INVESTIGATION OF NOVEL ROUTES IN THE SYNTHESIS OF TiNF AND COMPOUNDS IN THE Ti-N-O-F SYSTEM

by

Aimable Ngendahimana

Submitted in Partial Fulfillment of the Requirements

for the Degree of

Master of Science

in the

Chemistry

Program

YOUNGSTOWN STATE UNIVERSITY

May, 2010

INVESTIGATION OF NOVEL ROUTES IN THE SYNTHESIS OF TiNF
AND COMPOUNDS IN THE Ti-N-O-F SYSTEM

Aimable Ngendahimana

I hereby release this thesis to the public. I understand that this thesis will be made available from the OhioLINK ETD Center and the Maag Library Circulation Desk for public access. I also authorize the University or other individuals to make copies of this thesis as needed for scholarly research.

Signature:

Aimable Ngendahimana, Student Date

Approvals:

Dr. Timothy R. Wagner, Thesis Advisor Date

Dr. Allen D. Hunter, Committee Member Date

Dr. Clovis A. Linkous, Committee Member Date

Dr. Peter J. Kasvinsky, Dean of School of Graduate Studies & Research Date

ABSTRACT

Titanium nitride fluoride, TiNF, an anion exchange derivative of titanium dioxide, has been a target for synthetic inorganic chemists for some time. No true TiNF compound has been reported to date. A novel route for the synthesis of a TiNF phase has been outlined and tested. The method involves the use of a titanium complex as a precursor for the formation of TiNF and/or a Titanium Oxynitride Fluoride, 'Ti-N-O-F'. A suitable precursor, bis (diethylamidofluoro) titanium $[F_2(Et_2N)_2Ti]_4$ was identified, synthesized, its single crystal structure was determined, and it was used to test the proposed synthetic route towards TiNF. In this work, we propose that titanium complexes of the general formula $[F_2(Et_2N)_2Ti]_4$ undergo a thermal decomposition reaction involving a β-elimination of volatile ethylene from the amide ligands and subsequent loss of equally volatile ammonium fluoride, thus leaving at the end of the thermal decomposition as the only non-volatile product TiNF after all other products escape as gases or highly volatile solids. In the presence of fortuitous air and moisture the non-volatile TiNF is expected to undergo partial hydrolysis to form a 'Ti-N-O-F' phase. The thermal decomposition reaction of $TiF_2(NEt_2)_2$ has been investigated via Thermal Gravimetric Analysis and the properties of the non-volatile product were analyzed using Powder X-Ray Diffraction, Electron Microscopy and X-Ray Photoelectron Spectroscopy. In a second synthesis route, doping of TiO_2 with nitrogen has been achieved by reacting TiO_2 with urea. The amount of nitrogen doped into TiO_2 using urea is 8.62% by atomic concentration which is about twice the amount of nitrogen doped into TiO_2 using other known methods.

ACKNOWLEDGEMENTS

My first acknowledgement is to thank my research advisor, Dr. Timothy R. Wagner, for guiding me throughout my research and graduate studies. He has positively contributed to my professional and academic growth, by involving me into materials research, the kind of field of study I have always wanted to get trained in. I thank him for his patience and the encouragement he portrayed while I was working under his supervision. I would like to thank Dr. Allen D. Hunter for offering me a job, to work at the YSU analytical materials instrumentation facility. This was, indeed an excellent opportunity for me to gain experience in crystallography. I also want to thank Dr. Hunter for allowing me to participate in the out-reach program for chemical education in Africa. Such activities allowed me to keep in touch with my former professors and mentors while pursuing further education at YSU. I would like to thank Dr. Zeller for he has always been ready to assist in carrying out my research. I highly appreciate his input in my graduate studies and research. I want to thank Dr. Clovis A. Linkous for accepting to be on my thesis oral defense committee. He has tremendously contributed to my graduate studies and research experience, through his chemical instrumentation class as well as research interactions.

I also want to thank Rachel Kusnic for collecting XPS data and Materials Research Laboratory of Struthers for making their equipments available in my research. I thank all the professors at YSU, who have taught me and worked with me, as a teaching assistant. They have taught me how to be a better student as well as a better teacher. I would like to thank Dr. Howard D. Mettee, for sparing some time to play tennis with me. It helped me to refresh my mind as well as to improve my health.

I would like to dedicate the research work done and described in this thesis to my friends Helen and Ron Stauffer for they have been truly a blessing to me and to my family. They have been our ‘Grand Parents’ and role models!

TABLE OF CONTENTS

PAGE

TITLE PAGE.....i

SIGNATURE PAGE.....ii

ABSTRACT.....iii

ACKNOWLEDGEMENTS.....iv

TABLE OF CONTENTS.....vi

LIST OF TABLES.....x

LIST OF FIGURES.....xi

CHAPTERS

1. INTRODUCTION TO MATERIALS CHEMISTRY 1

1.1 General Background..... 1

1.2 Materials Chemistry as a Catalyst for Development..... 3

1.3 Categories of Materials Chemistry..... 4

1.3.1 Organic Materials Chemistry 4

1.3.2 Inorganic Materials Chemistry..... 5

1.3.3 Metal Oxides Materials..... 6

2. INORGANIC NITRIDE OXIDE-FLUORIDES MATERIALS 14

2.1 Nitrogen Doping..... 14

2.2 Metal Oxynitrides 14

2.2.1 Introduction 14

2.2.2 Previous Syntheses of Metal Oxynitrides 15

2.3 Nitride-Fluorides 24

3. STATEMENT OF THE PROBLEM AND GENERAL APPROACH 30

3.1 The Research Question 30

3.2 Motivation of the Research 30

3.3 Potential Molecular Precursors for the Synthesis of TiNF Materials 31

3.4 Coordination Compounds 32

3.5 Coordination Compounds as Molecular Precursors for the synthesis of TiNF 34

3.6 Sol-Gel Technique 35

3.7 Hypothesis 37

3.8 Objectives of the Research 40

4. SYNTHETIC METHODS 41

4.1 Air-Sensitive Chemistry 41

4.2 Schlenk Line Techniques 41

4.2.1 Starting up a Schlenk Line 42

4.2.2 Schlenk Vessels 45

4.2.3 Needle-Puncture Stoppers and Hypodermic Needles 46

4.2.4 Transfer of Air Sensitive Reagents 47

4.2.5 Refluxing 48

4.2.6 Distillation 49

4.2.7 Stirring 50

4.3 Solvent Purification 50

4.3.1 Degassing 50

4.3.2 Freeze-Pump-Thaw 50

4.3.3 Purging 51

4.3.4 Drying Agents 51

4.4 Maintenance of Low Temperature 53

4.4.1 Simple Cold Baths 53

4.4.2 Constant Temperature Cold Baths 53

4.5 Glove Bags 54

4.6 Glove Box 55

4.7 Tube Furnace 56

5. CHARACTERIZATION METHODS 57

5.1 Single Crystal X-ray Diffraction Analysis 57

5.2 Thermal Gravimetric Analysis (TGA) 58

5.3 Powder X-Ray Diffraction (PXRD) Analysis 59

5.4 Scanning Electron Microscopy (SEM) 62

5.5 X-ray Photoelectron Spectroscopy (XPS) 64

5.5.1 Instrumentation 64

5.5.2 XPS spectra vs Oxidation States 65

6. EXPERMENTAL RESULTS AND DISCUSSION 67

6.1 Sol-Gel Synthesis of TiO_2 67

6.2 Synthesis of bis(diethylamidofluoro) titanium 68

6.2.1 Synthesis of Ti $(NEt_2)_4$ 69

6.2.3 Synthesis of $[TiF_2(NEt_2)_2]_4$ 71

6.2.4 Single-Crystal Data Collection and Analysis of $[TiF_2(NEt_2)_2]_4$ 72

6.3 Thermal Gravimetric Analysis of $[TiF_2(NEt_2)_2]_4$ 84

6.3.1 Thermal Decomposition Analysis of $[TiF_2(NEt_2)_2]_4$ 84

6.3.2 Thermal Decomposition of a bulk sample of $[TiF_2(NEt_2)_2]_4$ 89

6.4 XPS Analysis 93

7. ATTEMPTED SYNTHESIS OF TiN_xO_y COMPOUND VIA UREA ROUTE 96

7.1 Motivation 96

7.2 The Proposed Reaction Process of TiO2 with Urea 96

7.3 Experimental 97

7.4 Results and Discussion 98

8. CHEMICAL EDUCATION OUTREACH 106

8.1 CyberLabNet Project 106

8.2 Baraton Chemistry Professors Visit at YSU 107

8.3 Introducing Vernier Probes and Sensors at Baraton University 108

9. SUMMARY AND CONCLUSION 109

REFERENCES 112

APPENDIX A: Selected bond distances (Å) in bis(diethylamidefluoro) titanium 115

APPENDIX B: Principal mean square atomic displacements U in $[TiF_2(NEt_2)_2]$ 116

APPENDIX C: Rietveld Refinement of TiNxOy compound from urea-TiO_2 reaction 119

LIST OF TABLES

TABLE		PAGE
1.1	Lead-free Piezoelectric Materials……..	7
2.1	Structural Similarity between TiO_2 and $TiO_{2-x}N_x$……..	16
2.2	Nitrogen Content in the Green (A) and Yellow (B) Samples……	27
2.3	Neutron Diffraction Pattern of the Nitrogen and Fluorine Doped TiO_2…….	29
4.1	Common Drying Reagents……..	52
6.1	Intensity Statistics……	73
6.2	Crystal Data……	75
6.3	Data Collection……	76
6.4	Selected Bond Lengths ……..	78
6.5	Selected Bond Angles ……	78
6.6	Tube Furnace Program-1……..	90
6.7	Percentage Atomic Concentrations in the ‘Ti-N-O-F’ and TiO_2 Samples……..	94
7.1	Tube Furnace Program-2……	98
7.2	Percentage Atomic Concentrations in the TiN_xO_y Samples……	105

LIST OF FIGURES

FIGURE		PAGE
1.1	Imperfection in a crystal leading to superionic conductivity……..	8
1.2	Photodegradation of 1, 1-dichloro-2-chloroethene……	11
2.1	Photocatalytic activity of TiO_2 Vs $TiO_{2-x}N_x$.....	17
2.2	XRD patterns of TiO_2N by ammonolysis (b) and by hydrazine method (c)……	18
2.3	Binding energies corresponding to Ti-N and N-X (X= O, N, C)……	19
2.4	Powder XRD pattern of (a) $CaTaO_2N$ (b) $SrTaO_2N$ and (c) $BaTaO_2N$ synthesized using urea….	20
2.5	EDAX patterns of (a) $SrTaO_2N$ (b) $TaBaO_2N$ (c) $SrNbO_2N$ and (d) $NbBaO_2N$……..	21
2.6	Influence of nitrogen doping on the energy band gap of TiO_2……	23
2.7	N-doped TiO_2 materials……	26
2.8	Spectral response of TiO_2, CdS, and the variants of TiO_2……	27
4.1	Schematic of a Schlenkline Set-up……	44
4.2	Schlenk round-bottom flask……	46
4.3	A Schlenk filter……	46
4.4	Rubber-stoppers……	47
4.5	Cannula transfer……	48
4.6	Programmable tube furnace……	56
5.1	Schematic of a TGA instrument……	59
5.2	Geometric set-up of a powder X-ray diffractometer……	61
5.3	SEM imaging……..	63
5.4	XPS schematic……	65

5.5 XPS spectra of titanium dioxide…… 66

6.1 PXRD pattern match of TiO_2…… 68

6.2 Ortep plot of bis (diethylamodofluoro) titanium…… 80

6.3 Packing of bis (diethylamodofluoro) titanium…… 81

6.4 Sphere model of bis (diethylamodofluoro) titanium…… 82

6.5 Stick model of bis (diethylamodofluoro) titanium…… 83

6.6 TGA thermogram-1 of bis (diethylamodofluoro) titanium…… 84

6.7 TGA thermogram-2 of bis (diethylamodofluoro) titanium…… 86

6.8 TGA thermogram-3 of bis (diethylamodofluoro) titanium…… 86

6.9 TGA thermogram-4 of bis (diethylamodofluoro) titanium…… 87

6.10 TGA thermogram-5…… 87

6.11 Overlay of the representative thermograms…… 88

6.12 PXRD pattern of the decomposition product of bis (diethylamodofluoro) titanium… 91

6.13 SEM micrograph of TiO_2 anatase…… 92

6.14 SEM micrograph corresponding to the decomposition product…… 93

6.15 XPS spectra for the analysis of 'Ti-N-O-F'…… 94

7.1 PXRD pattern for TiN_xO_y…… 99

7.2 XPS spectra for the blue sample of TiN_xO_y…… 101

7.3 Titanium curve fitting for the whole sample…… 101

7.4 XPS spectra for the green Sample…… 102

7.5 Oxygen curve fitting for the green phase…… 103

7.6 Oxygen curve fitting for the blue phase…… 103

7.7 Nitrogen curve fitting for the green sample…… 104

7.8 Nitrogen curve fitting for the blue sample…… 104

Chapter 1

Introduction to Materials Chemistry

1.1 General Background

Materials chemistry is the chemistry of the design, synthesis and characterization of assemblies of molecules whose properties arise from interactions between them. It is an interdisciplinary field in which a good understanding of the principles of both chemistry and materials science, and sometimes physics and biology, is required. It is very important to note that simply synthesizing a material is not materials chemistry but chemical synthesis. Although it is recognized that synthesis is a major part of what chemists do, the sub-discipline, materials chemistry, must include an element of application, function or novel design that is beyond the simple chemical reactivity of the species in question. Design refers to the design at the atomic or molecular level and design at greater length scale becomes materials science and engineering. Work on novel materials that may show potential applications is part of materials chemistry in which chemists may generate new types of materials with previously unknown properties leading to unimagined applications (Chaitanya *et al.,* 1996).

Chemistry has always been an indispensable contributor to the development and improvement of new materials. Materials are synthesized from chemical precursors and assembled using processes requiring chemical transformations. Of the six major classes of products produced by the chemical industry – fuels, commodity chemicals, polymers,

agricultural chemicals, pharmaceuticals and specialty chemicals – two contribute directly to materials chemistry. Synthetic organic polymers constitute a major class of materials, and specialty chemicals (e.g. paints, corrosion inhibitors, lubricants, adhesives and adhesion promoters, electronics chemicals) are essential components of many assembled materials systems. Until recently, chemistry has been relatively inactive in other major areas of materials: metallurgy has attracted little activity from chemists, and only in the last few years has chemistry again become involved in ceramics.

To develop ideas about the sub-discipline of materials chemistry, it is useful to look at some of the processes and priorities of researchers in the parent discipline itself. As mentioned above, much materials chemistry is motivated by the discovery and development of materials that may be exploited for desired applications. While this is an essential motivating factor, there is a need to have some scope of purely studying the structure and properties of materials. Chemists therefore generate new materials often before their potential applications become fully conceived. Today, the work of most materials chemists is focused on producing functional device materials and the discipline is often seen as being focused on the production of materials with electrical, optical or magnetic applications. Materials chemistry can also encompass structural properties such as strength or flexibility, but the current focus of chemists mainly involves other types of functionality. This might however change in the future. Therefore, rather than purely investigating properties, the materials chemist tries to manipulate the synthetic process to produce a desired end product. The relationship

between method of synthesis and design of the final end product is crucial for a materials chemist.

1.2 Materials Chemistry as a Catalyst for Development

Materials are so ubiquitous and so pervasive that we often take them for granted. Yet they play a very crucial role in our lives, in practically all manufacturing industries, in research and in development. Materials have a generality comparable to that of energy and information and the three together comprise all technology. Materials chemistry is the foundation upon which all these technological changes are built. New materials made from more abundant raw materials can be made as substitutes for old ones which might have been fabricated from ecologically less desirable raw materials or simply from raw materials that are scarce. For example development of catalysts based on abundant materials could significantly reduce demand for platinum catalysts commonly used for treating automobile exhaust gases and for use in chemical processes (Chaitanya *et al.,* 1996). Such innovations can play a significant role in the economy, in raising the standard of living, in minimizing demand for energy and in improving environmental quality. Another example worth mentioning is silicon nitride. Its excellent strength, thermal shock resistance and oxidation behavior have made it a material of choice for gas turbine engines (Yan *et al.,* 1994.). As there continues to be demand for new and improved products, research in materials chemistry will continue to play a large role in design and synthesis of these materials.

1.3 Categories of Materials Chemistry

1.3.1 Organic Materials Chemistry

Organic materials are mostly polymers which have dominated the plastic, rubber and elastomeric industry. In general, polymers can be divided into two categories: natural and synthetic polymers. Examples of naturally occurring polymers include cellulose, starch, lignin, chitin and various polysaccharides. In fact the first attempt to make a synthetic fiber was done by altering the natural polymer cellulose by John Wesley Hyatt in 1870 (Yan *et. al* 1994.). He treated cellulose nitrate (an explosive material made by exposing cotton plant fibers to nitric and sulfuric acids) with alcohol and camphor to obtain a hard and shiny material that is moldable. In 1887 Count Hilaire de Chardonnet created a related product when he learned to spin cellulose nitrate into Chardonnet silk, the first synthetic fiber to enter production (Lilliane *et al.,* 2003.). Both cellulose nitrate and Chardonnet silk were polymers created by altering natural polymers.

In 1909 the American inventor Leo Baekelan made the first truly synthetic polymer by treating carbolic acid, a derivative of coal tar, with formaldehyde under heat and pressure. The product Bakelite was hard, immune to harsh chemicals, electrically insulating, and heat resistant. Such characteristics made Bakelite useful for many applications such as making household goods and electrical parts. Since then chemical and materials engineering have come up with polymers that have exceptional mechanical properties such as stiffness, toughness and low creep that make them

valuable in the manufacture of structural products, like gears, bearings and electronic devices. For example, polyamides are crystalline and have good impact strength, toughness and abrasion resistance.

1.3.2 Inorganic Materials Chemistry

Inorganic materials are commonly divided into pure inorganic materials such as ceramics and alloys, and organic-inorganic hybrid materials such as coordination polymers, organometallic polymers and even framework materials. The hybrid materials which are often polymeric in nature all have one general idea in common: by combining inorganic and organic compounds, it is likely possible to develop materials with special properties. Synthesis of such compounds can lead to formation of functional materials suitable for solving important technological problems.

For example polysiloxanes, which are probably the most commercially valuable and familiar inorganic polymers, have a number of important properties such as: (1) they can be formulated to be electrically insulative or conductive, (2) they have low chemical reactivity and toxicity, and (3) they have high gas permeability, and are therefore suitable for medical applications. Inorganic polymers and hybrid materials have yielded numerous important technological materials but there are also numerous non-polymeric and purely inorganic materials with equally important applications in many high tech applications. Commonly targeted purely inorganic compounds include: molecular inorganic superconductors, magnetic materials, materials for non-linear optics, photocatalysts, semiconductors and many others.

Since it is not possible to exhaustively describe all inorganic materials, the following sections will concentrate on inorganic oxides because they are the most commonly synthesized class of inorganic compounds.

1.3.3 Metal Oxides Materials

Inorganic oxides have emerged as materials of interest in the electronic industry, and especially superconductor industry. These oxide materials have many interesting electronic properties which cannot be fully discussed in this chapter. However, a few of these properties need to be discussed in order to shed more light on how important inorganic oxides materials are.

Dielectrics

A dielectric material is a poor conductor of electricity but an efficient supporter of electric fields while dissipating minimal energy in the form of heat. Dielectric properties are measured in terms of dielectric loss, dielectric constant and dielectric strength. The lower the dielectric loss (the proportion of energy lost as heat) the more effective is a dielectric material. Metal oxides such as aluminum oxide have a high dielectric constant which means that they are not able to withstand intense electrostatic fields but nevertheless have made it possible to manufacture high value capacitors with low physical volume (Thirumal *et al.,* 2002.).

Piezoelectrics

Metal oxides such as lithium niobate and lithium tantalate exhibit the so called piezoelectric effect. A piezoelectric material produces an electrical charge when mechanical stress is applied and conversely when mechanically deformed, a piezoelectric substance produces an electric field (Cochet-Muchy *et al.* 2002). One necessary condition for a compound to be piezoelectric is for the materials to be non-centrosymmetric. As an application example, piezoelectric materials can be used in a car's airbag to detect the intensity of a shock and send an electrical signal which triggers the airbag. Lead oxide-based piezoelectric ceramics are widely used in various applications such as transducers, filters, oscillators and actuators. The toxicity and high vapor pressure of lead oxide has lead to the need to process environmentally benign lead-free piezoelectrics examples of which are shown in **Table 1.1.**

Table 1.1 Examples of Lead-free Piezoelectric Materials (Shrout *et al*., 2008.)

Material	$\varepsilon_r/\varepsilon_0$	Loss	d_{33} (pC/N)	k_p	k_{33}	T_c (°C)	T_{O-T}/T_d (°C)
$BaTiO_3$	1,700	0.01	190	0.36	0.5	115	0
$BaTiO_3$-$CaTiO_3$-Co	1,420	0.005	150	0.31	0.46	105	−45
$(K_{0.5}Na_{0.5})NbO_3$ (HP)	500	0.02	127	0.46	0.6	420	
$(K_{0.5}Na_{0.5})NbO_3$	290	0.04	80	0.35	0.51	420	195
KNN-Li (7%)	950	0.084	240	0.45	0.64	460	~20
KNN-Li3%; Ta20% (LF3)	920–1,256	0.024–0.02	190–230	0.46–0.505	0.62	310–323	50–70
KNN-LF4[a]	1,570	/	410	0.61	/	253	25
KNN-$SrTiO_3$ (5%)	950	/	200	0.37	/	277	27
KNN-$LiTaO_3$ (5%)	570	0.04	200	0.36	/	430	55
KNN-$LiNbO_3$ (6%)	500	0.04	235	0.42	0.61	460	70
KNN-$LiSbO_3$ (5%)	1,288	0.019	283	0.50	/	392	45
NBT-KBT-LBT	1,550	0.034	216	0.401	/	350	160
NBT-KBT-BT	820	0.03	145	0.162	0.519	302	224
NBT-KBT-BT (MPB)	730	0.02	173	0.33	0.59	290	162
NBT-KBT-BT	770	0.034	183	0.367	0.619	290	100
NBT-BT	665	0.028	64 (d_{31})	0.28(k_{31})	/	/	/
NN-BT10%	1,000	0.015	147	/	/	235	/
NBT-KBT50%	825	0.03	150	0.22	/	320	210
SBT-KBT90	870	0.04	110	0.15	0.507	296	/
SBT-KBT85	1,000	0.05	120	0.16	0.491	250	/
BBT-KBT90	837	0.05	140	0.23	0.538	297	144
BBT-KBT80	630	0.04	95	0.15	0.361	290	238
$Sr_2NaNb_5O_{15}$[a]	1,100	/	120	/	/	280	/

[a]Textured ceramics; T_{O-T}: Orthorhombic to tetragonal phase transition; HP: Hot Pressed; NN: $NaNbO_3$; NBT: $(Na_{0.5}Bi_{0.5})TiO_3$; KBT: $(K_{0.5}Bi_{0.5})TiO_3$; LBT: $(Li_{0.5}Bi_{0.5})TiO_3$; BT: $BaTiO_3$; SBT: $(Sr_{0.7}Bi_{0.2})TiO_3$; BBT: $(Ba_{0.7}Bi_{0.2})TiO_3$; KNN: $(K_{0.5}Na_{0.5})NbO_3$; T_d: depolarization temperature.

Superionic conductors

Superionic conductors are materials that allow macroscopic movement of ions through their structure. This movement causes exceptionally high (liquid-like) values of ionic conductivity in the solid state (Sunandana *et al.,* 2004). Superionic conductivity typically occurs at high temperatures and is characterized by rapid diffusion of a significant fraction of one of the constituent species within an essentially rigid framework formed by other atomic species. A good example of a superionic oxide conductor is zirconium dioxide doped with calcium oxide and yttrium oxide which conducts oxygen ions. This property makes it useful in making oxygen sensors. It is paramount to mention that superionic conductors have numerous other technological applications ranging from mobile phones and laptop computers to high energy storage devices for next generation 'clean' electric vehicles. The theory of super conductivity is not a simple one. It includes details of crystal defects and activation energies of the ions involved in super conductivity. The crystal defects leading to superionic conductivity are described in **Figure 1.1**.

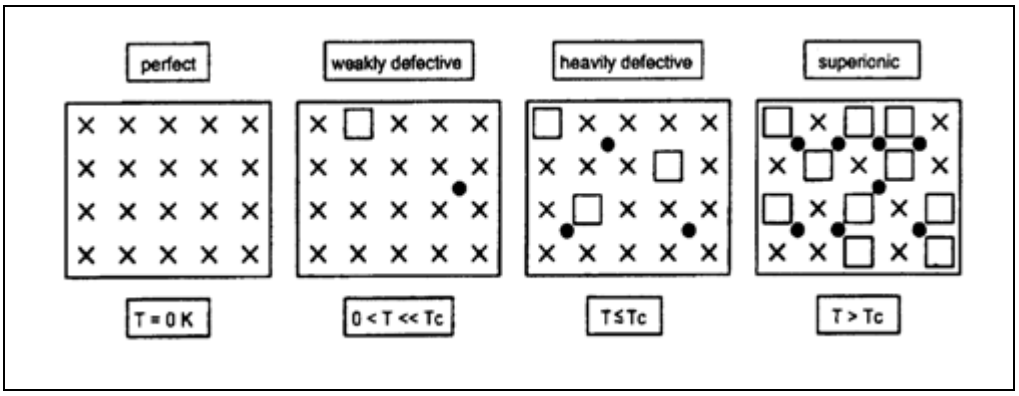

Figure 1.1 Imperfection in a crystal leading to superionic conductivity at $T>T_c$ (Sunandana *et al*., 2004)

Variable resistors

Metal oxides such as zinc oxides are used in manufacturing varistors. Usually a metal oxide varistor contains a ceramic mass of zinc oxide grains, in a matrix of other metal oxides such as cobalt or manganese, sandwiched between two metal plates. Varistors have high resistance at low voltages and a low resistance at high voltage! How does this happen? This happens because the boundary between each grain and its neighbor forms a diode junction, which allows current to flow in one direction. The mass of randomly oriented grains is electrically equivalent to a network of back to back diode pairs, each pair parallel with many other pairs. So when a small voltage is applied across the electrodes, only a tiny current flows because of a reverse leakage occurring through the diode junctions. When a large voltage is applied, the diode junction breaks down due to a combination of thermionic emission and electron tunneling, and large current flows.

Thermistors

The word “thermistor” is a short form of “thermal resistor”. A thermistor is an electronic component that exhibits a large change in resistance with a change in its body temperature. Many metal oxides such titanium, cobalt, nickel, iron and copper oxides have been used in the manufacture of thermistors. The fabrication of thermistors uses basic ceramic technology in which a mixture of two or more metal oxide powders are combined with a suitable binder, formed to desired geometry, dried and sintered at high temperatures. By varying the types of oxides powders used, their relative

proportions, the sintering atmosphere, the sintering atmosphere and the sintering temperature a wide range of thermal resistors can be obtained.

Ferromagnets and Ferroelectrics

Some materials, especially metals and metal oxides can exhibit ferromagnetic properties. Ferromagnetism is a physical phenomenon by which materials exhibit a strong attraction to magnetic fields and are able to retain their magnetic properties after the external field is switched off (Straus *et al.,* 2003). Ferromagnetism is explained better by noting that ferromagnetic materials have some unpaired electrons so their atoms have a net magnetic moment. In contrast to paramagnetic materials, where the magnetic moments of neighboring atoms or molecules are independent of each other, ferromagnetism originates from the existence of magnetic domains in which the magnetic moments are aligned. Examples of ferromagnetic metal oxides include $NiOFe_2O_3$, $CuOFe_2O_3$, $MnOFe_2O_3$ and $MgOFe_2O_3$. Ferromagnets are used in transformers, tape recording/data storage devices, and in the fabrication of electromagnets.

Photo-catalysts

Another application of metal oxides is photocatalysis. Indeed, work described in this thesis is largely aimed at development of new and better photocatalysts. As photocatalysis is not a subject that is necessarily known to every inorganic chemist, a brief description of the origins of photocatalysis is given in this Section.

Photocatalysis is a light assisted process. In catalysis, a chemical process or transformation is accelerated by a catalyst that is usually present in small managed quantities and which is not consumed in the reaction. Thus a catalyst permits reactions or processes to take place more effectively or under milder conditions than would otherwise be possible. It allows a reaction to take another pathway that otherwise would be kinetically not possible. A photocatalyst is similar to a catalyst, in that it is not consumed in a reaction, but it facilitates a process that otherwise would not be possible. In contrast to a traditional catalyst it does however not lower an activation barrier for a process; instead it allows the process to overcome this barrier with the help of energy provided by light. Thus, light has to initiate the reaction, by exciting the "catalytic" material. A well known photocatalyst is semiconducting TiO_2 (Michalow *et al.*, 2009.). It can be for example used to degrade organic pollutants from the environment (e.g., water contaminated by chlorinated organics) in the presence of a UV-light source as shown in **Figure 1.2** below.

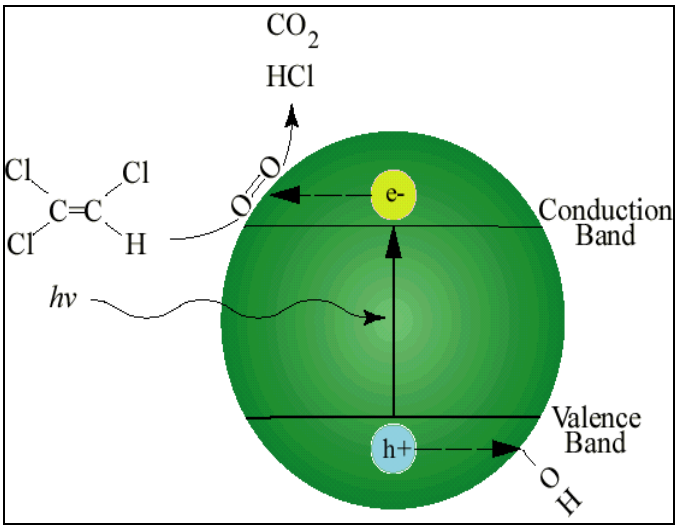

Figure 1.2 Photo-degradation of 1,1-dichloro-2-chloroethene
http://www.chem.purdue.edu/raftery/research/photocat.pdf (accessed Sept, 2009)

In the case of TiO_2, UV light is used to create electron-hole pairs in semiconducting TiO_2. The electrons then react with oxygen molecules as shown in the diagram above, to produce $O^{- -}$ ions and the holes react with surface OH^- groups to form hydroxyl radicals ($OH^{\cdot}$). If organic molecules are present, they can be attacked by these radical species, as shown in **Figure 1.2**, to degrade them into gaseous and/or harmless inorganic products such as CO_2, H_2O, and chloride anions if chlorine atoms were present in the molecule. Also important is a similar application where a TiO_2 photocatalyst is embedded in organic materials such as plastics to induce photo-aging. The presence of TiO_2 in these plastic materials will lead to a degradation that reduces the lifetime of such usually non-biodegradable materials. Therefore photocatalysts are a very important set of materials that has provided solutions to environmental problems and continues to attract research attention in other areas such as energy conversion technologies.

After realizing the potential of light in chemical and physical processes, materials chemists have continually searched for new photocatalysts. One limit to the first photocatalysts used (such as TiO_2) was the need to use energetic UV light to induce any reactions as these semiconductors did usually not absorb in the visible spectrum. By doping metal oxides with cations and anions, it is possible to extend the energy band gap of metal oxides such as TiO_2 into the visible region of the solar spectrum and therefore make these photocatalysts useful for a wider range of applications. For example, one way to make variants of metal oxides (and thus vary their band gap) is anion substitution to form compounds such as nitride fluorides, oxyfluorides,

oxynitrides and oxynitridefluorides. In the next chapter, the chemistry of nitridation and fluoridation will be discussed.

Chapter 2

Inorganic Nitride Oxide-Fluoride Materials

2.1 Nitrogen Doping

By doping metal oxides with nitrogen, several researchers have been able to extend the optical absorption of various metal oxides into the visible region. Many different nitriding agents are commonly used but the most widely used ones are: 1) ammonia 2) molecular nitrogen 3) urea, 4) hydrazines and 5) triethylamine. New metal oxide variants known as metal oxynitrides and also nitride fluorides have been synthesized using these nitriding agents.

2.2 Metal Oxynitrides

2.2.1 Introduction

Metal oxynitrides can be described as variants of metal oxides made by anion substitution which can have significant impact on its properties. For instance, a partial substitution on the O^{2-} sites by N^{3-} in TiO_2 leads to the formation of N-doped TiO_2 by carrying out this substitution it becomes possible to tune the photocatalytic behavior of the parent metal oxide. The partial substitution of O^{2-} by N^{3-} narrows the band gap of the parent oxide by shifting the valence band edge upwards. Oxynitrides therefore possess band gaps falling in the visible region, a property which makes them useful as photocatalysts and non-toxic pigments.

Therefore, oxynitrides are also investigated as potential photocatalitically active materials. They have attracted attention because current oxide photocatalysts such as TiO_2 are wide-gap semiconductors for which UV-light is necessary to produce electron-hole pairs by photo excitation. However, the UV-spectrum is just about 10% of the solar spectrum. A catalyst that would make use of the whole visible spectrum would be much more efficient and could be used in many more applications, e.g. for environmental clean up using sun light. Colored materials that absorb in the visible region of the spectrum, such as nitride type compounds, are promising candidates for visible-light-driven photocatalysis. In the literature two main applications are described. The first one concerns the use of nitrogen doped oxides to decompose polluting molecules in air or water. Among them, a tremendous number of publications highlight activity of nitrogen-doped titania with visible light as the energy source. The second group of applications that make use of oxynitrides as photocatalysts is devoted to water decomposition under visible light irradiation to produce hydrogen and/or oxygen.

2.2.2 Previous Synthesis of Metal Oxynitrides

Synthesis via Ammonolysis

The synthesis of metal oxynitride by ammonolysis often involves heat treatment of a metal oxide in NH_3 for prolonged periods of time. Michalow *et al.* (2009) synthesized and characterized nitrogen doped TiO_2 nanopowders by reacting titanium oxides with ammonia gas at temperatures of 550 °C (heating rate: 10 K/min) in a rotating cavity quartz (SiO_2) reactor with an internal diameter of 30 mm (Chang *et al.,*

2006). This synthesis involved two steps. The first step was to synthesize TiO_2 powders using a flame spray technique and the second was to carry out ammonolysis as described above. Ammonolysis was done on the TiO_2 synthesized by flame spray technique (F-TiO_2) as well as on TiO_2-25, which is a mixture of both polymorphic forms (anatase and rutile) of TiO_2. The results obtained show that doping TiO_2 with nitrogen slightly alters its unit cell parameters as summarized in **Table 2.1.** Note that F-TiO_2 in the table refers to the TiO_2 made by flame spray technique and P-25 refers to the polymorphic form of TiO_2

Table 2.1 Structural Similarity between TiO_2 and $TiO_{2-x}N_x$ (Michalow *et al*., 2009.)

Sample	F-TiO_2		F-$TiO_{2-x}N_x$		P-TiO_2		P-$TiO_{2-x}N_x$	
	Anatase	Rutile	Anatase	Rutile	Anatase	Rutile	Anatase	Rutile
Fraction (wt.%)	91.07 ± 0.45	8.93 ± 0.20	88.23 ± 0.56	11.77 ± 0.26	83.13 ± 0.39	16.87 ± 0.14	82.75 ± 0.47	17.25 ± 0.17
Average crystallite size (nm)	27.72	11.85	20.96	10.87	20.58	34.99	21.06	32.41
Lattice parameter, *a* (nm)	0.3786 ± 0.0001	0.4592 ± 0.0001	0.3787 ± 0.0001	0.4591 ± 0.0001	0.3786 ± 0.0001	0.4594 ± 0.0001	0.3787 ± 0.0001	0.4595 ± 0.0001
Lattice parameter, *c* (nm)	0.9505 ± 0.0001	0.2956 ± 0.0001	0.9503 ± 0.0001	0.2958 ± 0.0001	0.9508 ± 0.0001	0.29588 ± 0.0001	0.9507 ± 0.0001	0.2960 ± 0.0001
Cell volume (nm^3)	0.1362 ± 0.0001	0.0623 ± 0.0001	0.1363 ± 0.0001	0.0623 ± 0.0001	0.1362 ± 0.0001	0.0624 ± 0.0001	0.1363 ± 0.0001	0.0625 ± 0.0001

In addition it was shown that nitrogen doped TiO_2 has some photocatalytic activity. In this case, an experiment was performed to compare how various TiO_2 and $TiO_{2-X}N_X$ (X « 0.1) compounds decolorized methylene blue (MB). The graph in **Figure 2.1,** summarizes their results.

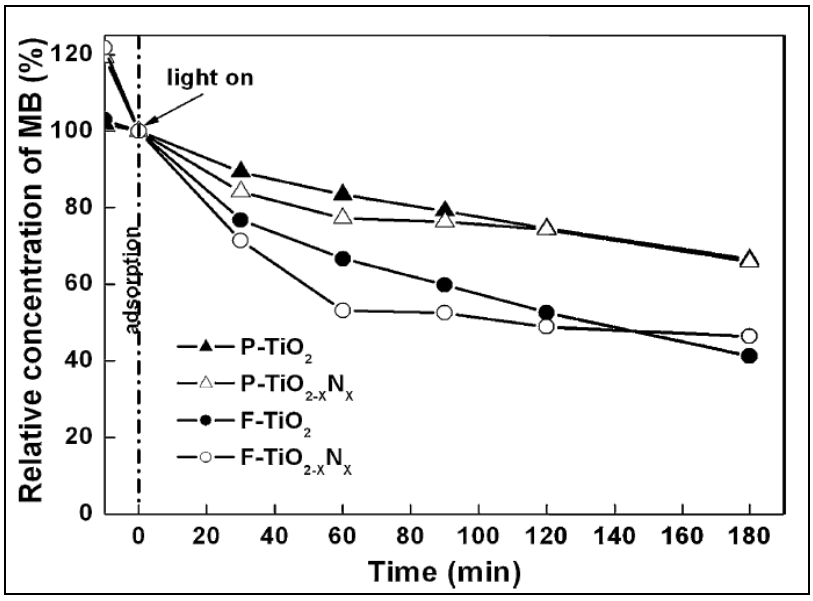

Figure 2.1 Photocatalytic activities of TiO_2 vs $TiO_{2-x}N_x$ (Michalow *et al.*, 2009.)

Synthesis via Hydrazine

Hydrazine is a reactive chemical and it ignites in air at relatively low temperature in a highly exothermic reaction. Li *et al.* (2007) in their paper demonstrated a wet method to prepare nitrogen-doped TiO_2 using hydrazine as the nitrogen source. The method is simple and does not require calcination at high temperatures. In their experiment, 10 mL titanium (IV) tetraisopropoxide was added dropwise to 200 mL deionized water without any other reagent under vigorous stirring. The obtained products were filtered and rinsed with deionized water several times, then dried at 60°C to form white powders. The powders were dipped in hydrazine hydrate (80%) for 12 hours, then filtered and dried at 110°C for three hours in air. XRD patterns for non-sintered TiO_2 (denoted as T60), pure sintered TiO_2 (denoted as TH) and the yellow nitrogen doped TiO_2 obtained are shown in **Figure 2.2**. Pattern (a) is for the T60, pattern

(b) is the TH and pattern (c) is for the yellow nitrogen doped TiO_2. The XRD patterns of the nitrogen-doped TiO_2 are similar to that of TiO_2 and $TiO_{2-x}N_x$ obtained via ammonolysis has a similar PXRD pattern to that of $TiO_{2-x}N_x$ obtained via the hydrazine route.

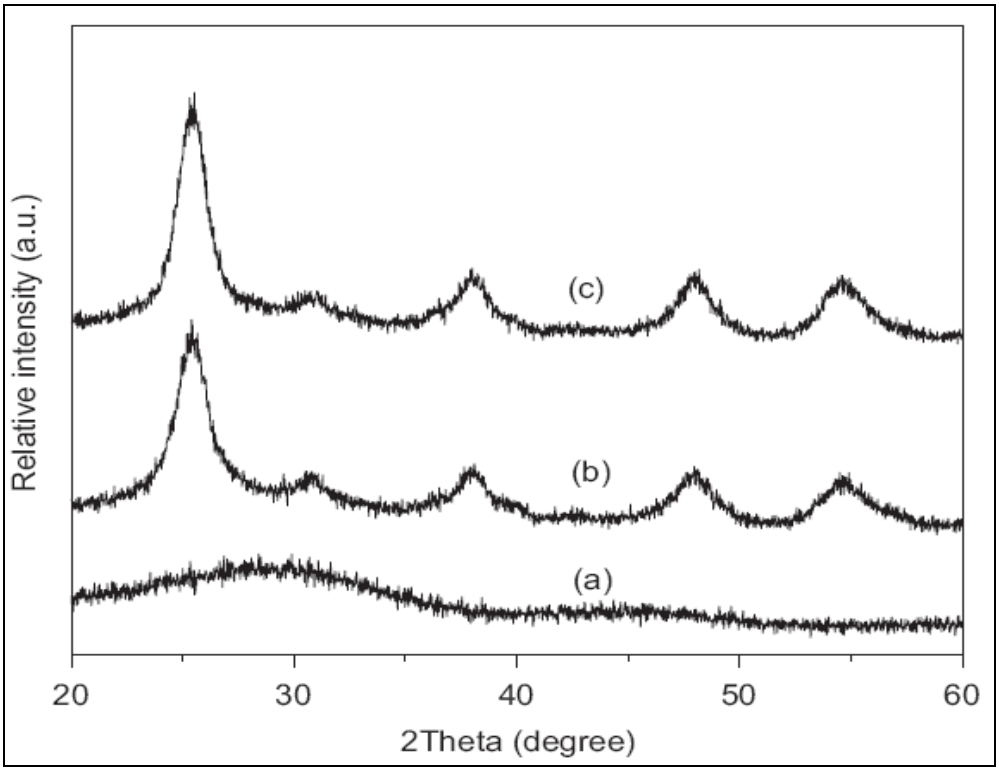

Figure 2.2 XRD patterns of TiO2-xNx by ammonolysis (b) and by hydrazine method (c) (Li *et al*., 2007.).

In their research, Li *et al.* (2007) show that a Ti-N bond existed in the $TiO_{2-x}N_x$ products, using XPS. The Ti-N is located at 396.6 eV (Li *et al*., 2007). Other nitrogen bonds such as N-O, N-N, and N-C are located at 399.6 eV. These bond energies are quite close as shown in **Figure 2.3**, and a keen observation is needed to distinguish them.

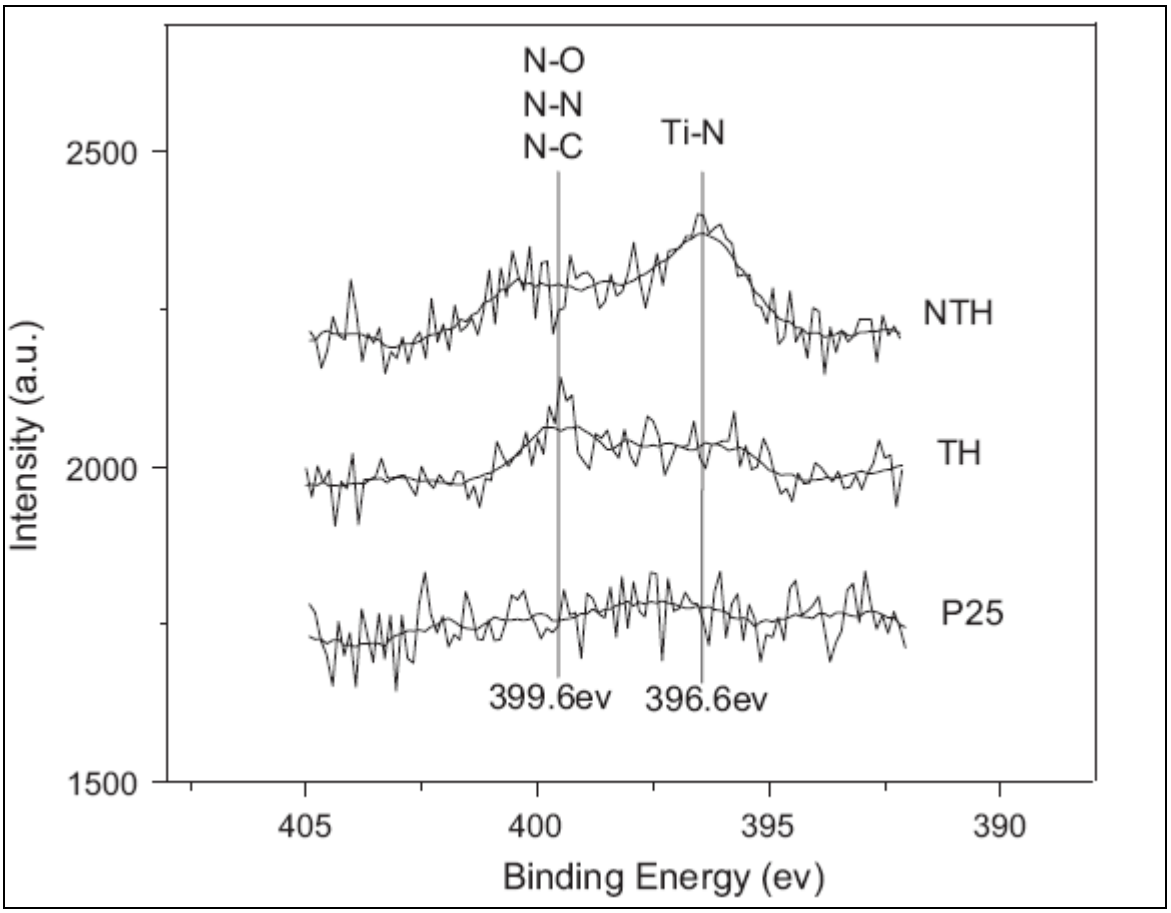

Figure 2.3 Binding energies corresponding to Ti-N and N-X (X= O, N, C) (*Li et al*., 2007).

Synthesis via Urea

Several binary and ternary metal oxynitrides have been prepared using urea as a nitridation agent. The method generally involves heating a suitable metal compound such as a halide or an oxide in admixture with urea at an appropriate temperature. The urea route makes it possible to start with a solid mixture of metal oxides and urea and to effect nitridation by the ammonia formed in situ by the decomposition of urea (Gomathi *et al.*, 2009). This method has successfully led to the synthesis of $CaTaO_2N$, $SrTaO_2N$ and $BaTaO_2N$ by heating Ta_2O_5 with $CaCO_3$, $SrCO_3$ and $BaCO_3$ in a mixture with excess urea at around 1200K. XRD patterns for the products are shown in **Figure 2.4**.

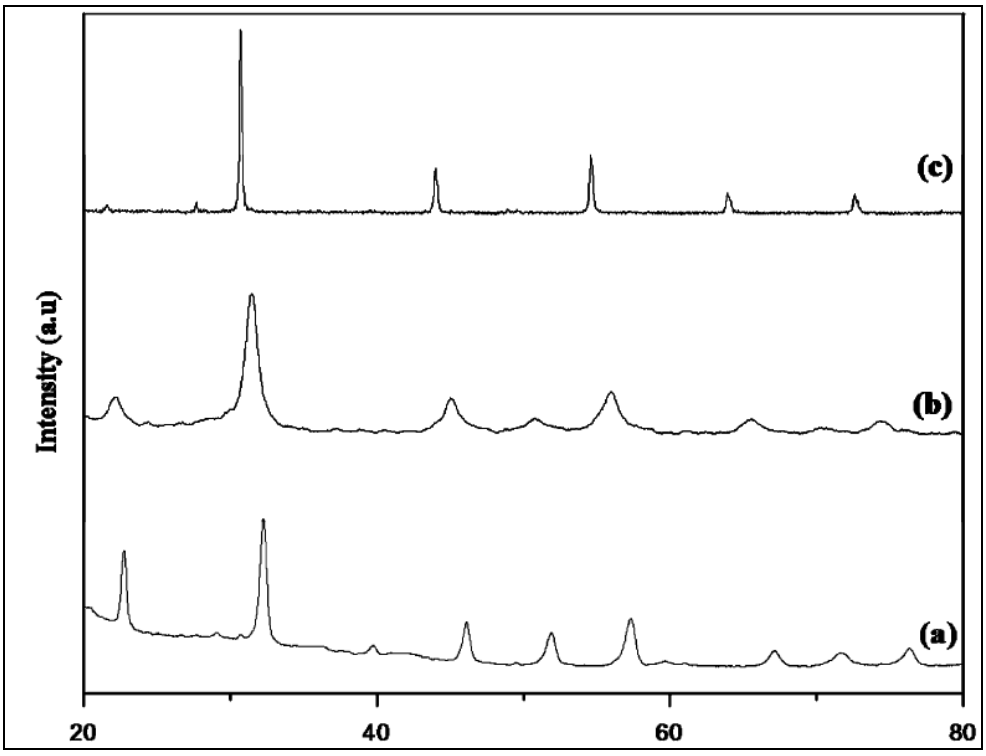

Figure 2.4 Powder XRD pattern of (a) $CaTaO_2N$ (b) $SrTaO_2N$ and (c) $BaTaO_2N$synthesized using urea (Gomathi *et al*., 2009).

Various compounds synthesized via the urea route were further characterized by EDAX as shown in **Figure 2.5**. Each spectrum shows a considerable amount of nitrogen doping at approximately 0.6 KeV.

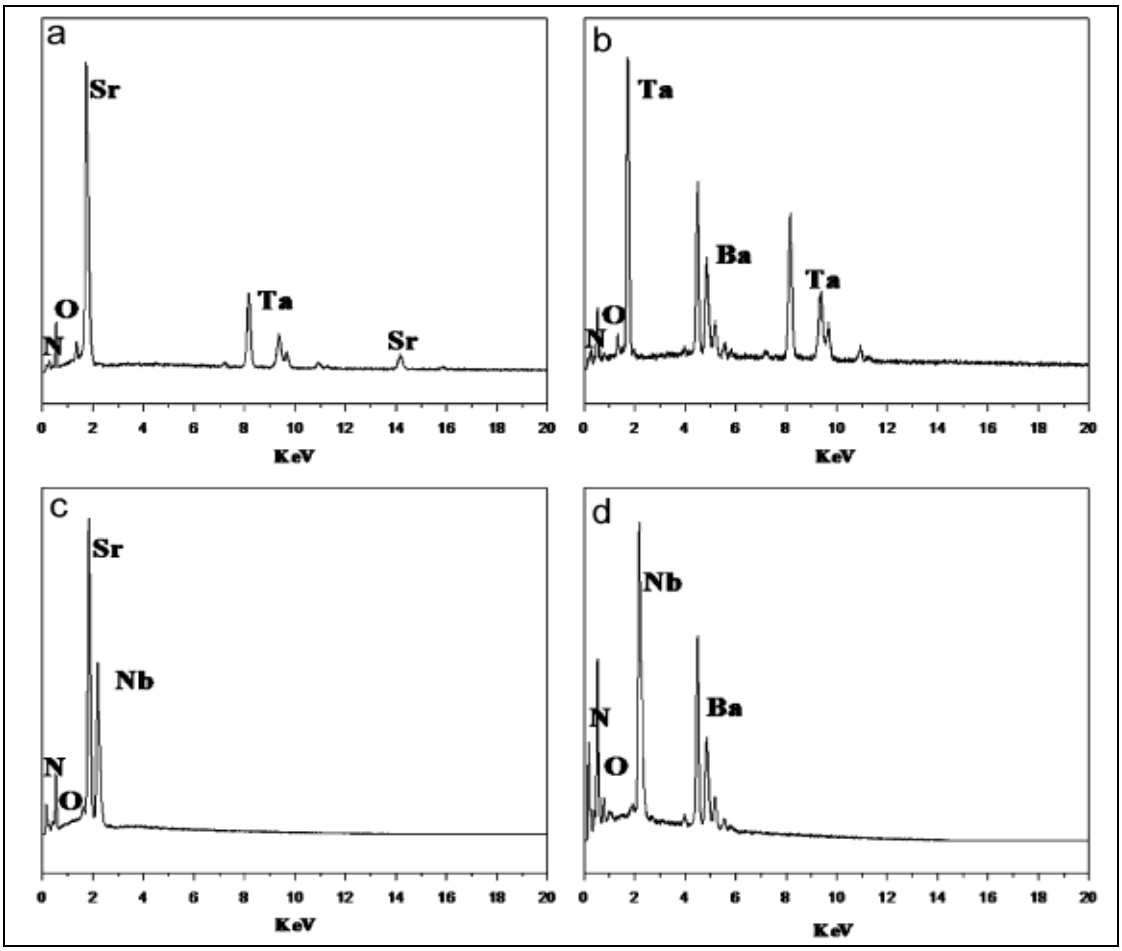

Figure 2.5 EDAX patterns of (a) $SrTaO_2N$ (b) $TaBaO_2N$ (c) $SrNbO_2N$ and (d) $NbBaO_2N$ synthesized using urea (Gomathi *et al*., 2009).

Synthesis using Alkyl ammonium Salt

Triethylamine was used by Gole *et al.* (2004) as a nitriding agent in the synthesis of $TiO_{2-x}N_x$. In their work, two types of TiO_2 nanoparticles were doped with nitrogen: the

first were colloidal TiO_2 nanoparticles and the second a partially agglomerated gel (solution) of TiO_2 nanoparticles. These two types of particles lead to the formation of yellow and orange products respectively. Using a typical sol-gel synthesis experiment, they were able to synthesize TiO_2 particles with varying sizes. In the first synthesis, a 5mL aliquot of $Ti[OCH(CH_3)_2]_4$, dissolved in isopropanol, was added drop wise to 900 mL of distilled water at a pH of 2. Characterization of the resulting particles was done by TEM, giving particle sizes ranging from 3 to 11 nm. However in an alternative synthesis using a mixture of water and acetic acid, particles of 5 to 20 nm in size were obtained. In this case, 250 mL of doubly ionized water and 80 mL of acetic acid were combined in a 1L flask as the mixture was cooled to 0°C. Then a 10 mL aliquot of 2-propanol followed by 3.7 mL of $Ti[OCH(CH_3)_2]_4$ was slowly added via dropping funnel. Continued stirring for 24 hours produced a clear colloidal solution with particle sizes ranging from 5 nm to 20 nm.

Before nitridation of the resulting nanoparticle colloids was done, palladium was introduced to the colloids, in the form of palladium chloride. In order to form an alkylammonium salt, triethylamine was introduced and agitation of the mixture was done for several hours. After treatment with triethylamine, the nanocolloid solution formed deep yellow crystallites while the partially agglomerated nanoparticle gel solution lead to the formation of orange crystallites. Optical properties of the two types of $TiO_{2-x}N_x$, the yellow and the orange types, were investigated.

As shown in **Figure 2.6**, the reflectance spectrum of P25-TiO_2 sharply rises at approximately 380 nm, the reflectance spectrum for the nitride, $TiO_{2-X}N_X$ crystallites generated from the nanoparticle solutions, rises sharply at around 450 nm, and the corresponding spectrum for nitrided $TiO_{2-X}N_X$, partially agglomerated nanoparticles, rise at 550 nm.

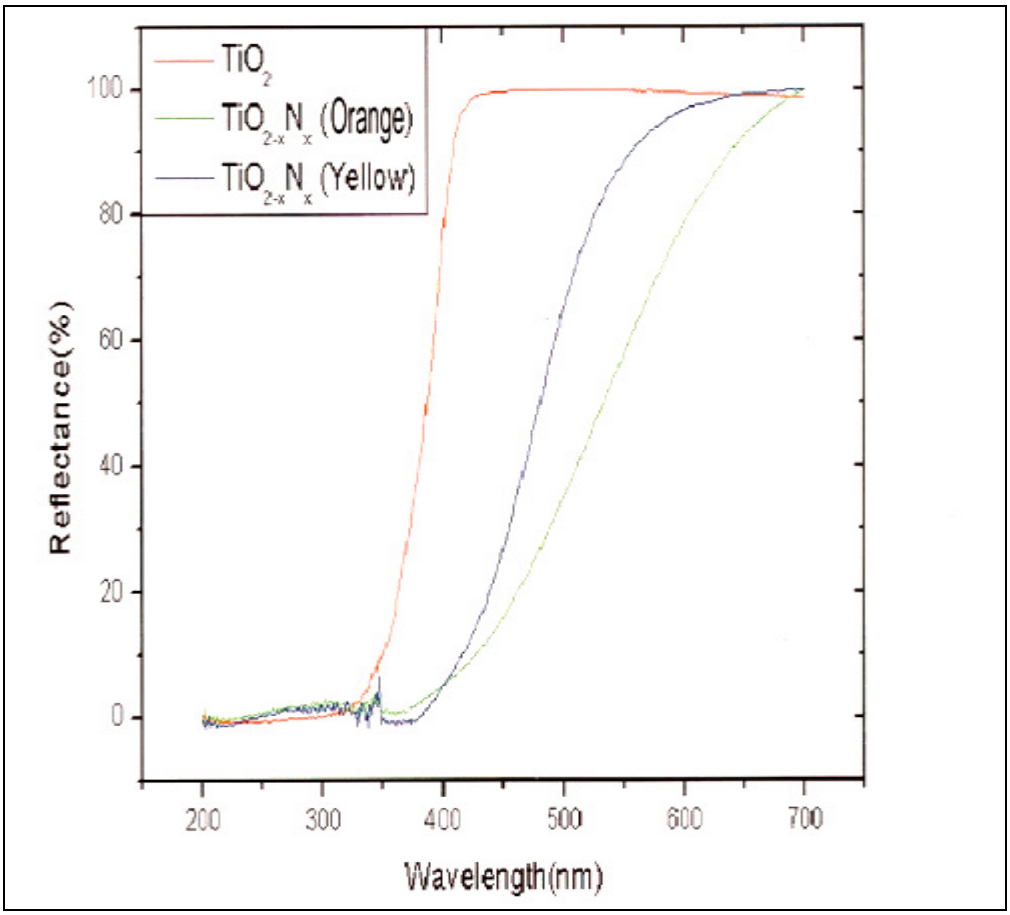

Figure 2.6 Influence of nitrogen doping on the energy band gap of TiO_2 (Gole *et al*., 2004).

2.3 NITRIDE-FLUORIDES

Inorganic nitride-fluorides have been a relatively unexplored area of materials chemistry. While tens of thousands of inorganic oxides have been studied, only about forty nitride-fluorides have been reported over the past forty years. Nitride-fluorides and oxides have structural similarities due to the fact that the substitution $2O^- \rightarrow N^{3-} + F^-$ conserves the cation-to-anion ratio and does not significantly alter the average anion radius. At the same time, differing electronegativities of nitrogen and fluorine give these phases electronic structures and local coordination environments that are distinctively different form their oxide analogs.

One of the earliest relevant studies was published by Andersson, pertaining to his work on magnesium-nitride-fluorides (Stephen *et al*., 1997). Andersson prepared his samples by reacting magnesium powder with MgF_2 in a nitrogen gas atmosphere. His work yielded three different phases having two compositions: Mg_3NF_3, L-Mg_2NF (low temperature form) and H-Mg_2NF (high-temperature form). The L-Mg_2NF and H-Mg_2NF forms were prepared at reaction temperatures of 900 °C and 1350 °C respectively. The compositions were deduced by both density measurements and structure determinations. In the structure, magnesium is coordinated to three nitrogen and two fluorine atoms, with a sixth long bond to fluorine. The H-Mg_2NF sample was found to be isostructural to MgO at temperatures between 1250 °C and 1350 °C. After the work of Andersson, another group reported the synthesis of calcium, strontium and barium nitride-fluorides. Erlich, Linz and Siefert (1970) conducted this synthesis by using 3 to 1 mole ratios of the metal to metal-fluoride for the Sr_2NF and Ba_2NF syntheses, and a 4 to

1 ratio for the Ca_2NF synthesis. The reaction mixtures were annealed in an inert argon environment at a temperature of 1000°C for 24 hours and then reacted in nitrogen gas for 5 hours at 450°C. Following this treatment, the calcium, strontium and barium reaction mixtures were sintered in nitrogen gas flow for 24 hours at 1000°C, 950°C, and 700°C, respectively.

In addition to the main group compounds discussed above, some transitional metal nitride-fluorides have been reported. For example in 1971, Marchand and others reported their syntheses of five phases of zinc nitride–fluoride compounds obtained by combining Zn_3N_2 and ZnF_2 in nickel crucibles (Nicklow *et al.,* 2002.). The five phases were the following: α-Zn_2NF, β-Zn_2NF, β-Zn_2NF, α-$Zn_9N_4F_6$ and $Zn_7N_4F_2$. More recently, Wüstefeld *et al.* (1998) have reported their study of the preparation and structural characterization of titanium nitride-fluoride. A powder sample of titanium was prepared by ammonolysis of activated $(NH_4)_2TiF_6$, and characterized by Rietveld analysis. The compound was found to be isostructural with the anatase form of TiO_2.

More relevant to the research work described in Chapter 3 of this thesis is the work done by Seibel, Woodward, Wagner *et al* . (2009). Three basic research questions were posed in their paper: “Can phase pure TiNF be prepared? And if so what are its properties? Which reactions lead to the formation of TiNF?“ The paper goes on to suggest that if TiNF cannot be prepared then, simultaneous substitution of nitrogen and fluorine into TiO_2 could lead to interesting photocatalytic properties. However, there are many questions that come along with this idea. The first question is “what is the

relationship between composition, color and photocatalytic properties?" and the second is "and how can the composition be controlled?"

Synthesis done by Seibel *et al.* (2009) led to the formation of TiO_2 doped with both nitrogen and fluorine. By carrying out pyroammonolysis of $(NH_4)_2TiF_6$ under fortuitous presence of oxygen through H_2O traces, they obtained a green phase type material (denoted as sample A). Exposure of this product to humidity at elevated temperatures leads to a yellow phase material denoted as sample B. Another green phase (sample D) was prepared by using a different starting material ($TiOF_2$). It was prepared by heating $TiOF_2$ in flowing NH_3 for 96 hours at 370 °C in a silica glass reactor. Pictures of the samples described above are shown in **Figure 2.7** below:

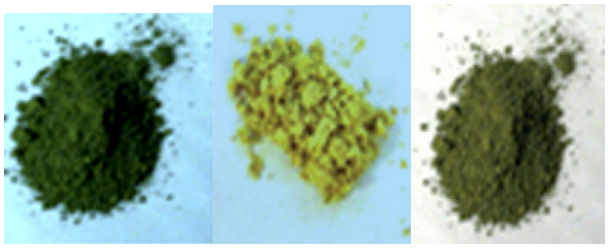

Sample A Sample B Sample D

Figure 2.7 TiO_2 doped with nitrogen and fluorine (Seibel *et al*. 2009).

Elemental analysis was done using an Exeter Analytical CE 440 Elemental Analyzer, in a set up for combustion analysis of nitrides. A summary of elemental analysis on sample A and B is shown in **Table 2.2.**

Table 2.2 Nitrogen Content in the Green A and Yellow B Samples (Siebel *et al*., 2009.)

Sample	N (g/kg)	Ti^{3+} (mmol/g)	Ti^{3+}/Ti in $TiO_{2-\delta}$	Composition
Green A	8.5(2)	0.133(21)	0.010(1)	$TiN_{0.05}O_{1.89}F_{0.06}$
Yellow B	6.2(3)	0.000	—	$TiN_{0.04}O_{1.92}F_{0.04}$

In order to evaluate the spectral response, a UV-visible diffuse reflectance spectrometer was used to measure absorbance of the three phases (sample A,B and D) and the response was compared to that of an intrinsic semiconductor, in this case CdS as shown in **Figure 2.8.**

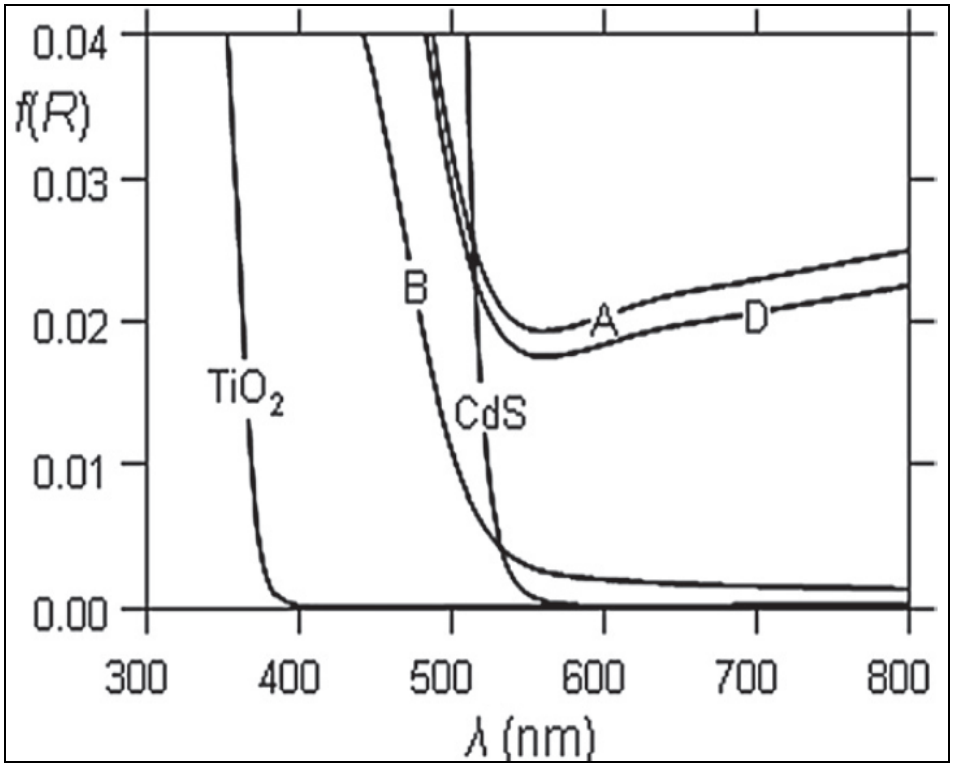

Figure 2.8 Spectral responses of TiO_2, CdS, and the variants of TiO_2 (Sample A, B, C, D) (Seibel *et al*., 2009).

According to this research, it was shown that the green and the yellow phases have similar band-gap energies (2.3 - 2.4 eV). These values represent a decrease by 0.7 -

0.8 eV with respect to pure TiO_2. Indeed a semiconductor with a band gap of this size is supposed to be yellow. Therefore, sample B (yellow phase) was the only material possessing the anticipated optical response! However, when the green phase $TiN_{0.05}O_{1.89}F_{0.06}$ was treated in wet air at 600 °C it became brilliant yellow $TiN_{0.04}O_{1.92}F_{0.04}$ mainly because of hydrolysis of excess F^- and oxidation of $Ti^{3+}$to Ti^{4+}. The explanation given is that the yellow and the green colors appear under increasing dopant contents in a homogeneity range adjacent to titanium dioxide, in which the green color is linked with the formation of about 1% of Ti^{3+} at the Ti site. This argument is further supported by the observation that, by heating the yellow phase at relatively high temperatures, it becomes a white product because of further hydrolysis into a white product. The color change is associated with further hydrolysis of F^- and N^{3-}.

Having done elemental analysis, and knowing the composition of the green and the yellow phases, additional analysis was performed to check how the dopants would affect the unit-cell parameters and the bond distances of the two phases. This was achieved using neutron powder diffraction (NPD). The unit cell parameters and bond distances for both phases, green and yellow, were compared with the corresponding values of TiO_2 as shown in **Table 2.3**.

Table 2.3 Neutron Diffraction Data of the Nitrogen and Fluorine Doped TiO_2 (Seibel et al., 2009)

Sample	Site coordinates	*a*, *c* (Å)	*V* (Å³)	Ti–O (Å)
A (green) $TiN_{0.05}O_{1.89}F_{0.06}$	4a (cation) 0 ¾ ⅛	3.7970(0)	136.959(4)	1.9850(5) × 2
	8e (anion) 0 ¼ 0.0840(1)	9.4994(1)		1.9381(1) × 4
B (yellow) $TiN_{0.04}O_{1.92}F_{0.04}$	4a (cation) 0 ¾ ⅛	3.7887(2)	136.570(19)	1.9795(9) × 2
	8e (anion) 0 ¼ 0.0831(1)	9.5244(5)		1.9359(2) × 4
Anatase (white) TiO_2	4a (cation) 0 ¾ ⅛	3.784(1)	136.25	1.9800(3) × 2
	8e (anion) 0 ¼ 0.0831(2)	9.514(1)		1.9336(6) × 4

The results show the expected decrease in bond distances and unit-cell volume upon progressing from sample A (the green phase) containing reduced titanium, to the sample B where titanium is fully oxidized to Ti^{4+}.

Chapter 3

Statement of the Problem and General Approach

3.1 The Research Question

Can a true TiNF or $TiN_xO_{2-X}F_X$ compound (for x > 0.1) compound be synthesized via decomposition of a suitable titanium complex precursor, or perhaps a simpler method?

3.2 Motivation of the Research

As described in the introduction a potentially intriguing nitride fluoride is TiNF. The corresponding oxide, TiO_2, has a number of important properties. Its band gap (E_g ≈3.1 eV) and refractive index (n > 2.5) make it an ideal white pigment. In particular the introduction of nitrogen is known to decrease the band gap. This type of band gap tailoring is potentially attractive because a reduction of the band gap could be exploited to prepare new yellow, orange or red pigments that could replace highly toxic compounds that are traditionally used for these hues (CdS, $PbCrO_4$, HgS, etc.). (Seibel *et al.*, 2009).

Most of the work done in the syntheses of nitride-fluoride materials has focused on the use of ammonolysis. Less investigated is thermal decomposition of coordination complex precursors as e.g. described earlier for $(NH_4)_2TiF_6$ in the attempted synthesis of TiNF. Thermal decomposition of metal complex precursors has experienced a surge in interest in the areas of mixed metal oxides (Hamid *et al*., 2006), for example, in the

synthesis of magnetically active materials but it has received relatively little attention for the synthesis of mixed anion metal compounds. Investigating this alternative route for the synthesis of nitride-fluorides might thus yield significant new information towards the synthesis of metal nitride fluorides.

3.3 Potential Molecular Precursors for the Synthesis of TiNF Materials

There are a number of complexes which contain titanium nitrogen and fluorine within one molecule and these could serve as molecular precursors in the synthesis of a phase containing Ti, N, and F. An ideal precursor should not contain oxygen atoms as the high affinity of Ti^{4+} towards oxygen would probably lead to preferred retention of oxygen rather than of the desired N and F ions. A typical example of a coordination complex that fulfills these requirements would for example be: the various forms of bis(dimethylmidofluoro) titanium, $[F_2(Me_2N)_2Ti]_n$: hexakis (μ_2-dimethylamido)-hexakis (μ_2-fluoro)-hexakis(dimethylamino)-hexafluoro-hexa-titanium,tetrakis(μ_2-fluoro)-tetrakis(μ_2-dimethylamido)-tetrafluorotetrakis (dimethylamido)-tetra-titanium [(μ_2-Me_2N)μ_2-$F(Me_2N)FTi]_4$. These compounds have a high content for the desired metal in the desired oxidation state of Ti^{4+}as well as the required N and F content. Even more important than the pure composition, is however the structural makeup of the complexes and the ligands. In the above listed complexes the Ti-N and Ti-F bonds are preformed. Some of both the fluorine as well as the nitrogen atoms have even already established bridges between neighboring titanium ions, which constitute the first step of the condensation process towards the infinite TiNF lattice. Another important aspect of the precursor is the structure of the organic ligands. On the one hand they should be

sterically bulky enough to shield the complex from humidity to avoid quick hydrolization. On the other hand the organic groups should allow for a kinetically accessible decomposition pathway that leads to volatile side products that can be carried away in a gas stream upon decomposition of the complex. By using such metal complexes to synthesize TiNF (or other nitride fluorides), it is hoped that very high purity products can be obtained which might, in turn, exhibit better physical and electrical properties, with a good potential for technological applications.

3.4 Coordination Compounds

The study of metal complexes falls under the field of coordination chemistry, and this area can be classified into more subfields depending on the nature of the ligands involved in coordination. Broadly speaking there are classical coordination complexes (Werner complexes), bioinorganic complexes, clusters and organometallic compounds. Ligands in classical coordination compounds bind to metals almost exclusively via "their lone pairs" of electrons residing on the main group atoms of the ligands. Typical ligands are H_2O, NH_3, halogenides, cyanide and similar ligands. Examples are e.g. $[Co(EDTA)]^-$], $[Co(NH_3)_6]Cl_3$ & $K_3[Fe(C_2O_4)_3]$. Organometallic compounds are characterized by having at least one covalent metal-carbon bond and exhibit usually a low oxidation state of the metal. In organometallic compounds ligands are organic groups such as alkenes, alkynes, alkyls as well as "organic-like" ligands such as phosphines, hydride, and carbon dioxide, as e.g. in $(C_5H_5)Fe(CO_2)_2CH_3$. In bioinorganic compounds, ligands are those provided by nature, especially including the side chains of amino acids and many co-

factors such as porphyrins. In cluster compounds ligands are all of the above but in addition there are also metal-metal bonds found. A good example is $Ru_3(CO)_{12}$.

In order to avoid a common misconception, it should be again clarified that organometallic compounds are organic compounds containing metal-carbon bonds, thus compounds where metals are bonded to organic moieties through heteroatoms such as oxygen, nitrogen and sulfur are not organometallic compounds. They should instead be classified under one of the other classes of coordination compounds. Nevertheless all these compounds are potential molecular precursors in the synthesis of pure inorganic materials. A well known example is the use of metal alkoxides which have gained a wide industrial application in the preparation of inorganic oxides and particularly silicon dioxide (Nathan *et al*., 2006.). Metal alkoxides can be considered as derivatives of alcohols in which hydroxyl hydrogen is replaced by a metal. Metal alkoxides are frequently associated by intermolecular forces into tight complexes. Double metal alkoxides are complexes of metal alkoxides containing two different metal atoms which are connected by a bridging oxygen atom of the alkoxides (called a μ-O bridge). These double metal alkoxides would be desirable where a mixed metal oxide is to be synthesized. Excessive condensation into even larger entities should however be avoided as formation, isolation and purification of one single precursor then becomes very difficult.

3.5 Coordination Compounds as Molecular Precursors for the Synthesis of TiNF

Organometallic chemical vapor deposition (OMCVD) is the use of high purity volatile liquid or solid organometallic compounds to obtain a solid thin film upon decomposition. The term is often used not only for organometallic compounds *per se*, but for all molecular charge neutral metal complexes with a high vapor pressure. Several reaction types have been used in semiconductor device fabrication, including thermal decomposition, oxidation, reduction, hydrolysis, ammonolysis, polymerization, and processes such as sputtering which depend on physical mass transport (Akiyo et. al 1986). Organometallic compounds that decompose into inorganic materials during vapor deposition have the advantage that they often have quite high vapor pressures when compared to other compounds used in traditional Chemical Vapor decomposition (CVD). As molecular compounds they can also be often easily purified by methods such as chromatography, crystallization, distillation or sublimation and are thus often available in the high purity necessary for e.g. the fabrication of integrated circuits.

Many researchers have worked on molecular precursors that would help to deliver a final phase of interest, e.g. a certain metal oxide, metal, or mixture of the two, and with certain morphological features such as crystallite shape or grain size. For example, several researchers showed that they were able to synthesize heterometallic molybdenum complexes that could be used as single-source precursors in fabrication of coatings and for the preparation of mesoporous materials (Nathan *et al*., 2006 & Thurtson *et al*., 2002). Elsewhere, scientists continue to develop heterobimetallic

precursors in order to synthesize nanostructures and nanoparticles. Because we are going to be concerned with solid state titanium compounds in the later chapters, it is very crucial to look at some of the substances that would act as molecular precursors in the synthesis of titanium compounds. As we proceed a special focus will be on metal complexes containing Ti, N, and F which would have potential use in the synthesis of ceramic nitride materials.

3.6 Sol-Gel Technique.

The sol-gel technique has been a popular method for preparing specialty metal oxides glasses and ceramics by hydrolyzing a chemical precursor or mixture of chemical precursors that pass sequentially through a solution state and a gel state before being dehydrated to a glass or a ceramic. Sol-gel technology has expanded dramatically since 1980 with development of a variety of techniques to prepare fibers, microspheres, thin films, fine powders and monoliths. Applications for sol-gel technology include protective coatings, catalysts, piezoelectric devices, wave guides, lenses, high strength ceramics, superconductors, insulating materials and nuclear waste encapsulation.

Preparation of metal oxides by the sol-gel route proceeds through three basic steps: The first is partial hydrolysis of metal alkoxides to form reactive monomers; the second is polycondensation of these monomers to form colloid-like oligomers (sol formation); and thirdly, additional hydrolysis to promote polymerization and cross-linking leading to a 3-dimensional matrix (gel formation) (Stephen *et al*., 1997). Although

presented sequentially, these reactions occur simultaneously after the initial processing stage. The technique is summarized below:

i) **MONOMER FORMATION (PARTIAL HYDROLYSIS)**

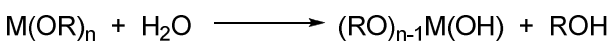

ii) **SOL FORMATION (POLYCONDENSATION**)

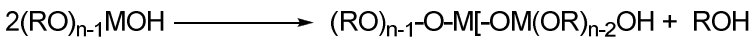

iii) **GELATION (CROSS-LINKING)**

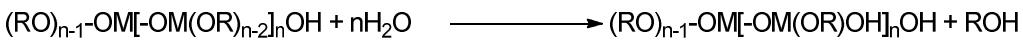

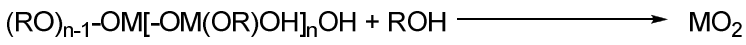

As polymerization and cross-linking progress, the viscosity of the sol gradually increases until the sol transition point is reached. At this point the viscosity abruptly increases and gelation occurs. Further increases in cross linking are promoted by drying and other dehydration methods. Maximum density can be achieved by densification, a process in which the isolated gel is heated above its glass transition temperature. The densification rate and transition (sintering) temperature are influenced primarily by the morphology and composition of the gel. Researchers who use sol-gel techniques often take into account several synthesizing factors such as pH values, ion ratios and dispersing agents. For example, in the research paper published by Limin *et al.*(2006) on

the synthesis of M-type Ba hexaaferrites, it was reported that $BaF_{12}O_{19}$ was optimally synthesized with a pH value of 7 and a citric acid/metal ratio of three.

Both sol-gel synthesis and the thermal decomposition techniques require the presence of a coordination complex as a molecular precursor in order to obtain extended solid molecules.

3.7 Hypothesis

As stated in the introduction a compound such as $[F_2(Me_2N)_2Ti]_n$ has many of the requirements needed for a precursor for the formation of TiNF. It has a high content of the desired metal in the oxidation state of Ti^{4+}as well as a high N and F content. Ti-N and Ti-F bonds are preformed and some of the fluorine as well as the nitrogen atoms have already established bridges between neighboring titanium ions, which constitute the first step of the condensation process towards the infinite TiNF lattice. On the other hand the organic groups should allow for a kinetically accessible decomposition pathway that leads to volatile side products that can be carried away in a gas stream upon decomposition of the complex. For a compound such as $[F_2(Me_2N)_2Ti]_n$ such a decomposition pathway with a low activation barrier is not given as nitrogen-methyl bonds would need to be broken in at least one step, a process that would involve an α-elimination which is commonly associated with a high activation barrier, and thus high decomposition temperatures.

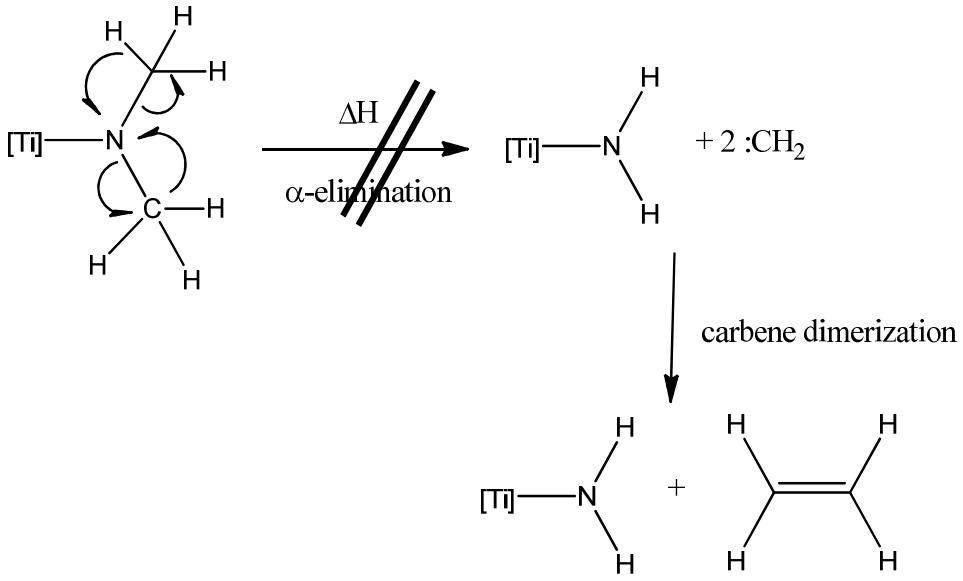

This problem can be avoided by substituting the methyl groups on the amide by alkyl groups that have a β-hydrogen, thus opening the possibility of β-elimination, which commonly has a much lower activation barrier. Possible amides that possess hydrogen in β-position would e.g. be ethyl or isopropyl rather than methyl. β-elimination would be expected to proceed as shown in the scheme below:

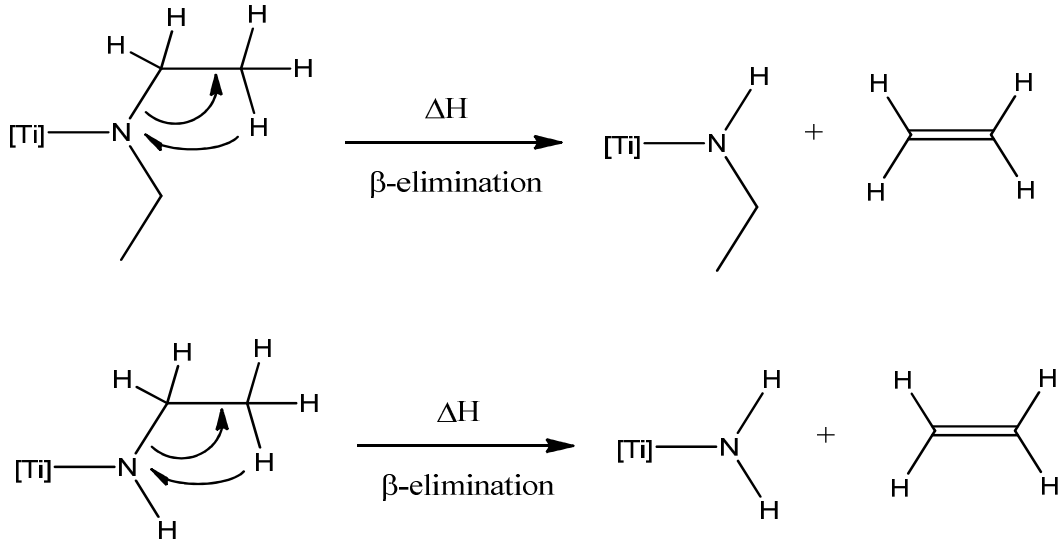

The formed ethylene would be released as a gas and the remaining in situ formed complex would be of the composition $[TiF_2(NH_2)_2]_4$. Upon further heating, $[TiF_2(NH_2)_2]_4$ would decompose into NH_4F and TiNF (if it exists!). The released NH_4F would finally sublime off as NH_3 and HF gases. The total reaction would thus read as follows:

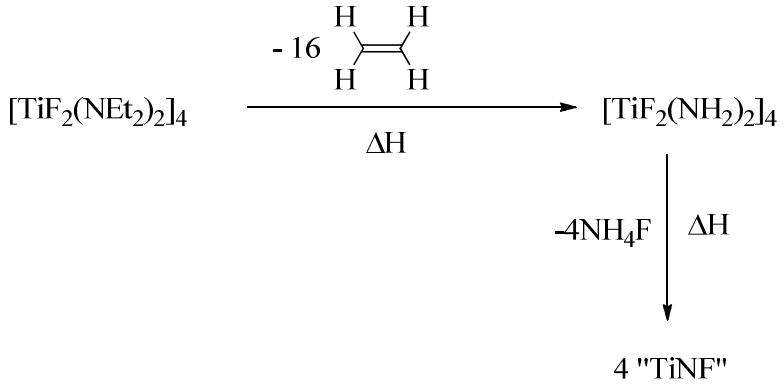

According to this hypothesis, about 448.8 g of ethylene gas should be released for every one mole (920.64 g) of bis(diethylamido fluoro) titanium decomposed. Thus in theory, we expect to observe a 48.75% mass loss during the first step. During the second decomposition step, we expect to observe a mass loss of 148.148 g for every mole of $[TiF_2(NH_2)_2]_4$. Thus a total mass of about 596.948 g per mole of $[TiF_2(NEt_2)_2]_4$ should be theoretically observed for the above mentioned hypothesis. Therefore at the end of decomposition a total of 64.84% drop in mass is expected. The expected end product should therefore have 35.16% of the original mass.

As the reaction involves multiple steps two β-eliminations per ethyl group and loss of several molecules of ammonium fluoride, it could be expected that some of these steps occur in parallel to each other, i.e. some of the NH_4F elimination might

precede β-eliminations of ethylene, thus there might be no two step mechanism but only one decomposition step, or more than two steps.

Once formed the stability of the compound towards traces of water or oxygen might impact its isolation, and even if pure TiNF is formed it might be isolated as a partially oxygenated species, thus “Ti-N-O-F”.

3.8 Objectives of the Research.

- Identify and synthesize suitable titanium complex precursors for thermal synthesis of “Ti-N-O-F”
- Investigate the thermal decomposition of the synthesized precursors
- Carry out structural characterization of the resulting “Ti-N-O-F” compound by a variety of techniques including powder XRD, XRF, SEM, XPS etc

Chapter 4

Synthetic Methods

4.1 Air-Sensitive Chemistry

Chemists use a variety of techniques in order to carry out reactions in inert atmosphere that are free of reactive gases such as oxygen, water vapor, carbon dioxide and many others. Effectiveness of these techniques can vary in the way they prevent access of air, ease in setting up, and their convenience in use. The two main techniques used are glove bags and glove boxes, which maintain all reagents and equipment under an inert atmosphere within one large enclosure, and Schlenk line techniques, which utilize flasks and other glassware that are kept under an inert atmosphere via individual connections to vacuum pumps and inert gas lines. The following chapter will discuss some of these techniques that are relevant in the synthesis of organometallic complexes and other air and humidity sensitive compounds.

4.2 Schlenk Line Techniques

The main technique used for the reactions carried out in the current project was the Schlenk line approach. The success of the research that involves air and humidity sensitive materials relies heavily on the proper setup and handling of the Schlenk line. A basic Schlenk line is composed of a vacuum pump able to achieve a vacuum of at least 10^{-3} mbar (usually an oil pump), a gas cylinder with the inert gas (usually ultra high purity nitrogen or argon), and a vacuum manifold with connected hoses that allow to

connect individual flasks and other chemical glassware to be attached to either the vacuum or the inert gas lines. Schlenk glassware is equipped with inert gas adapters, and by repeated switching between vacuum and inert gas the interior of the flasks can be filled entirely will inert gas. Afterwards the flasks are kept under a slight positive pressure of inert gas to maintain the unreactive atmosphere. In order to protect the pump from solvents and vapors that might get trapped in the oil and reduce the lifetime of the pump, the Schlenk line is usually equipped with one or more traps that are cooled from the outside with liquid nitrogen or dry ice. Often the Schlenk line is also equipped with a vacuum gauge.

4.2.1 Starting up a Schlenk line

The following paragraphs describe the operation of a Schlenk line; a schematic of which is shown in **Figure 4.1.** There are many small variations in the set up and operation of such a line between different laboratories, and the guidelines given below describe the best practices used in the labs at the YSU Department of Chemistry. Other laboratories might follow slightly different procedures.

In order to have a properly set up Schlenk line, as shown in **Figure 4.1**, one first needs to check that the inert gas cylinder is sufficiently filled for the experiment(s) planned, and that all the glassware and equipment for the day is available and usable. In the next step one should check that all connectors and joints in the Schlenk line are well sealed. If necessary they have to be adjusted and/or regreased. Ordinary high vacuum grease should not be used when working with Schlenk lines as this grease is usually

soluble in many organic solvents. Dissolution of the grease might not only lead to a leaking Schlenk line, but the grease will also contaminate the reaction mixtures, and joints tend to lock up and become unmovable. Preferable are thus fluorinated greases such as Apiezon M which are not soluble in organic solvents or water.

As a habit, before starting a Schlenk line, one needs to make sure that the Dewar traps are filled with liquid nitrogen. If the vacuum traps have solvent in them, empty the solvent in the waste container, grease them properly and reconnect them back to the vacuum line, fill the traps with nitrogen and wrap the top with a cloth towel, wait a moment and then start the pump with all valves properly closed. It is important to not let the dewars stand with liquid nitrogen in them over night to avoid accumulation of liquid oxygen in the traps. If liquid oxygen forms inside the traps in the presence of organic compounds, it might lead to an explosion. For this reason the traps should also not be left in the liquid nitrogen for more than a few minutes when the vacuum pump is not switched on. Once the traps are set and the pump is on, it is advisable to purge the gas line gently for five to ten minutes but also taking care that the pressure on the nitrogen tank does not go beyond 5 psi.

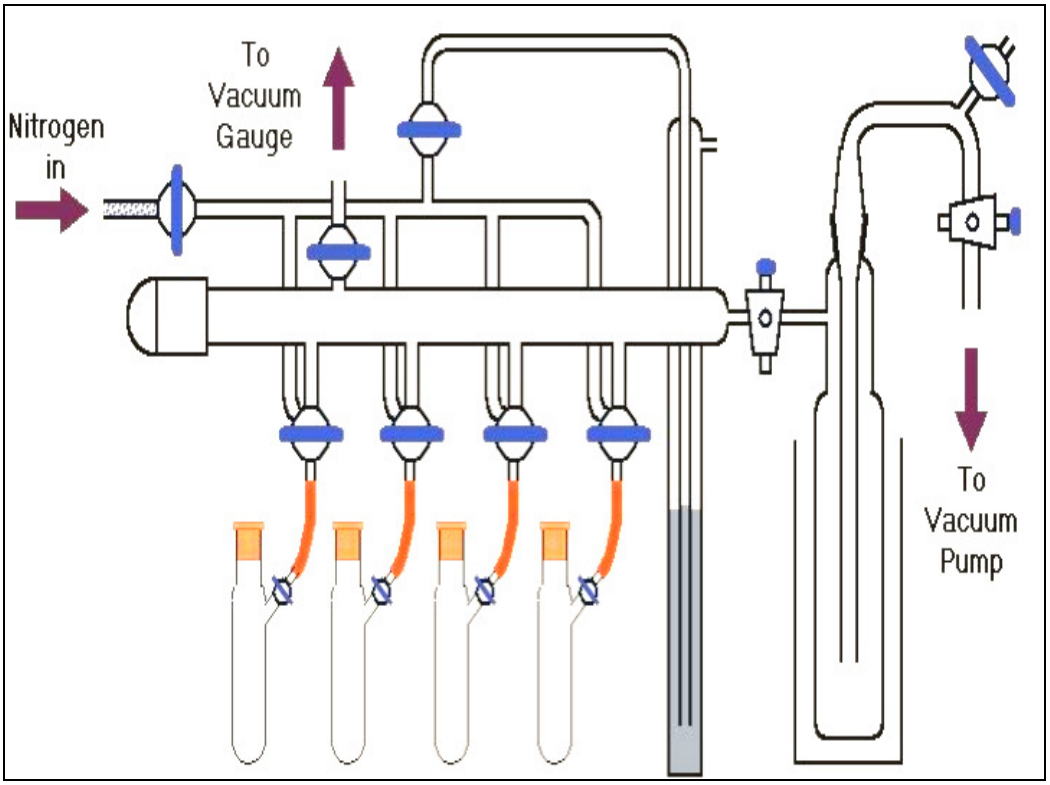

Figure 4.1 A schematic of a Schlenk line set up
http://www.chem.mun.ca/homes/fmkhome/Schlenks.htm (accessed August 2009)

4.2.2 Schlenk Vessels

Schlenk vessels such as those shown in **Figure 4.2** and **Figure 4.3** have an outlet that can be attached to a vacuum line via flexible hoses and an inlet that can be stoppered with a glass stopper. Examples of Schlenk vessels include Schlenk flasks, Schlenk tubes, Schlenk filters and other glassware as shown below. After connecting a vessel to the Schlenk line it is first evacuated for several minutes and then filled with the inert gas (via switching between the two at the manifold). The procedure is repeated at least twice to assure complete removal of all reactive gases from the inside of the vessel. In the case of reactions very sensitive to humidity, the glassware should be heated with a heat gun while under vacuum to assure removal of all adsorbed traces of water from the surface of the glass. If a vacuum gauge is available, complete removal of adsorbed water can be monitored via the pressure reading which should be around 1 to 2×10^{-3} mbar. Once completely under inert gas the vessel can be charged with the reagents. Solid reagents should be added first, followed by an additional careful evacuation of the vessel. Light solids should - if they are not reactive themselves - be added with all valves closed to avoid the sample from being blown away. After all solids are added a positive pressure of an inert atmosphere should be maintained at all times, especially when transferring reagents into the Schlenk vessel. Liquids are best transferred via syringes and needles; see below. In each step it is important to consider if there is any way air could get into the system, and if the possibility exists, then the container should to be evacuated and filled with inert gas again three times immediately. (This should be done carefully if any of the reagents or solvents is low

boiling to avoid loss of a reagent due to excessive evaporation or contamination of the hoses and manifold with reagent or solvent).

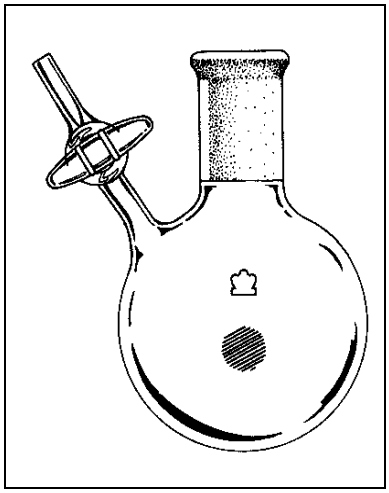

Figure 4.2 Schlenk round-bottom flask

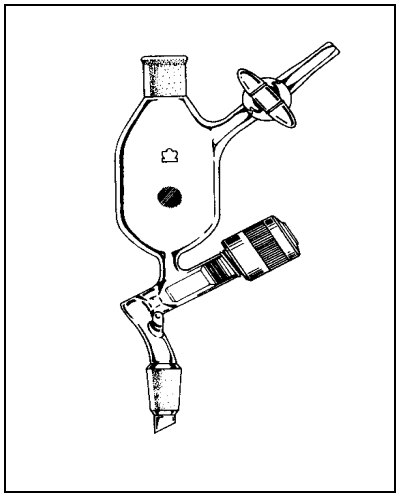

Figure 4.3 Schlenk filter

http://depts.washington.edu/chemcrs/bulkdisk/chem317A (accessed August, 2008)

4.2.3 Needle-puncture stoppers and Hypodermic needles

A convenient method for transferring a liquid to or from a vessel without introducing air is by means of a hypodermic needle inserted through a special rubber septum, such as that used for serum bottles. A typical needle puncture septum is hollow to within a short distance of the top. The sleeve like extension folds down over the neck of the glass tubing and holds the stopper (**Figure 4.4**) securely in position during handling. The sleeve should be additionally secured with some wire wrapped tightly around. The diaphragm can be easily punctured with a syringe needle and seals automatically after the needle is withdrawn (when punctured too often septa start to leak and need to be replaced).

Figure 4.4 Rubber-stoppers
http://punjabindustryexport.com/prods/rubber/
(accessed August 2008)

4.2.4 Transfer of Air Sensitive Reagents

A common technique for transferring liquid reagents from one container to another, without introducing air into the liquid reagents, is known as cannula transfer. A cannula is essentially a two-ended needle with both ends sharpened. When transferring a solution from one flask to another one the following should be done:

1. The flask from which the solution is to be transferred from should be at a slightly higher elevation than the receiving flask.

2. Make sure the flask from which a solution will be transferred from (left flask in **Figure 4.5**) is pressurized. Insert the transfer needle into the top of the flask just atop of the solution and let the needle flush for a few minutes.

3. Insert the other end of the transfer needle into the pressurized receiving flask.

4. Insert an exit needle into the septum of the receiving flask to allow for the pressure to escape. Then close the valve of the receiving container.

5. Lower the cannula into the liquid to be transferred. The liquid should start to transfer into the receiving flask.

6. When complete, open the nitrogen valve at the receiving flask, then remove the exit needle

7. Remove the cannula carefully by pointing the ends away from any person.

8. Immediately after clean all cannulas with an appropriate solvent to avoid clogging with precipitates that result from formation of decomposition products and precipitates.

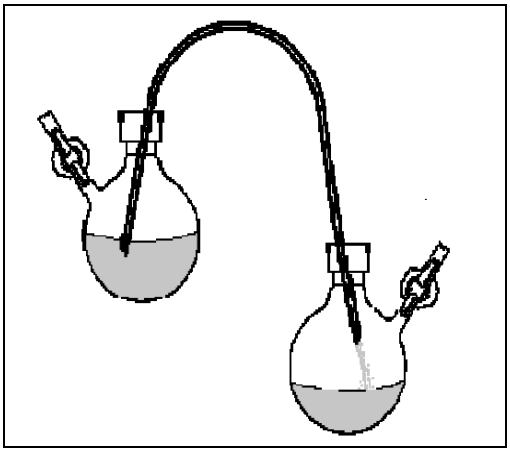

Figure 4.5 Cannula transfer
http://www.sas.org/E-Bulletin/2003-05-16/labNotes/body.html
(Accessed August 2008)

4.2.5 Refluxing

Heating to reflux of a solvent (often abbreviated as refluxing) is required when it is necessary to maintain a solution at its boiling point for an extended period of time while carrying out a reaction. The operation is usually carried out using a ground-glass

flask and a condenser. Heating is usually accomplished with a heating mantle or - if a more accurate temperature control is needed - with a hot bath (e.g. a water bath for lower temperatures, an oil bath for temperatures above 70 °C). When using a hot bath the bath temperature should be monitored via a thermometer. When access of moisture to the refluxing liquid is to be prevented the process should be done under Schlenk-line conditions. As heating of the solvent in an enclosed environment will create pressure, one of the inert gas connectors has to be kept open to the manifold during heating, maintaining of temperature and cooling. This connector should be above the condenser (as otherwise the boiling solvent would be condensing into hoses and manifold).

4.2.6 Distillation

Heating mantles are very convenient for supplying heat to the distillation flask, but in the later stages of distillation, they can cause overheating of the flask walls above the liquid level and thereby decompose any thermally unstable compounds of the liquid mixture. Therefore, whenever thermally unstable compounds are subjected to distillation, a liquid such as water or oil should be used to supply heat to the distilling solution. If the compound being distilled is pure or if it is being distilled essentially from non-volatile impurities, the operation can be used as a determination of the boiling point. It is important that the bulb of the thermometer lie entirely below the level of the side of the side arm of the distillation head and that, at the time of reading, liquid be condensing on the upper part of the thermometer and flowing back down over the bulb.

4.2.7 Stirring

Magnetic stirring makes it possible to stir solutions in a closed system such as a Schlenk vessel. In magnetic stirring a small glass or plastic-encased bar magnet is placed in the bottom of the reaction vessel and is caused to spin by rotation of a larger magnet beneath the reaction vessel with a variable speed motor. Again, magnetic stirring is ideal for stirring a mixture in that the space directly over the reaction vessel is completely unobstructed. Therefore it is the method of choice when working with air sensitive compounds. Magnetic stirring requires the use of not magnetic materials for hot or cold bath containers, e.g. glass or aluminum jars rather than steel pans.

4.3 Solvent purification

4.3.1 Degassing

Removal of air and moisture was carried out to avoid hydrolysis of the titanium complexes under investigation. The following are some of the common methods employed in a typical inorganic or organic laboratory setting.

4.3.2 Freeze-Pump-Thaw

A solvent is put in a sealed Schlenk flask which is then immersed in liquid nitrogen. When the solvent is completely frozen, the flask is opened to a high vacuum then pumped 2-3 minutes, with the flask still immersed in liquid nitrogen. Then the solvent is allowed to melt after closing the Schlenk flask. After the liquid is completely melted the tube is immersed in liquid nitrogen again and the process is repeated usually three times until no gas bubbles are observed any more during melting. After the last cycle, the Schlenk flask is filled with inert gas. Solvents degassed by the Freeze-Pump-

Thaw technique can be stocked for several weeks if kept properly sealed in a Schlenk flask. The Freeze-Pump-Thaw technique is especially useful when degassing low boiling or small amounts of liquids (e.g., deuterated solvents). It is not convenient for larger amounts of solvents.

4.3.3 Purging

This is a technique commonly used when a large amount of solvents need to be degassed. As the name implies, purging involves bubbling of an inert gas through the solvent for about ten to thirty minutes. While purging, care should be taken to prevent excessive solvent evaporation. A proper Schlenk flask or tube is connected to an inert gas line and then filled about two thirds with the solvent and equipped with a rubber septum. A needle hooked up to the inert gas line is pierced through the septum and immersed deep into the liquid, and a second short needle is used for relieving pressure. When finished, first the long needle is raised above the solvent level, then the inert gas connector is opened and finally the needles are removed from the pressurized vessel. If the solvent is intended to be stored the rubber septum should be replaced by a glass stopper.

4.3.4 Drying Agents

Again, it is necessary to purify a solvent before use to avoid a deleterious side reaction caused by an impurity. Usually water is the most significant impurity in a solvent and therefore most purification schemes are essentially schemes for the removal of water. In the following table (**Table 4.1**) some important drying agents are shown with remarks concerning their use.

Table 4.1 Common Drying Agents

Drying agent	Remarks
Alkali metals (sodium, potassium, sodium, potassium alloys)	-Never used to dry acidic solvents or solvents having oxidizing power. -Chlorinated hydrocarbons must never be treated with alkali metals. -Used together with benzophenone. This forms a blue radical anion in the absence of protic species and oxygen.
Lithium aluminum hydride	-Removes protic species. -Oxidizing solvents must be avoided. -Should never be heated with a solvent over 100 °C - Should not be used on solvents highly contaminated with protic species or oxidizing agents
Calcium Hydride	-Insoluble in all solvents with which it does not react with. -Protic impurities are very efficiently removed by refluxing a solvent with the powdered reagent good for chlorinated solvents (methylene chloride & chloroform).
Phosphorous Pentoxide	-Reacts vigorously with water to form syrupy phosphoric acid principally used to dry hydrocarbons and their halogenated derivatives
Molecular sieves	-Molecular sieves are used to absorb water and moisture from the solvent. It is important to put dry molecular sieves in a vessel that is used to purge nitrogen through a solvent.

4.4 Maintenance of Low Temperature

4.4.1 Simple Cold Baths

When it is necessary to carry out a reaction at about 3°C, simple ice baths can be used. In such cases, several methods, each relying on the occasional attention of the experimenter, can be used.

In the interval between room temperature and about 12°C, flowing tap water is usually adequate. From this point to 0°C, a stirred water bath to which crushed ice is occasionally added can be used. For the same temperature interval, a mixture of ice and aqueous hydrochloric acid can be used. The temperature can be maintained by siphoning off some of the dilute HCl solution and adding fresh ice and 12 M HCl. Temperatures between about -10°C and -78°C are conveniently maintained by the occasional addition of dry ice chunks to a stirred bath of ethyl alcohol or acetone. Temperatures below -78°C usually require cooling of a liquid with liquid nitrogen with constant-temperature slush baths.

4.4.2 Constant Temperature Cold Baths

Except for the ice-water bath, slush baths are prepared in a hood by slowly adding liquid nitrogen to the stirred liquids in dewars until the consistency of a thick milk shake is achieved. Care must be taken not to add too much liquid nitrogen, or else a difficult-to-melt solid mass may form.

The dry ice bath is unique. It is strictly not a slush bath, and it is made by slowly adding crushed dry ice and a liquid, such as 95% percent ethanol, to a Dewar. If the dry

ice is added too rapidly, or if too much liquid is present, the liquid may be thrown out of the Dewar by the violent evolution of CO_2. The final bath should consist of a pile of dry-ice chunks with just enough liquid present to bring the liquid level within 1 or 2 cm of the top of the pile. It is difficult to submerge a reaction vessel in a dry ice bath after the bath has been prepared due to heavy CO_2 evolution when immersing the warm vessel; therefore it is best to place the apparatus in the Dewar before preparing the bath. Other low-freezing liquids such as acetone or isopropanol can be used.

4.5 Glove Bags

One of the simplest methods for providing an inert atmosphere for chemical manipulations is to enclose the entire apparatus in a transparent polyethylene bag that is under a positive pressure of inert gas. The bag is provided with inward pointing gloves that facilitate the handling of objects within the bag. A nitrogen or argon inlet tube is inserted into the narrow opening at the top of the bag and secured with a rubber band. The materials to be handled are introduced through the front flap and the bag is purged of air by a repeated inflating and deflating of the bag. The flap is then loosely folded and clipped and the gas flow is adjusted so as to maintain the bag in a barely inflated state. The operator then inserts his hands in the gloves and carries out the required manipulations. Glove bags provide an adequate environment for modestly sensitive materials. They are not suitable for really oxygen or nitrogen sensitive materials and should never be used with highly reactive materials such as e.g. butyl lithium.

4.6 Glove Box

Reagents too sensitive for a glove bag can instead be handled in a Glove Box. A glove box has two main parts: a large box filled with an inert gas fitted with a window and gloves in which manipulations are carried out; and a lock through which material is moved in and out of the box. The main box is fitted with a manostat that maintains the pressure slightly above the atmospheric pressure by allowing pure inert gas to enter when the pressure rises too high to a certain value. The gas in the box is constantly circulated through a purification 'train' of hot activated copper (to remove oxygen) and molecular sieves (to remove water vapor). Using this method oxygen and water concentrations can be kept in the low ppm range if the glove box is well maintained.

Material to be introduced into the box is placed in the lock while the inner door is clamped shut. The outer door is then closed and the lock is evacuated to a relatively low pressure. The lock is filled again with inert gas from the main box via a valve and the lock is re-evacuated and the process is repeated several times. Finally after the lock is filled again the inner door is opened so that the material in the lock can be transferred into the box. Material to be removed is placed in the lock, the inner door is closed and then the outer door is opened. It is helpful to apply talcum powder to the hands and gloves before working in the box and to wear an auxiliary pair of tight-fitting rubber gloves to keep the main gloves clean for others to use.

4.7 Tube Furnace

Solid state chemists mostly use furnaces to carry out reactions at high but controlled temperatures. There are many types of furnaces, each with their own capabilities and limitations. In our research, tube furnaces were used. A tube furnace is designed to heat a tube that is usually 50 to 100 cm in length and from 25 to 100 mm in diameter. Samples are placed inside the tube in ceramic or metal boats using a long push rod. The tube is surrounded by heating elements which may have a thermocouple. Furnace tubes usually have an end protruding about 10 centimeters from the hot hallow. This end does not get very hot thus an adapter may be connected to the tube at this end. Therefore, it is possible to connect an adapter for nitrogen gas if an inert atmosphere is needed. In a typical set up, (as shown in **Figure 4.6**) gas flows in one end of the tube and carries any evolved gases out at the other. Usually a bubbler is added to allow monitoring of gas flow.

Figure 4.6 Programmable tube furnace

Chapter 5

Characterization Methods

5.1 Single Crystal X-ray Diffraction Analysis

In X-ray diffraction analysis, electrons inside a single crystal sample act as a diffraction grid and interact with an incoming beam of X-rays to produce diffraction patterns. In practice, thousands of these diffraction patterns are collected and used to trace the electron densities in a single crystal sample by using a complex mathematical procedure. In fact, an electron-density contour map obtained from the diffraction patterns tells us the relative electron densities at various locations in a molecule. The densities reach a maximum near the center of each atom, thus making it possible to determine the positions of the nuclei and hence the geometric parameters of the molecule.

The X-ray diffraction technique is the preferred method to determine the crystal structure and thus the molecular structure of our target compounds. In this work, a SMART APEX Bruker X-ray diffractometer is used to obtain X-ray diffraction data, and the actual structure solution and refinement is carried out using the SHELXTL suite of programs. At the end of a structure solution a CIF file is prepared to show the results of the diffraction experiment, and includes information such as such as atom types and positions, and bond lengths and bond angles in a commonly accepted format.

A refinement program such as SHELXTL is used to refine the experimental data/model to come up with a crystal structure that makes chemical sense. Particularly, the number and the lengths of bonds as well as the coordination geometry of an atom in a structure should be critically examined. For example, a nitrogen atom appearing to make four single bonds might not be a nitrogen atom or else it would have to carry a positive charge! Therefore a thorough examination of the CIF file is needed when checking the validity of the proposed crystal structure. Moreover, other statistical indicators such as regression factors and goodness of fit must be within acceptable limits.

5.2 Thermal Gravimetric Analysis (TGA)

Once the crystal structure of a titanium complex precursor is solved, then its thermal decomposition reaction can be investigated using a technique known as Thermogravimetric Analysis (TGA). This instrument has to be connected to a nitrogen or argon tank to have an inert atmosphere in the sample holder before and during its operation.

In practice, a TGA instrument (see **Figure 5.1**) measures the weight loss or gain of a material as a function of temperature. As the precursor complex thermally decomposes in the TGA chamber, it loses weight due to a loss of volatile products that escape as gases. Given that the decomposition happens in an inert atmosphere, we do not expect to see a weight gain. As the analysis proceeds, a careful observation of the temperature ranges over which the thermal decomposition occurs must be made. These

temperature ranges are useful in designing thermal ramps and holds to be used during those critical reaction periods when decomposing larger amounts of materials than can be done in the TGA.

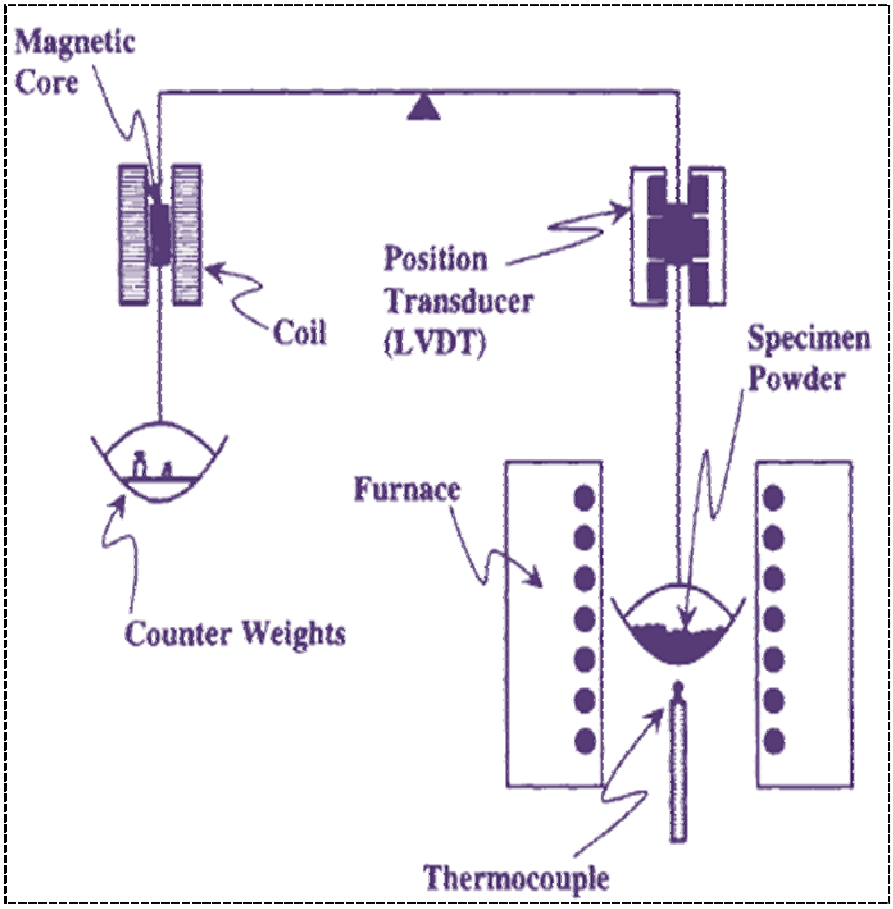

Figure 5.1 A schematic of a TGA instrument
http://physicalchemistryresources.com/Book5_sections/TA_Applications%20Thermogravimetric%20AnalysisHTML_1.htm (accessed August 2008)

5.3 Powder X-Ray Diffraction (PXRD) Analysis

A solid material that is polycrystalline and non-amorphous can be analyzed using X-ray powder diffraction in a manner similar to that of single crystal X-ray analysis, except that instead of obtaining a diffraction pattern with spots, we obtain lines.

Therefore refinements programs with X-ray powder diffraction data are different from those used for single crystal data.

The experiments conducted in this thesis have used the Bragg-Brentano geometry. For this configuration (**Figure 5.2**) it is important that the sample specimen should exhibit a plane or flattened surface. This can be achieved by using a microscope slide to pack the powder well onto the sample holder and leveling it smoothly and evenly.

Once the diffraction pattern/peak pattern is obtained, a database search and match can be done to see which experimental peaks correspond to those peaks already calculated and stored in the database. The main difference to single crystal refinement is that the whole pattern is fitted against the structural model, while in single crystal diffraction the numerical hkl intensities are used. Thus, in a manner similar to that of single crystal analysis, various statistical indicators such as regression factors and the weighted regression factors can be used to check the validity of the proposed powder structure.

Unlike single-crystal X-ray data, powder X-ray data are collected as peaks with each peak measuring a d-spacing that represents a family of all lattice planes having that spacing. In addition, each peak has an intensity which differs from other peaks in the pattern, and overlap with other nearby peaks may occur. In a powder diffraction pattern, the strongest peak is assigned an intensity value of 100% and the other peaks are scaled relative to that value. Variations in measured intensities are strongly related

to the scattering intensity of the components of the crystal structure as well as their arrangement in the lattice.

A diffraction pattern is collected by varying the angle of incidence of the incoming X-Ray beam by θ and the scattering angle by 2θ while measuring the scattering intensity I(2θ) as a function of the latter. In inorganic synthesis, we are mostly concerned with unit-cell parameters, space group, phase identification and at times phase abundance. Also it might be necessary to carry out time and temperature dependent X-ray diffraction. In that case a diffractometer equipped with a hot stage can be used.

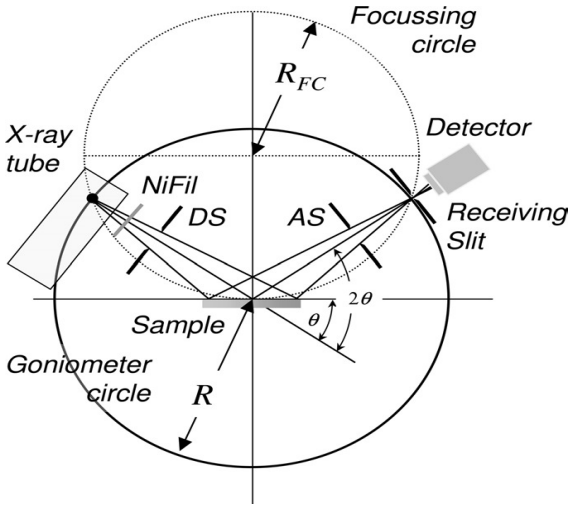

Figure 5.2 Geometic set-up of a powder X-ray diffractometer

http://www.wiley-vch.de/books/sample/3527310525_c01.pdf (Accessed August, 2008)

5.4 Scanning Electron Microscopy

A scanning electron microscope (SEM) is an instrument capable of producing high resolution images of a sample surface at large magnification not achievable with optical microscopy. **Figure 5.3** depicts a typical configuration for imaging in the SEM. Due to the manner in which the image is created, SEM images have a characteristic three-dimensional appearance and are useful for judging the surface structure of the sample. In an SEM, electrons are thermionically emitted from a tungsten or lanthanum hexaboride (LaB_6) cathode and are accelerated towards an anode. Tungsten is used because of its high melting point and low vapor pressure, thereby allowing it to be heated for electron emission. The electron beam, which typically has an energy ranging from a few hundred eV to 100 KeV, is focused by one or two condenser lenses into a beam with a very fine focal spot sized 0.4 nm to 5 nm. The beam passes through pairs of scanning coils or pairs of deflector plates in the electron optical column, typically in the objective lens which deflects the beam horizontally and vertically so that it scans in a raster fashion over a rectangular area of the sample surface. When the primary electron beam interacts with the sample, the electrons lose energy by repeated scattering and absorption within a teardrop-shaped volume of the specimen known as the interaction volume, which extends from less than 100 nm to around 5 µm into the surface. The size of the interaction volume depends on the electrons' landing energy, the atomic number of the specimen and the specimens' density. The energy exchange between the electron beam and the sample results in the emission of electrons and electromagnetic radiation, which can then be detected to produce an image.

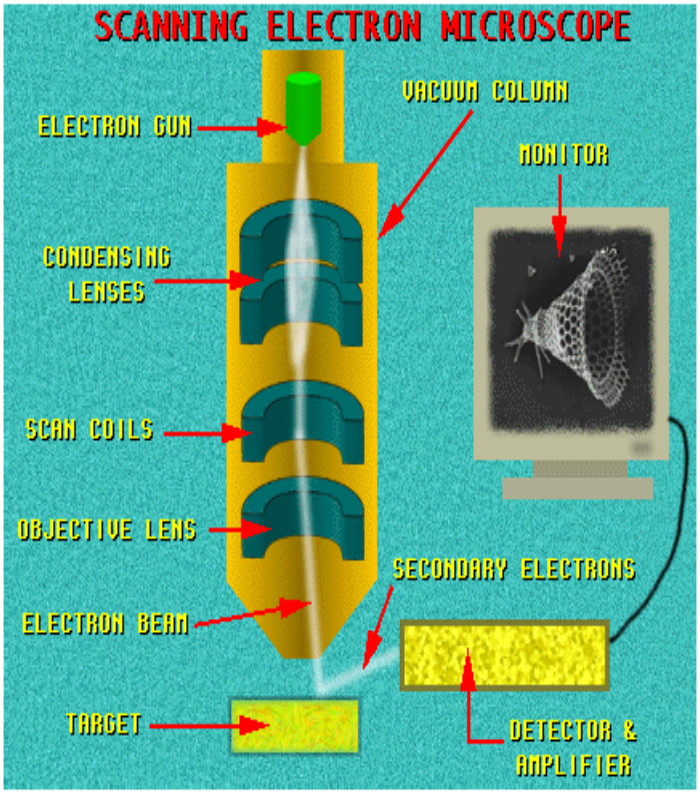

Figure 5.3 SEM imaging
http://materialscience.uoregon.edu/ttsem/sem_mos.gif (accessed April, 2010)

5.5 X-ray Photoelectron Spectroscopy (XPS)

In XPS, an X-ray beam of known energy *hv* is used to displace an electron e^- from a K orbital of energy E_b. The process can be represented as

$$A + hv \rightarrow A^{+}* + e^{-}$$

The kinetic energy of the emitted electrons is recorded. The spectrum thus consists of a plot of the number of emitted electrons, or the power of the electron beam, as a function of the energy of the emitted electrons. The kinetic energy of the emitted electron E_k can then be measured in an electron spectrometer. The binding energy of the electron E_b can then be calculated using the following equation:

$$E_b = hv - E_k - w$$

The symbol w is the work function of the spectrometer, a factor that corrects for the electrostatic environment in which the electron is formed and measured. The binding energy of an electron is characteristic of the atom and orbital that emits the electron.

5.5.1 Instrumentation

Just like any other optical spectroscopic techniques, XPS (see **Figure 5.4**) has four main components: (1) a source, (2) a sample holder, (3) an analyzer which has the same function as a monochromator, and (4) a detector. Other components include a signal processor and a read-out.

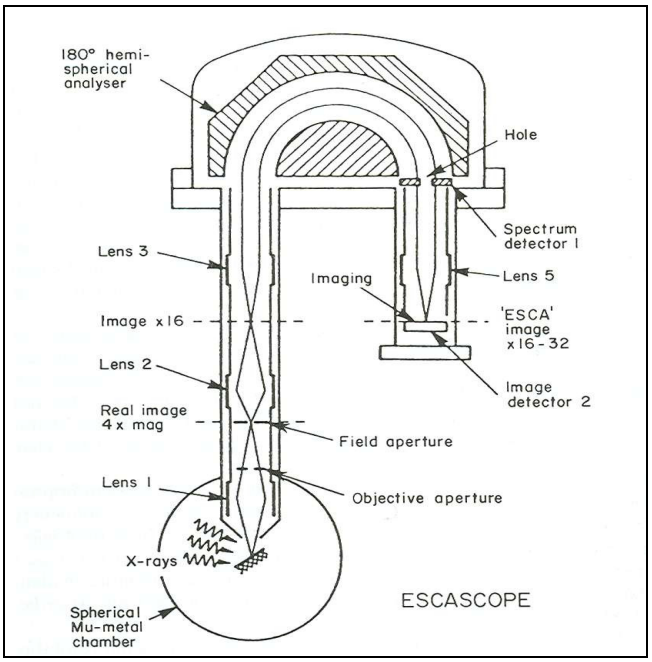

Figure 5.4 XPS schematic
http://www.fys.uio.no/funmat/school/workshops/2005/xps/instrument.pdf
(accessed May, 2010)

5.5.2 XPS Spectra vs Oxidation States

An XPS spectrum can show oxidation states of the elements present in a sample. This is important, for example, in investigating change in oxidation state of titanium when synthesizing variants of TiO_2 such as Ti-N-F. An example of a Ti^{4+} spectrum is shown in **Figure 5.5**.

When one of the peaks of a survey spectrum is examined under conditions of higher resolution, the position of the maximum depends to a small degree on the chemical environment of the atom responsible for the peak. Variations in the number of valence electrons and the type of bonds they form influence the binding energies of the core electrons. Binding energies increase as the oxidation state becomes more positive. This can be explained by assuming that the attraction of the nucleus for a core electron

is diminished by the presence of outer electrons. When one of these electrons is removed and the effective charge for the core electron is sensed, this leads to an increase in binding energy.

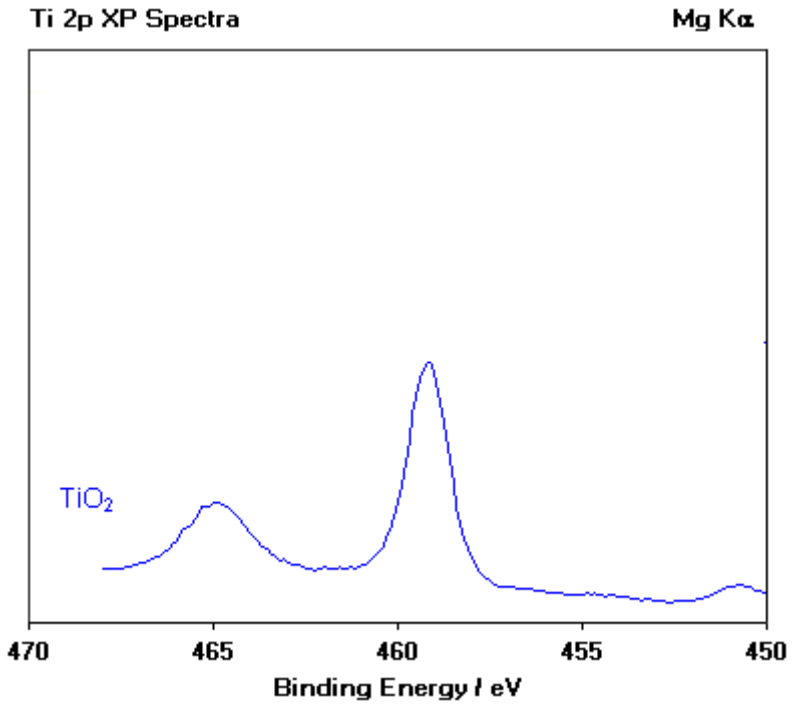

Figure 5.5 XPS spectra of titanium dioxide
http://www.jhu.edu/~chem/fairbr/surfacelab/xps.html (accessed May, 2009)

Chapter 6

Experimental Results and Discussion

6.1 Sol-Gel Synthesis of TiO_2

As discussed in the literature review, variants of TiO_2, such as TiO_2N and TiNF are expected to be isostructural to TiO_2-anatase. Therefore, the first task in this work was to synthesize TiO_2-anatase against which most of the data such as XRD, SEM micrographs, XPS and, in the long-run, photoconductivity would be compared. To synthesize TiO_2-anatase, 50 mL of titanium (tetra-isopropoxide) was slowly added to rapidly stirring dilute nitric acid (300 mL, 0.5% V/V). The mixture was then boiled until the total volume was reduced to 90 mL. This solution was then heated at 200°C in a sealed vessel for 15 hours. Finally 5.4 g of polyethylene glycol were added and the solution stirred for an additional 8 hours. The gel obtained was sintered at 500°C and analyzed by powder X-ray diffraction. The overall reaction can be written as:

$$0.25Ti[OCH(CH_3)_2]_4 \longrightarrow TiO_2 + 4\ HOCH(CH_3)_2$$

The powder XRD pattern of the final product is shown in **Figure 6.1**, and indicates that an anatase phase was synthesized. The characteristic broad peaks of the diffraction pattern suggest the formation of anatase particles with small size, probably nano-sized particles. There are two peaks which were not accounted for. The first one is at 2θ equals to 31^o and the second at 2θ equals to 27.5^o. One of the possible origins of

the two peaks could be the polyethylene glycol used to stabilize the gel, in the synthesis of TiO_2.

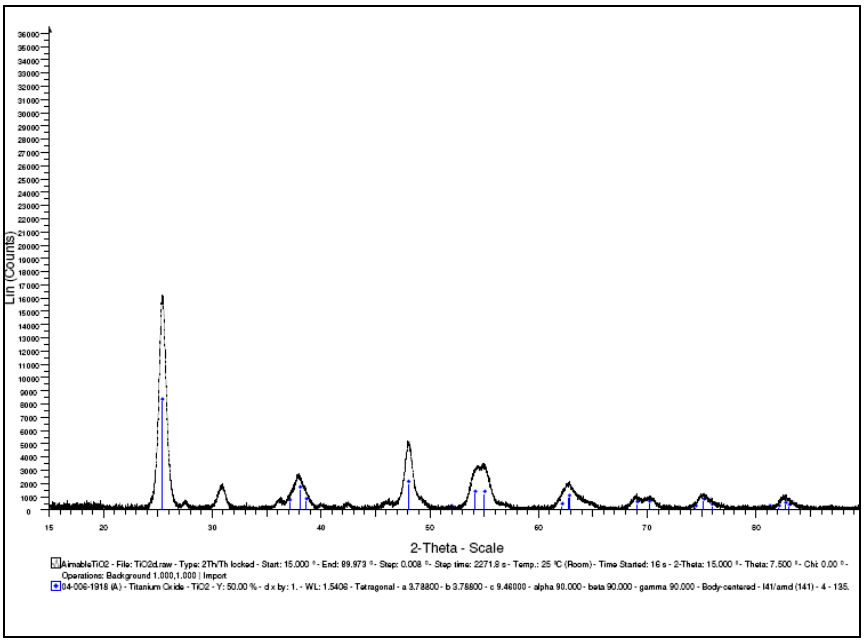

Figure 6.1 PXRD pattern match of TiO_2

6.2 Synthesis of bis (diethylamidofluoro) titanium

The synthesis of bis (diethylamidofluoro) titanium was done under inert gas using a Schlenk-line. The Schlenk line used was not an “all glass” Schlenk set-up. It was rather an improvised one, with plastic hose-pipes and rubber pipes at certain positions. Nevertheless, it served the purpose of ensuring a positive inert-gas flow in the course of the reaction. This synthesis of the titanium complex precursor involved two steps: preparation of $Ti(NEt_2)_4$ followed by the synthesis of $[TiF_2(NEt_2)_2]_4$. The third and final step planned was the thermal decomposition of this precursor to form TiNF.

6.2.1 Synthesis of $Ti(NEt_2)_4$

The overall synthesis of the title compound can be represented as:

$$TiCl_4 + 4HNEt_2 \longrightarrow Ti(NEt_2)_4$$

Prior to synthesis all solvents (ether, toluene and hexanes) were thoroughly degassed by bubbling of nitrogen gas through the solvent and dried using molecular sieves. Certain reagents such as diethyl amine were also thoroughly degassed and dried to ensure the removal of any dissolved air. All glassware and transfer needles were cleaned and dried in an oven to ensure complete removal of moisture.

After ensuring that all Schlenk vessels and reagents were free from moisture and air, the synthesis apparatus was set up as follows: a three necked round bottom Schlenk flask was evacuated and flushed with nitrogen three times to ensure a complete inert atmosphere inside the flask. A cold bath made by freezing methanol with liquid nitrogen was prepared and used to cool the flask before proceeding. All the transfers of reagents into the reaction flask were done using dry stainless steel needles.

The flask containing ether was purged with nitrogen such that no external air flowed into the flask, then the syringe and the needle were flushed with nitrogen three times before drawing ether solvent into the syringe and transferring it into the reaction flask. Using the flushed transfer needle, 200 mL of ether (ACROS) solvent was then transferred into the reaction flask. Next, a solution of BuLi (Aldrich, 1.6 M in hexanes, 100 mL, 10.25 g, and 0.16 moles) was transferred into the reaction flask containing

ether using a cannula transfer needle. In this transfer, a ruler was used to determine the level at which 100 mL of BuLi had been transferred. While stirring, an equimolar amount of diethyl amine (Sigma-Aldrich, ≥ 99 %, 16.62 mL, 11.7 g) was transferred into the reaction flask at -10 °C. Then, a solution of titanium tetrachloride (Aldrich, 99.995%, 4.38 mL, 7.58 g, 0.04 moles) was diluted into a degassed and dried toluene solution (Sigma-Aldrich, ≥99.5%, 100 mL) in a separate flask. The mixture was then transferred into the reaction vessel while slowly stirring. A positive pressure was maintained inside the reaction flask to avoid any infiltration by oxygen when carrying out the transfer. The reaction mixture was then heated to reflux of the solvent until a change in color from brown to red-orange appeared after approximately thirty minutes. At this point, a mixture of solid by-products and a red-orange solution had formed. This suspension was transferred into a Schlenk filter with a glass filter plate and the solids were filtered off into a round bottom flask. Excess ether solvent was removed under vacuum, and an additional 100 mL of toluene were added to the reaction vessel. The filtrate was then reduced to approximately half the original volume by evaporation under reduced pressure. The product was then distilled under vacuum at 112 °C. The distillates were collected in fractions using a Schlenk receiving flask that had three outlets. The three outlets made it possible to fix three more collecting flask onto the distillation set up. In addition a hot blower was used to reinforce the movement of the distillate into the condenser. At the collecting end a cold bath made of ice and salt was set up to allow quick condensation of the distillate as soon as it was collected. The distilled product was

further reduced and concentrated under vacuum to remove excess toluene. The Schlenk flask containing the product was filled with nitrogen and stored in the freezer at –18°C.

6.2.2 Synthesis of $[TiF_2(NEt_2)_2]_n$

The overall synthesis of the title compound is:

$$Ti(NEt_2)_4 + TiF_4 \longrightarrow [TiF_2(NEt_2)_2]_n$$

To incorporate fluorine into $Ti(NEt_2)_4$, titanium tetra-fluoride was reacted with $Ti(NEt_2)_4$ obtained in the previous reaction. Therefore TiF_4 (Alfa-Aesar, 98%, 4.95 g, 0.04 moles) were transferred into 100 mL of dried and degassed hexanes. The obtained solution was transferred to the reaction flask (containing 13.46 g of $Ti(NEt_2)_4$ 0.04 moles) on a Schlenk-line, using a stainless transfer needle. The reaction was allowed to proceed for 12 hours while stirring. Again using a stainless transfer needle, the product was transferred and filtered from the residue using a Schlenk-filter. The residue on the filter plate was washed with more hexane and the hexane solution was concentrated to half the original amount by gentle heating with a warm water bath while maintaining a light vacuum on the solution.

Crystals of the product were grown by cooling of the concentrated solution of the compound in hexanes (under nitrogen in small Schlenk flasks) to –18°C (freezer) for a period of several days. Crystals usually did form after about five days. The crystals of the target material, which are black, did typically form together with reddish to colorless crystals of an unidentified side product. Slow crystallization of freshly prepared samples

usually yielded a first crop of large well defined crystals of $[TiF_2(NEt_2)_2]_4$. Additional cooling then led to the formation of more $[TiF_2(NEt_2)_2]_4$ crystals mixed with crystals of the byproduct crystals. Pure material that was used in the thermal decomposition, TGA, DSC, and single crystal diffraction experiments was thus harvested from the first batch of crystals, and no total yield of the reaction was determined.

When dry, the black crystals are stable for a short time in air and can be handled, for example, for single crystal mounting or preparation of a TGA sample in air. When left in air for several minutes, the black crystals first start to lose color on the edges and then quickly soften and become a white soft and wet material, probably due to hydrolysis and release of diethyl amine. Once the decomposition starts it accelerates quickly, and is probably associated with the release of diethyl amine which acts as a solvent to accelerate the decomposition of the remainder of the material. Individual crystals under a microscope decompose at different rates, with those that start showing first signs of decomposition being totally decomposed quickly while other crystals might not yet be affected at all. After 10 to 15 minutes in air the material is however totally decomposed throughout.

6.2.3 Single-Crystal Data Collection and Analysis

To determine the crystal structure of the product, as well as having unambiguous proof of the identity of the compound, a single-crystal diffraction analysis was attempted. For mounting of single crystalline samples, a small amount of the crystalline product was transferred from the Schlenk tube onto a microscope slide in air and the

sample was immersed in mineral oil for easier handling of the crystals and selection of a crystal suitable for diffraction. Immersion in oil also extended the lifetime of the crystals in air to several hours. Decomposition did however proceed even in mineral oil. Several potential crystals were selected, transferred to the diffractometer and unit cell determinations were attempted in a stream of cold nitrogen gas at 100 K. With the crystals being non-transparent and dark red in color, selection of a suitable crystal proved difficult, and many of the samples tested were not single crystalline, but were intergrown or twinned. All did show a large mosaicity. Three full datasets were eventually collected. Intensity statistics for the best data set obtained using a Bruker AXS SMART APEX CCD diffractometer are shown in **Table 6.1**, and this data will be further discussed later.

Table 6.1 Intensity Statistics

Resolution	#Data	#Theory	%Complete	Redundancy	Mean I	Mean I/s	R(int)	Rsigma
Inf - 2.07	595	599	99.3	3.73	34.5	35.88	0.0236	0.0175
2.07 - 1.63	611	616	99.2	3.68	24.2	31.23	0.0249	0.0219
1.63 - 1.42	608	608	100.0	3.60	17.4	26.23	0.0327	0.0270
1.42 - 1.29	602	603	99.8	3.50	13.1	22.50	0.0409	0.0342
1.29 - 1.20	594	594	100.0	3.41	9.8	17.77	0.0495	0.0436
1.20 - 1.13	595	598	99.5	3.21	7.6	13.95	0.0582	0.0561
1.13 - 1.07	627	627	100.0	3.04	6.5	12.49	0.0654	0.0670
1.07 - 1.02	664	664	100.0	2.95	5.9	11.24	0.0788	0.0746
1.02 - 0.98	633	634	99.8	2.80	6.3	11.09	0.0743	0.0733
0.98 - 0.94	738	739	99.9	2.66	6.0	10.64	0.0770	0.0792
0.94 - 0.91	646	649	99.5	2.56	5.3	9.61	0.0916	0.0881
0.91 - 0.88	715	721	99.2	2.45	5.0	8.92	0.0961	0.0975
0.88 - 0.85	832	850	97.9	2.42	4.1	7.86	0.1092	0.1121
0.85 - 0.83	624	636	98.1	2.27	3.6	7.12	0.1200	0.1286
0.83 - 0.81	663	689	96.2	2.16	3.4	6.77	0.1312	0.1401
0.81 - 0.79	740	769	96.2	2.21	2.9	6.44	0.1413	0.1487
0.79 - 0.77	817	854	95.7	1.98	2.7	5.93	0.1503	0.1742
0.77 - 0.75	429	454	94.5	1.97	2.9	6.34	0.1528	0.1667
0.85 - 0.75	3568	3704	96.3	2.14	3.2	6.61	0.1340	0.1460
Inf - 0.75	11733	11904	98.6	2.78	8.6	13.58	0.0500	0.0545

As shown in **Table 6.2**, the crystal sample was red in color and had dimensions of 0.28 mm × 0.20 mm × 0.07 mm. A total of 9963 reflections were used determine the unit cell parameters of the monoclinic lattice. The a, b and c unit cell axes were determined to be 11.5734(15) Å, 37.163(5) Å and 12.1111(16) Å, respectively. The parameters are quite large, hence indicating the presence of a large unit cell. The fourth unit cell parameter β (°), which is the angle between the a and c cell axes, was determined to be 115.079(2). As for the structure refinement, a total of 11544 reflections were used in the final structure model. In addition, six constraints were imposed on the structure and all the hydrogen atoms were fixed in calculated positions. As seen from **Table 6.3**, the final regression factor (R) values did not appreciably minimize. For instance, a good R-value should be approximately the same as the R_{int} value of the data but the R-value obtained in this refinement was 11.5%, which is much larger than the 5.1% obtained for R_{int}. There is no obvious explanation for this R-value as the intensity statistics show that the diffraction data are of good quality.

Table 6.2 Crystal Data

Crystal data	
Chemical formula	$C_{32}H_{80}F_8N_8Ti_4$
M_r	920.64
Crystal system, space group	Monoclinic, $P2_1/c$
Temperature (K)	100
a, b, c (Å)	11.5734 (15), 37.163 (5), 12.1111 (16)
β (º)	115.079 (2)
V (Å^3)	4717.9 (11)
Z	4
F(000)	1952
Radiation type	Mo $K\alpha$
No. of reflections for cell measurement	9963
θ range (º) for cell measurement	2.3–31.1
μ (mm^{-1})	0.71
Crystal shape	Plate
Colour	Red
Crystal size (mm)	0.28 × 0.20 × 0.07

Table 6.3 Data Collection

Data collection	
Diffractometer	Bruker AXS *SMART APEX* CCD diffractometer
Radiation source	fine-focus sealed tube
Scan method	ω scans
Absorption correction	Multi-scan Apex2 v2008.2-4 (Bruker, 2008)
T_{min}, T_{max}	0.797, 0.951
No. of measured, independent and observed [$I > 2\sigma(I)$] reflections	32686, 11544, 9960
R_{int}	0.051
θ values (º)	θ_{max} = 28.3, θ_{min} = 1.9
Refinement	
$R[F^2 > 2\sigma(F^2)]$, $wR(F^2)$, S	0.115, 0.229, 1.30
No. of reflections	11544
No. of parameters	485
No. of restraints	6
H-atom treatment	H-atom parameters constrained
	$w = 1/[\sigma^2(F_o^2) + (0.P)^2 + 50.4507P]$ where $P = (F_o^2 + 2F_c^2)/3$
$\Delta\rangle_{max}$, $\Delta\rangle_{min}$ (e Å^{-3})	0.61, -0.98

In order to gauge the validity of the structure, the bond lengths and bond angles of the structure were examined. There are five types of bonded and non-bonded distances to consider. Ti–F bond lengths range from 1.817(4) Å to 2.236(3) Å, and Ti–N bonds range from 1.871(5) Å to 1.920(5) Å. The shortest Ti–Ti distances are 3.0861 Å. The C–N bond lengths between 1.467 Å and 1.482 Å, the C–C bonds between 1.520(5) Å and 1.535(5) Å. Selected bond lengths are listed in **Table 6.4**, and selected bond angles are presented in **Table 6.5**. Our experimental data show shorter Ti–N bond distances

that are less than 1.939 Å, which is the length listed as typical for this type of compound in International Tables For Crystallography, Volume C, 1995 (p. 733). This observation suggests the formation of a strong Ti–N bond in the bis(diethylamidofluoro) titanium. The International Tables (p. 759) also indicate that a standard Ti–F bond length for this compounds should be between 1.853 Å and 1.887 Å. Looking through Table 6.4, we see that only the F2-T1, F3-Ti2, F7-Ti3 & F8-Ti4 have bond distances (1.833(4) Å, 1.917(4) Å & 1.918(3) Å respectively) similar to the standard Ti–F bond distance, while the rest of the Ti–F bond distances are relatively larger than the standard value of 1.887 Å. The C–N bond distances are close to the standard values of 1.464 Å - 1.479 Å. The C–C bond distances between 1.520(5) Å and 1.535 (5) Å from our experiment are typical of a Csp^3–Csp^3 bond. The large Ti–Ti distance of 3.0861 Å is expected since the titanium atoms exist at the core of the molecular $[TiF_2(NEt_2)_2]_4$ and the distance between them is influenced by the ligands they are attached to (see **Figures 6.2, 6.3, 6.4** & **6.5**).

Table 6.4 Selected Bond Lengths

Coordinate bonds around Ti1		Coordinate bonds around Ti2		Coordinate bonds around Ti3		Coordinate bonds around Ti4	
F1—Ti1	2.015 (4)	F3—Ti2	1.917 (4)	F4—Ti3	2.147 (3)	F1—Ti4	2.015 (4)
F2—Ti1	1.833 (4)	F4—Ti2	2.196 (3)	F5—Ti3	2.006 (3)	F6—Ti4	2.236 (3)
F3—Ti1	2.168 (3)	F5—Ti2	2.009 (4)	F6—Ti3	2.201 (4)	F7—Ti4	2.168 (4)
F4—Ti1	2.230 (4)	F6—Ti2	2.142 (3)	F7—Ti3	1.918 (3)	F8—Ti4	1.817 (4)
N1—Ti1	1.907 (5)	N3—Ti2	1.888 (6)	N5—Ti3	1.884 (5)	N7—Ti4	1.913 (5)
N2—Ti1	1.905 (5)	N4—Ti2	1.884 (5)	N6—Ti3	1.871 (5)	N8—Ti4	1.920 (5)

Table 6.5 Selected bond angles

Bond	Bond angles
F2—Ti1—N2	98.1 (2)
F2—Ti1—N1	99.4 (2)
N2—Ti1—F1	96.53 (19)
N1—Ti1—F1	89.94 (19)
N2—Ti1—F3	88.68 (19)
N1—Ti1—F3	167.60 (19)
N2—Ti1—F3	88.68 (19)
N1—Ti1—F3	167.60 (19)
N2—Ti1—F4	158.98 (19)
N1—Ti1—F4	99.66 (19)

N4—Ti2—F3	100.8 (2)
N3—Ti2—F3	103.7 (2)
N4—Ti2—F5	106.1 (2)
N3—Ti2—F5	88.5 (2)
N4—Ti2—F6	93.71 (19)
N3—Ti2—F6	160.2 (2)
N6—Ti3—F7	104.01 (19)
N5—Ti3—F7	101.43 (19)
N6—Ti3—F5	87.82 (19)
N5—Ti3—F5	106.14 (19)
N6—Ti3—F4	161.90 (18)
N5—Ti3—F4	91.92 (19)
F8—Ti4—N7	97.5 (2)
F8—Ti4—N8	99.0 (2)
N7—Ti4—F1	97.5 (2)
N8—Ti4—F1	89.55 (19)
N7—Ti4—F7	88.40 (19)
N8—Ti4—F7	167.64 (19)
N7—Ti4—F6	159.1 (2)
N8—Ti4—F6	99.73 (18)

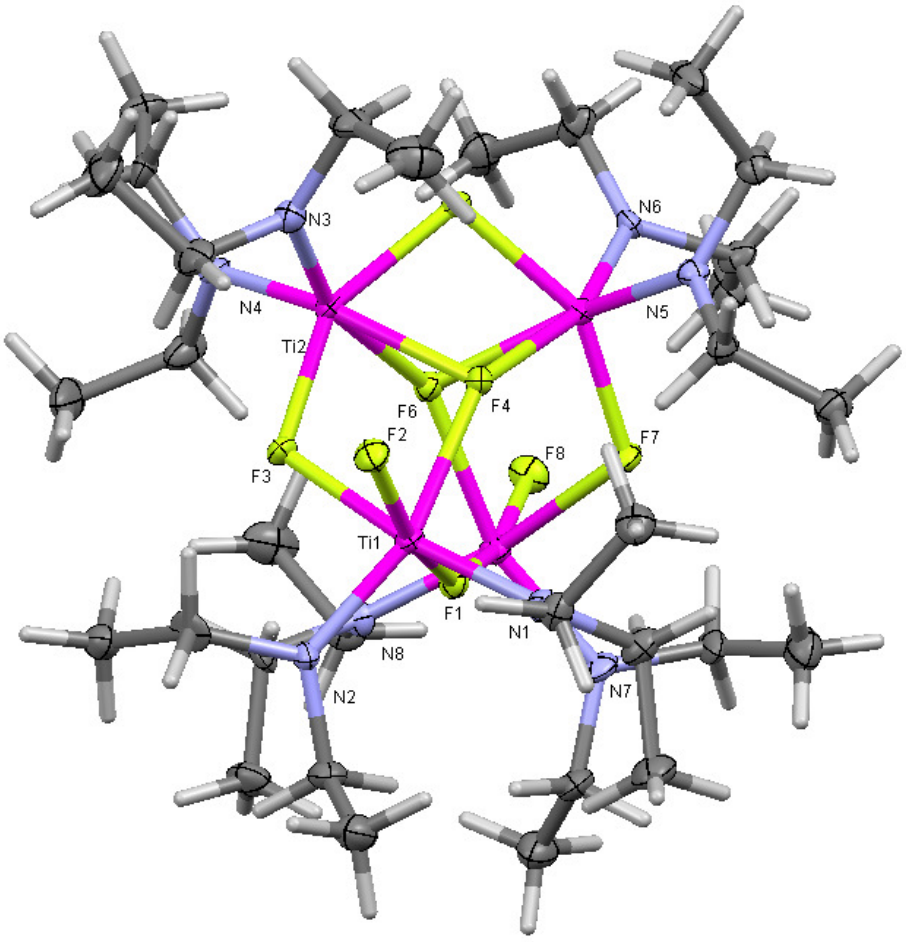

Figure 6.2 ORTEP plot of bis(diethylamidofluoro) titanium

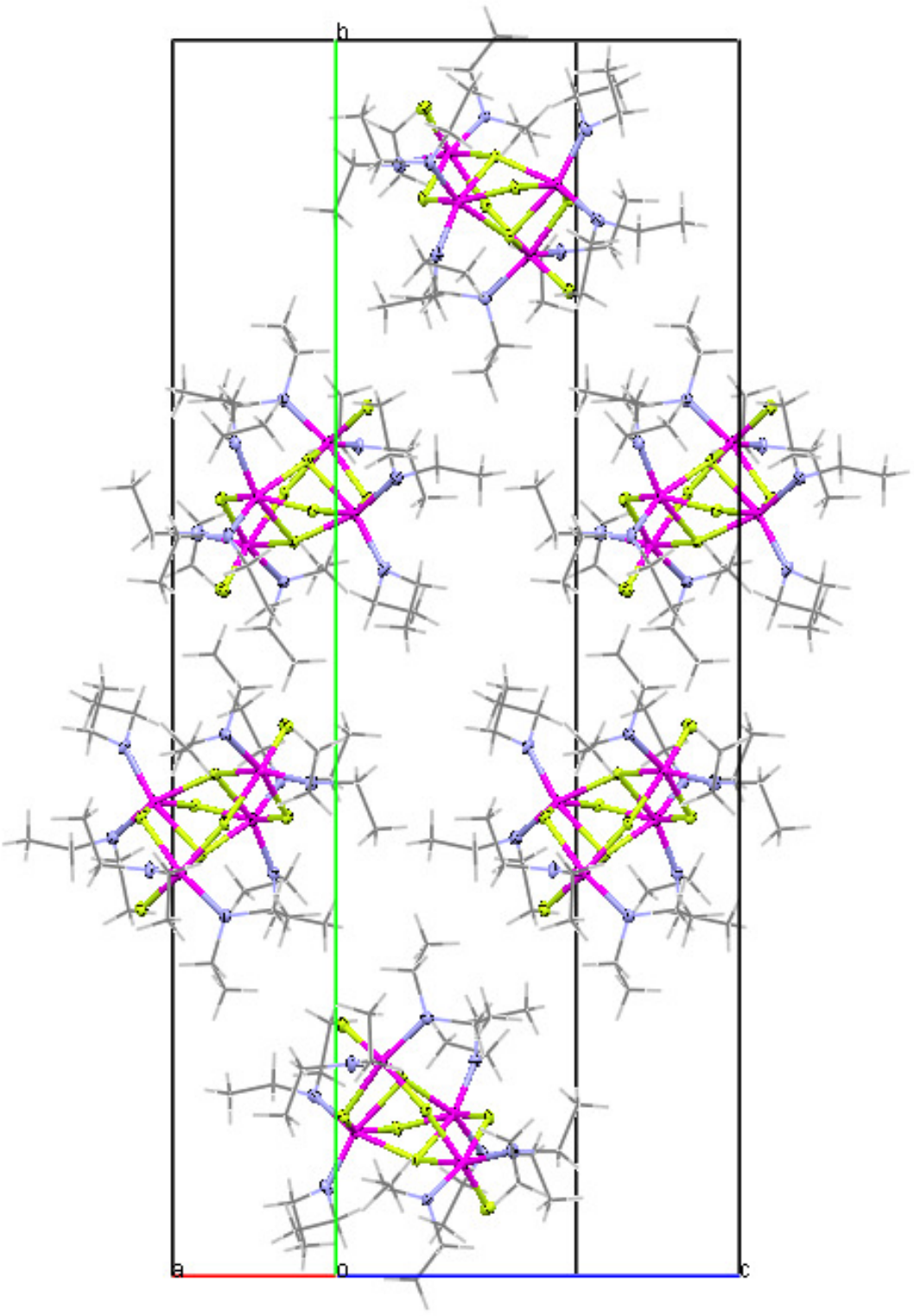

Figure 6.3 Packing of bis(diethylamidofluoro) titanium

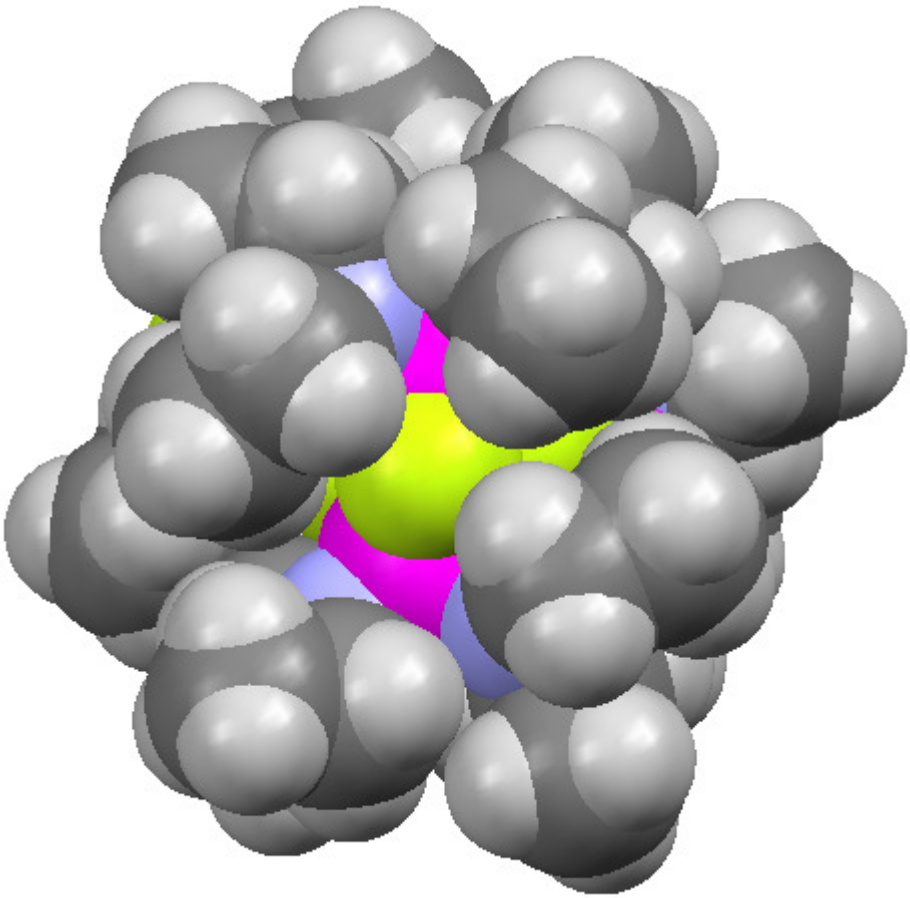

Figure 6.4 Sphere model of bis(diethylamidofluoro) titanium

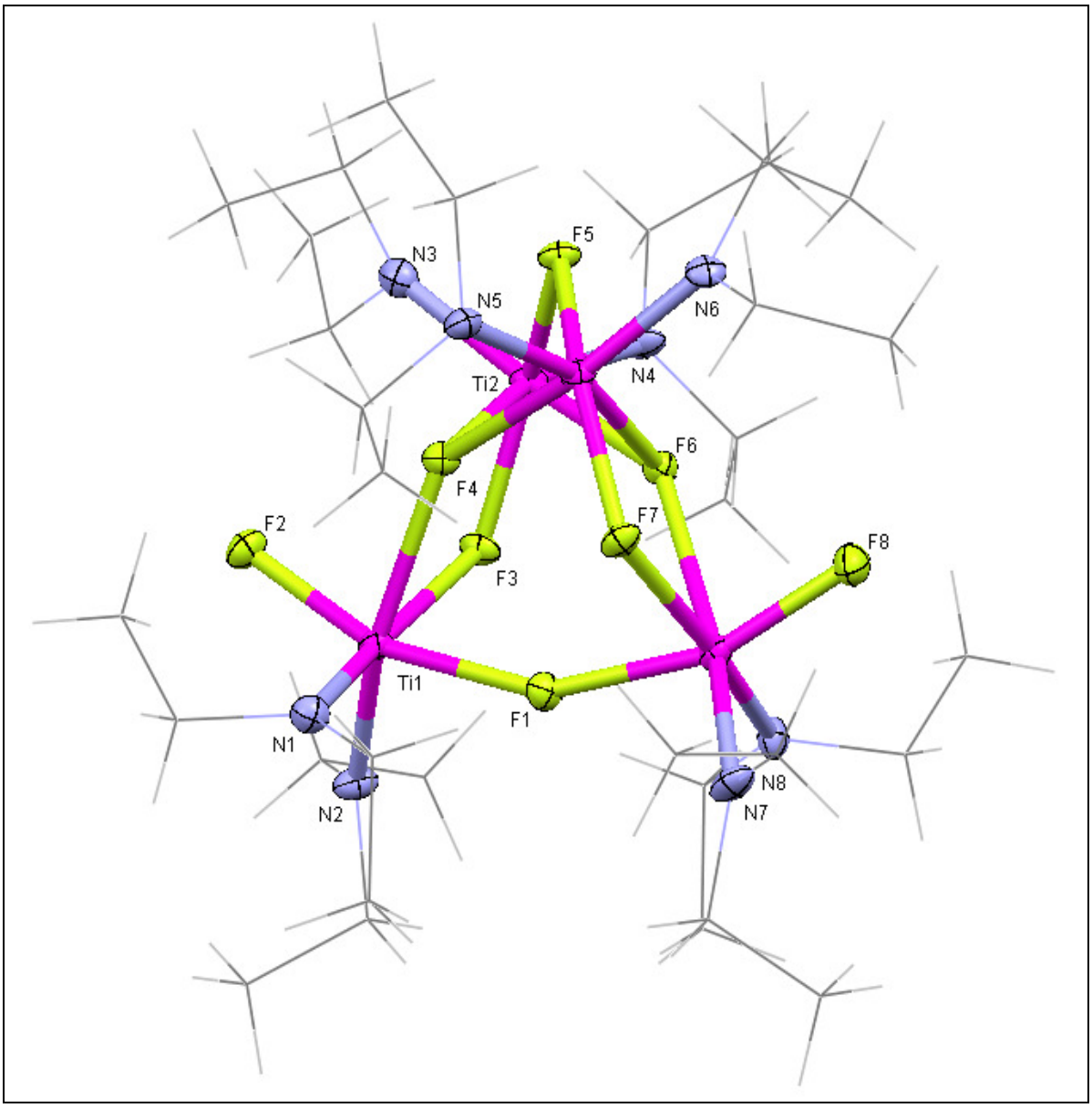

Figure 6.5 A stick model of bis(diethylamidofluoro) titanium

6. 3 Thermal Gravimetric Analysis of $[TiF_2(NEt_2)_2]_4$

6.3.1 Thermal Decomposition Analysis of $[TiF_2(NEt_2)_2]_4$

The TGA instrument was flushed with flowing nitrogen before and during operation. In addition the round bottom Schlenk flask containing the sample was evacuated and filled with nitrogen three times. About 3 to 4 mg of the sample was quickly transferred onto a TGA pan (i.e. aluminum pan) and the sample was quickly mounted into the furnace. The experimental parameters and results are shown in **Figure 6.6.**

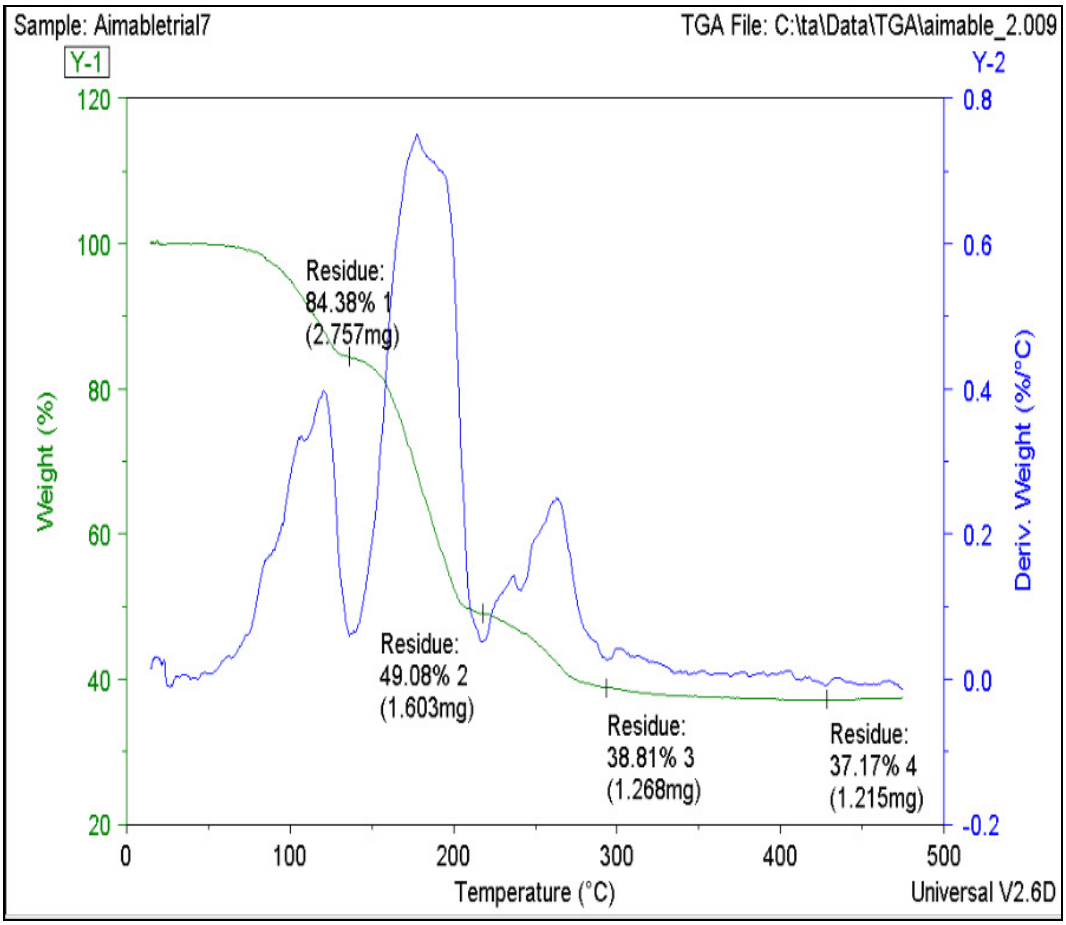

Figure 6.6 The TGA thermogram-1 of bis(diethylamodofluoro) titanium

The thermogram in **Figure 6.6** shows three decomposition steps. The first step corresponds to a loss of about 15.62% from the original weight. In practice the first loss is often associated with solvent loss. However our sample seemed to be quite dry and the compound did not contain any crystal solvent molecules as shown by the crystal structure determination. It is not clear if there was any solvent trapped within the dry crystals. This weight loss is likely associated with a first decomposition step of the material. The combined first and second step correspond to a total loss of about 50%, which is close to the theoretical value of about 48.75%. The final step corresponds to a total loss of about 63% and the theoretical value of the residue, i.e. the TiNF product, was expected to be about 35.5%. However the experimental value is about 37.17%.

Subsequent thermograms (in **Figures 6.7, 6.8, 6.9, 6.10 & 6.11**) show similar patterns to the one discussed in the preceding paragraph, however the expected weight losses did fluctuate significantly and were on average slightly lower than the theoretically expected value. The deviations from the expected weight loss are larger than could be expected due to measurement inaccuracies or instrument problems. The most likely cause of the deviations might be impurities in the starting material.

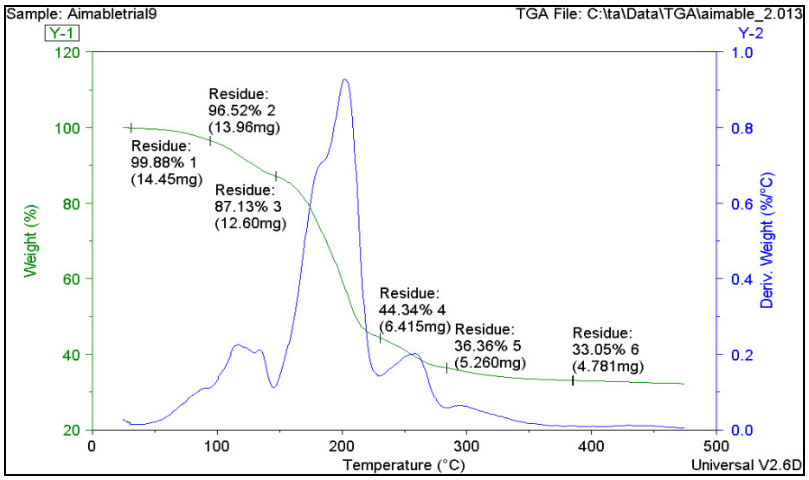

Figure 6.7 TGA thermogram-2 of bis (diethylamodofluoro) titanium

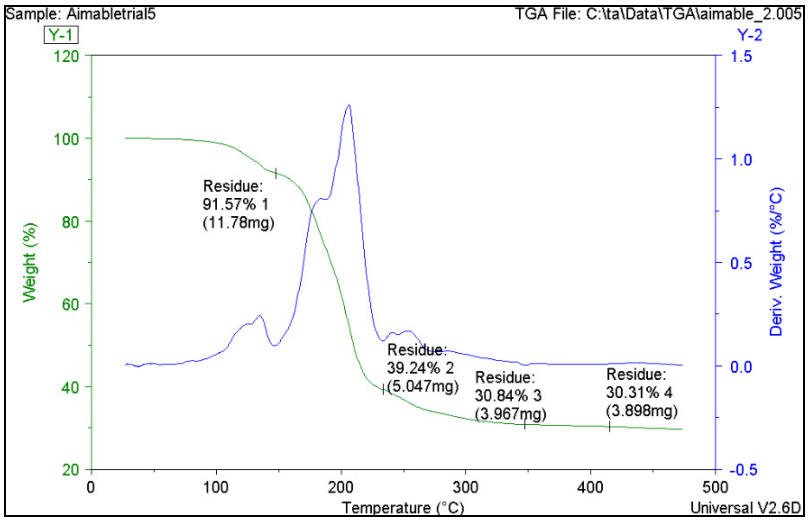

Figure 6.8 TGA thermogram-3 of bis (diethylamodofluoro) titanium.

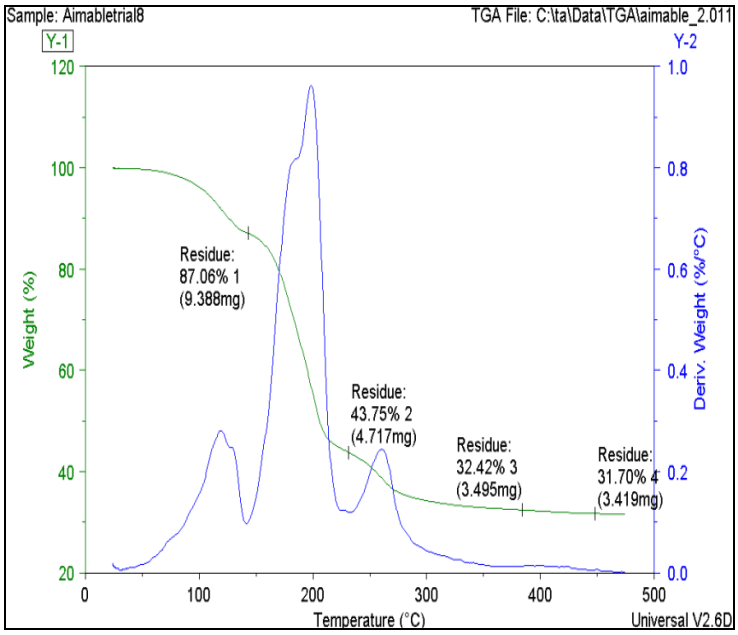

Figure 6.9 TGA thermogram-4 of bis (diethylamodofluoro) titanium.

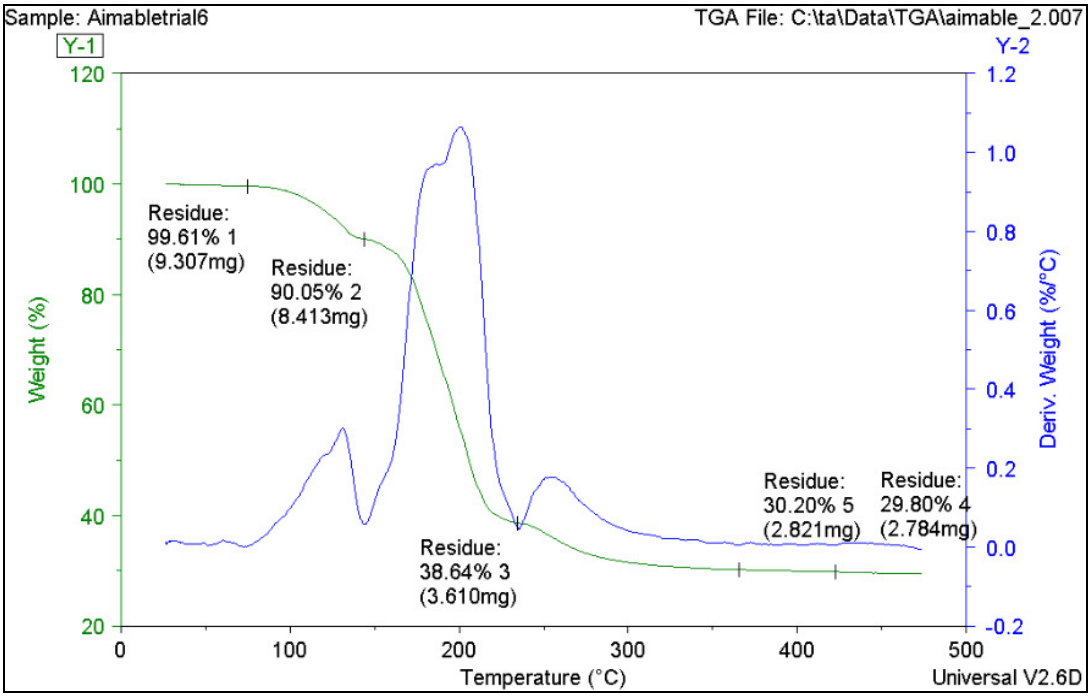

Figure 6.10 TGA thermogram-5 of bis (diethylamodofluoro) titanium.

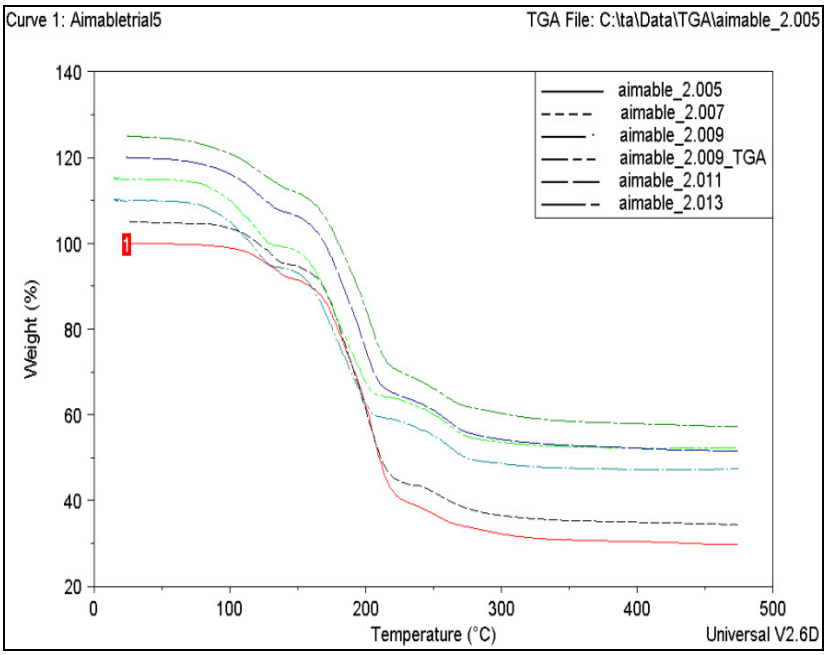

Figure 6.11 Overlay of the representative thermograms.

All of the TGA data does indicate that the thermal decomposition of the precursor proceeds in three characteristic steps. The first step is between 100°C and 150°C. The second step is found between 150°C and 200°C and the third between 200°C and 300°C. According to the thermograms obtained, the first step is about 13% of the original weight; the first and second combined about 50% - 56% of the original weight, and the third loss leads to 63% - 70% of the original mass weight.

According to the aforementioned hypothesis in Section 3.7, we expected to observe two decomposition steps, but the experimental thermograms show three steps. Also, it was expected that at the end of the decomposition reaction, 64.85% should have decomposed off, remaining with about 35% of the original weight.

The TGA results suggest that a similar overall decomposition, but different from the suggested mechanism in our hypothesis, could be occurring. The predicted loss in the first step is close to the combined experimental loss in the first and second decomposition steps. Looking at the thermogram in **Figure 6.6**, we see a loss of about 49% after the first two decomposition steps, which is close to the predicted first weight loss of 48.75%. The formation of a gassing white fume, resembling NH_4F when the TGA pan is unloaded from the furnace, could be a good source of information as to how the decomposition proceeds. The identity of this white fume could be determined by a mass spectrometer, if collected at the end of the decomposition.

6.3.2 Thermal Decomposition of a Bulk Sample of $[TiF_2(NEt_2)_2]_4$

The determination of the temperature at which a complete thermal decomposition occurs, gave us an idea of what temperature should be used in the decomposition bulk sample. Thus, a sample of $[TiF_2(NEt_2)_2]_4$ was decomposed in the inside of a tube furnace under nitrogen flow at a temperature of 300°C. Before mounting the sample inside the tube furnace, all the handling procedures were carried out inside a glove bag. A weighing balance, weighing crucibles, and spatulas were all put in a glove bag together with the flask containing $[TiF_2(NEt_2)_2]_4$. The bag was evacuated and filled with nitrogen three times. Using a dry clean spatula, 3.71 g of $[TiF_2(NEt_2)_2]_4$ sample was scooped from a Schlenk flask and placed in a quartz boat. The quartz boat was then placed in a tube. To avoid any infiltration of humidity into the sample, the tube was sealed and nitrogen gas was allowed to flow through. The tube containing the

sample was then mounted into the furnace, and the furnace program shown in **Table 6.6** was used to thermally decompose $[TiF_2(NEt_2)_2]_4$.

Table 6.6 Tube Furnace Program-1

Step 1	Step 2	Step 3
Ramp 60 °C/hr	Ramp 60 °C/hr	Ramp 60 °C/hr
Level at 100 °C	Level at 200 °C	Level 300 °C/hr
Dwell 1 hr	Dwell 10 hrs	Dwell 13 hrs

At the end of the tube furnace program, the sample was removed from the furnace and using a mortar and pestle, the sample was ground to obtain a dark green powder. From this point on the material was handled in air. The phases present in this powder were then analyzed using a powder X-ray diffractometer. As seen in **Figure 6.12,** there were three major phases whose peak patterns had a close match to the experimental peaks: anatase (titanium dioxide), ammonium titanium fluoride and ammonium titanium oxyfluoride. The dominant peak (71.30%) corresponded to the anatase phase and therefore this required a closer examination to establish if, this might be due to anatase or a variant of anatase. This was done in two ways; the first was examination via SEM and the second was a comparison of elemental analyses done on a standard anatase sample and the sample obtained after decomposition of the study sample.

The decomposition of the bulk sample in the tube furnace may not necessarily be an accurate representation of the decomposition inside a TGA. Therefore collecting and comparing PXRD data of freshly decomposed sample from the TGA is necessary. Also, after the decomposition, samples were handled in air and so decomposition of any

formed TiNF might have had occurred. In further studies samples will thus have to be handled under inert gas during all analysis steps, not only during synthesis, and controlled exposure of the samples to air and humidity has to be carried out.

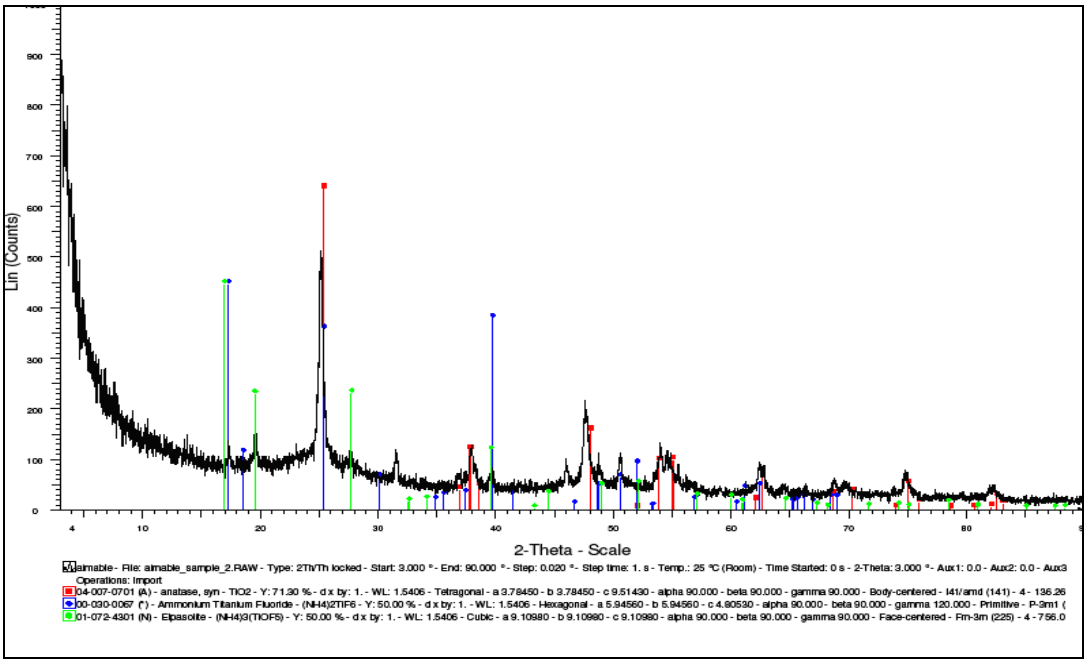

Figure 6.12 PXRD pattern of the decomposition of bis(diethylamodofluoro) titanium.

The SEM micrograph in **Figure 6.13** shows micro features of an anatase sample prepared by the sol-gel method. It has characteristic sharp edges that were not observed on the micrograph of the product obtained after decomposition of precursor (a) in the tube furnace. The absence of this unique feature of anatase suggests that the anatase pattern observed using powder XRD could be due to a variant of TiO_2 in which fluoride or nitride ions substitute for the oxygen anions in the TiO_2 lattice, hence changing its color from white to dark green. In order to verify this hypothesis, one would need neutron diffraction data, which could not be obtained at the moment. However, in

an attempt to carry out elemental analysis of the decomposition product, XPS scans were collected for both the standard TiO_2 anatase and for the decomposition product. A comparison of the elements present in both samples was done.

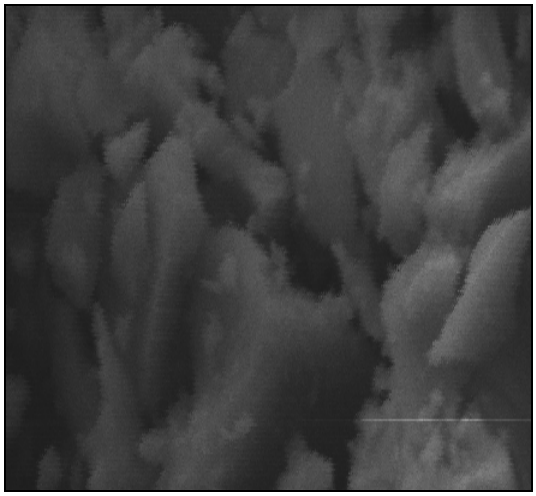

Figure 6.13 SEM micrograph corresponding to the decomposition product.

In addition to the Powder-XRD diffraction pattern, a further examination of the micro features of the product formed from the thermal decomposition of bis(diethylamidofluoro) titanium was carried out using SEM. Since the predominant peak pattern was closely matching that of TiO_2-anatase, it was expected that also the crystal habit could probably be the same. TiO_2-anatase can be easily identified due to its crystal habit which is pyramidal, possessing sharp edges, and its fractures are characterized by smoothly curving surfaces. These features were present in the standard TiO_2-anatase prepared in the lab as shown in **Figure 6.13**. However, a close examination of the decomposition product of bis(diethylamidofluoro) titanium does not show these micro features (see **Figure 6.14**) despite the fact that its XRD pattern is

predominantly close to that of TiO_2. These observations prompted us to utilize XPS as a tool to compare elemental composition of our TFTEA thermal decomposition product, and verify if indeed we had incorporated either nitrogen or fluorine into the TiO_2 lattice.

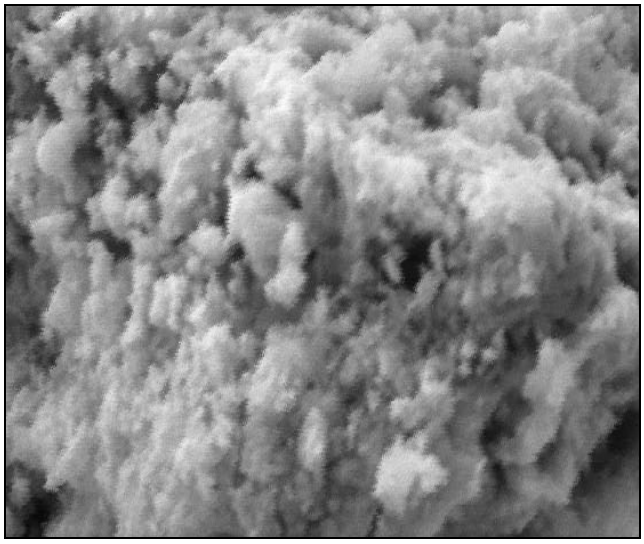

Figure 6.14 SEM micrograph of TiO_2 anatase.

6.4 XPS Analysis

Figure 6.15 shows that the sample "Ti-N-O-F" had five types of elements present. These are namely, carbon, nitrogen, titanium, oxygen and fluorine. The element of interest here is the nitrogen at 400eV. This is the inorganic nitrogen bound to titanium. Unfortunately, it is present in relatively low atomic concentration of about 4.9%. Therefore the presence of inorganic nitrogen in low concentration suggests the formation of (or decomposition to) a nitrogen-doped TiO_2 compound. Inorganic fluorine and oxygen were also present in almost equal ratio as seen from **Table 6.7**; oxygen was present at an atomic concentration of 23.54% while fluorine was at 18.86% atomic concentration. It should be mentioned as well that XPS is just a surface analysis

technique, and picks up elements such as carbon from the atmosphere, and this was evidently present in our data.

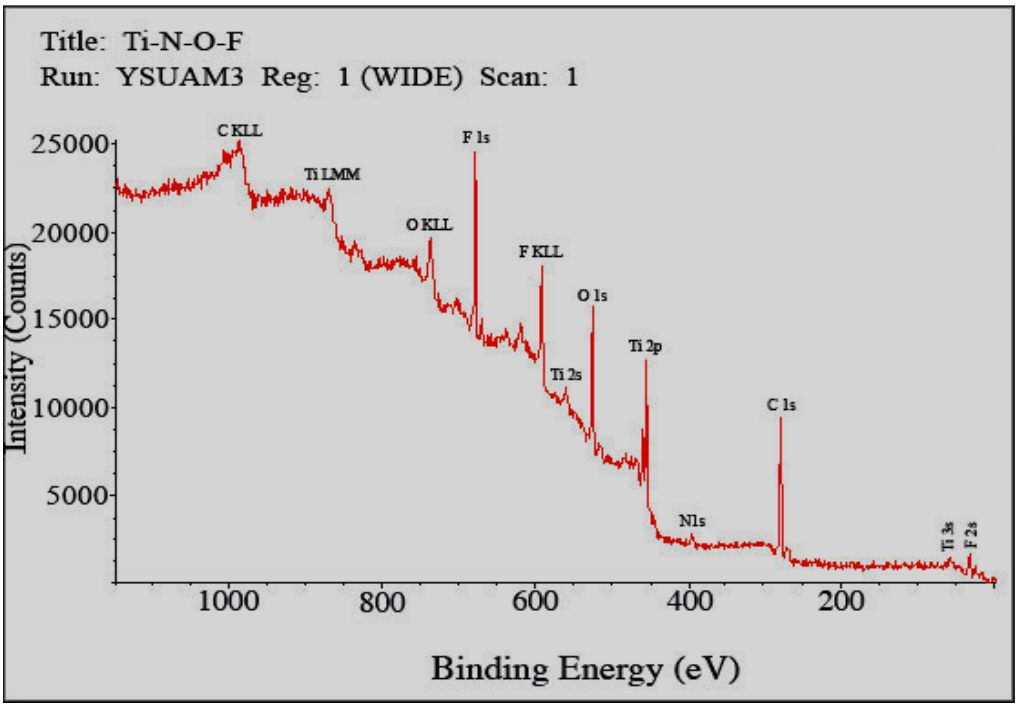

Figure 6.15 XPS spectra for the analysis of 'Ti-N-O-F'

Table 6.7 Percentage Atomic Concentrations in the 'Ti-N-O-F' and TiO_2 Samples

Sample	C	N	O	F	Na	S	Ti
TiO2(dirty)	21.15	-----	55.64	-----	1.46	1.54	20.21
TiO2(Clean)	18.38	-----	58.55	-----	1.75	0.54	20.78
'Ti-N-O-F'	41.45	4.90	23.54	18.86	-----	-----	11.26

In order to obtain more reliable data, a depth profile would be necessary in the future. Nevertheless, the XPS spectrum does suggest the formation of (or decomposition to) a compound made of titanium, oxygen, and fluorine. This compound is doped with nitrogen. The formation of N-doped compounds when trying to nitridate TiO_2 is a common occurrence from the literature, in fact a true TiNF compound has

never been made as the nitrogen tends to incorporate itself into the TiO_2 lattice as a dopant. Fortuitous oxygen presence in the "Ti-N-O-F" decomposition product probably occurred as soon as the reaction tube was exposed to the atmosphere while attempting to synthesize a true TiNF compound.

In addition, there seems to be some organic matter that was trapped in the "Ti-N-O-F" product. Looking at the XPS data for the standard TiO_2, we find that carbon content is about 11% by weight concentration which is mainly from the CO_2 from atmosphere. On the other hand, "Ti-N-O-F" has about 27.08% by weight concentration, which is about twice the carbon concentration in the standard TiO_2 sample. This increase in the carbon concentration in the "Ti-N-O-F" sample is likely due to addition of organic matter, trapped during decomposition of bis (diethylamidofluoro) titanium. Therefore to remove this organic matter from the "Ti-N-O-F" a careful choice of an organic solvent should be carried out and used to purify the "Ti-N-O-F". If using an organic solvent does not work out, then an effort to cleanly re-synthesize the precursor should be made. A different heating ramp and different (possibly higher) decomposition temperatures might also be able to influence the outcome of the decomposition reaction.

Chapter 7

Attempted Synthesis of TiN_xO_y via Urea Route

7.1 Motivation

The overall motivation of the work described in this chapter is to find an alternative for TiO_2 used in the development of TCON® ceramic-metallic interpenetrating phase composite materials produced by Fireline TCON, Inc. (FTi), a subsidiary of FireLine, Inc in Youngstown, Ohio. Attempts to produce TCON composites containing TiAl intermatallic phases have failed, apparently due to poor wettability of TiO_2 in the reaction system. By changing the surface morphology and lattice composition of TiO_2 through doping with nitrogen to produce $TiO_{2-x}N_x$, we propose that the reaction will be successful. Also important is the fact that urea is a relatively inexpensive commercial fertilizer available in large quantities, making this a potentially attractive approach for industrial scale-up.

7.2 The Proposed Reaction Process of TiO_2 and Urea

Carbamide, commonly known as urea, decomposes at around 190 °C to release ammonia, biuret, cyanuric acid, ammelide, ammeline and melamine. In this study, we propose that the ammonia released can be used to react with TiO_2 to produce $TiO_{2-x}N_x$. The proposed mechanism (Koscielska *et al*., 2005) for the reaction is indicated in the following equations:

$$NH_3 \longleftrightarrow 1/2\ N_2 + 3/2\ H_2$$

$$TiO_2 + (2\text{-}x)H_2 \longrightarrow TiO_x + (2\text{-}x)H_2O$$

$$TiO_x + NH_3 \longrightarrow TiN + H_2O$$

In these reactions, TiO_x represents reduced forms of titanium oxides, for example TiO, Ti_2O_3 and Ti_2O. The formation of these unstable titanium oxides leads to the agglomeration of TiN on their surface leading to the formation of a titanium oxynitride compound. The formation of a titanium compound in its reduced state would be detected in the XPS as well as PXRD, if a stable TiN compound is formed in the course of the reaction. The presence of inorganic nitrogen (nitrogen attached to a metal) would be detected in the XPS at around 396 eV.

7.3 Experimental

Titanium dioxide (TiO_2 anatase) used in this experiment was synthesized in a sol-gel reaction described previously. A mass of 3.32 g of TiO_2 was mixed with urea (Fisher Chemical, 99.99%, 60.06g, 1 mole), and the mixture was well ground using a mortar and pestle. A portion of this mixture weighing 8.63 g was placed in an alumina boat, which in turn was placed in a silica reaction tube. The tube was purged with N_2 gas three times, placed in a tube furnace, and kept under dynamic flow of nitrogen throughout the reaction. The tube furnace was run using the program shown in **Table 7.1**.

Table 7.1 Tube Furnace Program-2

Step 1	Ramp at 60 ^{o}C/hr Level at 190 ^{o}C Dwell for 3 hrs
Step 2	Ramp 60 ^{o}C/hr Level at 300 ^{o}C Dwell for 2 hrs
Step 3	Ramp 60 ^{o}C/hr Level at 1200 ^{o}C Dwell for 12 hrs
End	….

7.4 Results and Discussion

The initial reactants were all white in color but the reaction led to the formation of a product with varying colors. Thus the product contained different phases, dispersed essentially as a color gradient from one end of the boat to the other. Specifically, the sample consisted of a dark shiny blue powder on one end of the boat, followed by a green-yellow section, then a faint white section. Samples were analyzed using PXRD and XPS methods, and the PXRD pattern from a mixture of all three product colors is shown in **Figure 7.1**.

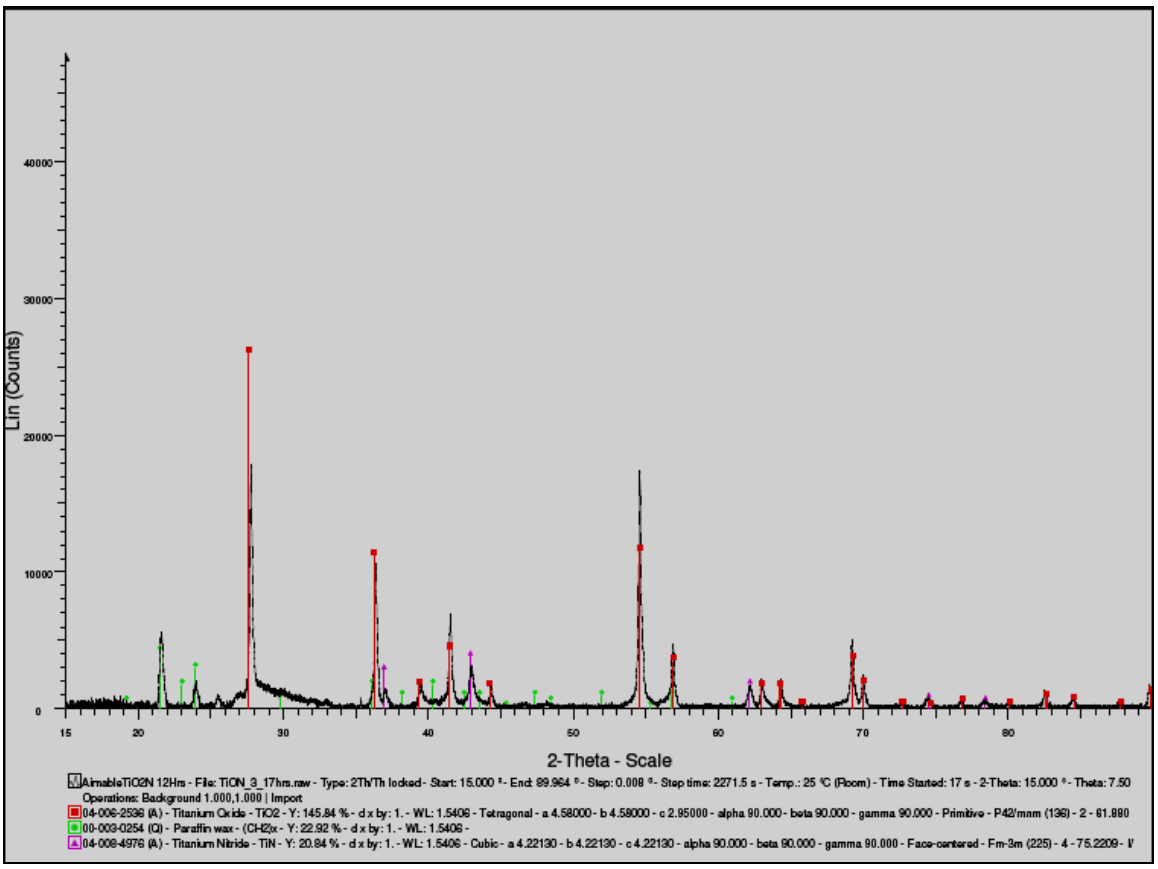

Figure 7.1 PXRD pattern for TiN_xO_y. The red pattern belongs to a TiO_2 rutile phase, the pink pattern belongs to a TiN phase & the green corresponds to the carbon wax used to support the sample.

The PXRD pattern in **Figure 7.1** (above) was matched and refined to the pattern of TiO_2 rutile and TiN. There were two peaks whose match could not be found but apparently they superimpose with the peaks belonging to paraffin wax, which was used for sample mounting. The peaks belonging to the TiN phase were also a good fit for the pattern belonging to an unstable phase of $TiO_{0.88}$, presumably because they both have the rocksalt structure. The patterns belonging to the reduced forms of titanium oxides were not refined as these oxides are not stable enough to survive in air and humidity for

long hours. They could react with the surrounding moisture and air or simply agglomerate the TiN onto their surface to form an oxynitride. As discussed below, more astonishing is the absence of a reduced form of titanium compound such as TiN in the XPS analysis, a somewhat contradictory result from the PXRD data. Also, puzzling is that, the shiny blue section was present in the largest amount by volume and was presumably the TiN phase which shows up very weakly in the PXRD pattern.

The XPS data for the blue phase indicate the presence of a Ti-N bond at around 396 eV as shown in the spectrum for the blue phase in **Figure 7.2**. In addition, the figure shows a Ti-O bond at around 530 eV. However, the Ti-O bond is shifted from the normal metal oxide position. The presence of N, which is more electronegative, in the vicinity of the oxygen could be responsible for this shift. XPS curve fitting results for titanium shown in **Figure 7.3** indicate that only a titanium compound with Ti^{4+} was formed. The change in color therefore is due to introduction of nitrogen into the TiO_2 lattice to form a TiN_xO_{2-X} compound. Further information on elemental analysis would be needed in order to come up with the necessary stoichiometry of the reaction. However, a close examination and comparison of the nitrogen XPS peak in the blue sample (**Figure 7.2**) to the one in the green sample (**Figure 7.4**) indicates that the blue sample has more nitrogen than the green one. This is evident from the relatively high intensity of the nitrogen peak in blue sample.

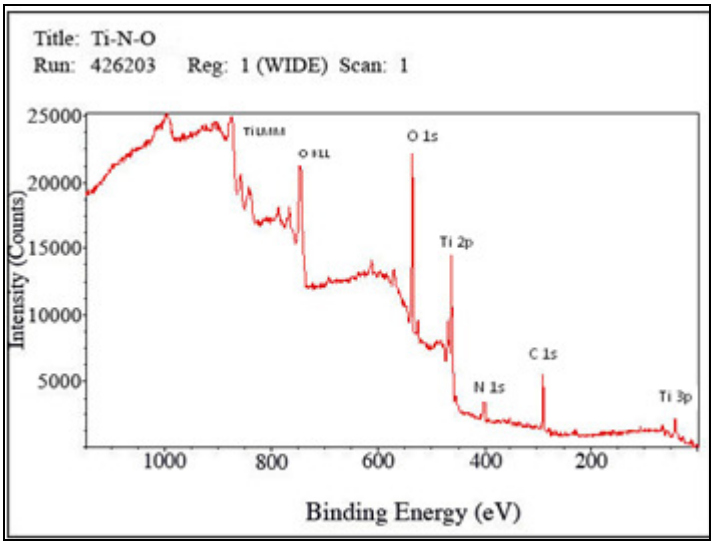

Figure 7.2 XPS spectra for the blue sample of TiN_xO_y

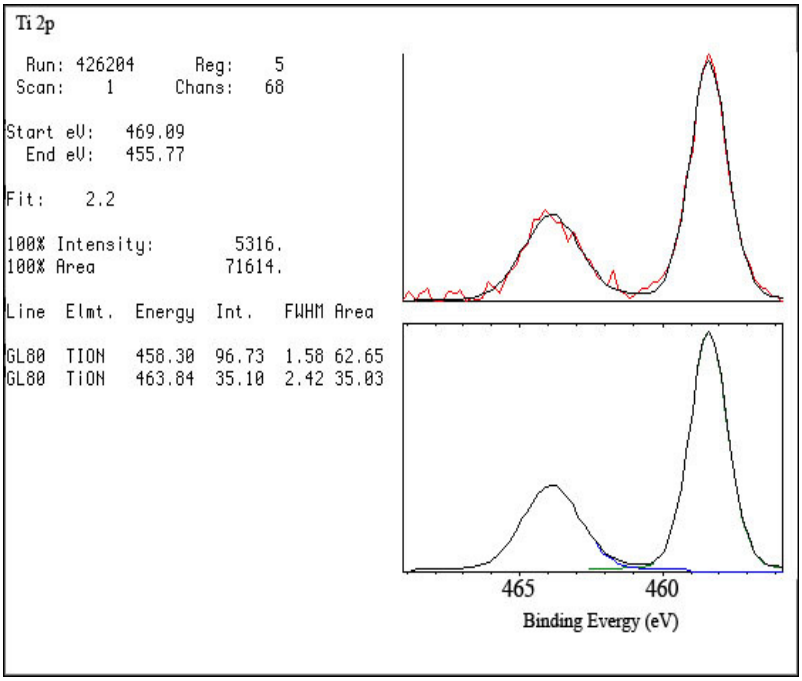

Figure 7.3 Titanium curve fitting for the whole sample

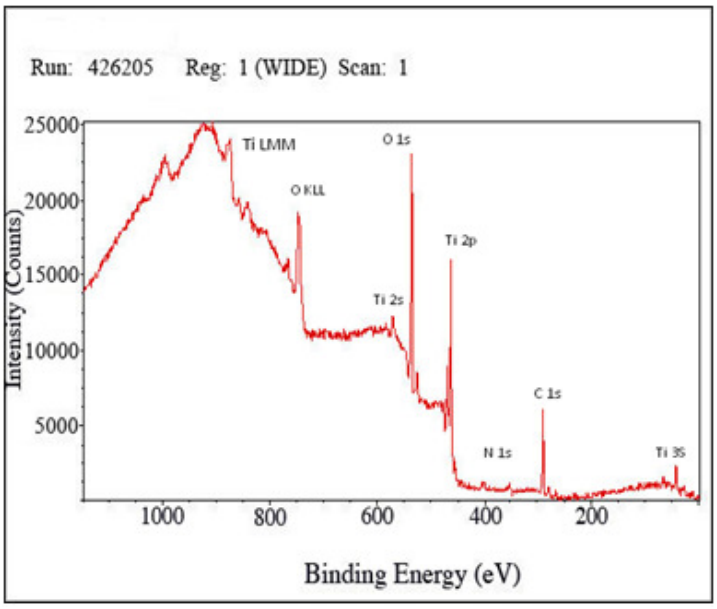

Figure 7.4 XPS spectra for the green sample

High resolution XPS data were collected for each element present in both the green and the blue samples, in order to see how the presence of nitrogen incorporated into the TiO_2 lattice affected the binding energy of oxygen in TiO_2. Initial observations suggest that the presence of nitrogen in the TiO_2 lattice lowers the binding energy of oxygen from 532 eV to approximately 530 eV (see **Figures 7.5** & **7.6**). Another interesting observation is that the nitrogen peak, which normally occurs at 396 eV (see **Figures 7.7** & **7.8**), is shifted towards lower binding energy (395 eV) in the blue sample. This observation is correlated to the amount of nitrogen in the respective samples as shown in **Table 7.2**. The blue sample has 8.62% atomic concentration of nitrogen and the green sample has 4.19% atomic concentration of nitrogen. Indeed, to the best of our knowledge, we have doubled the amount of nitrogen doped into TiO_2 using other known methods.

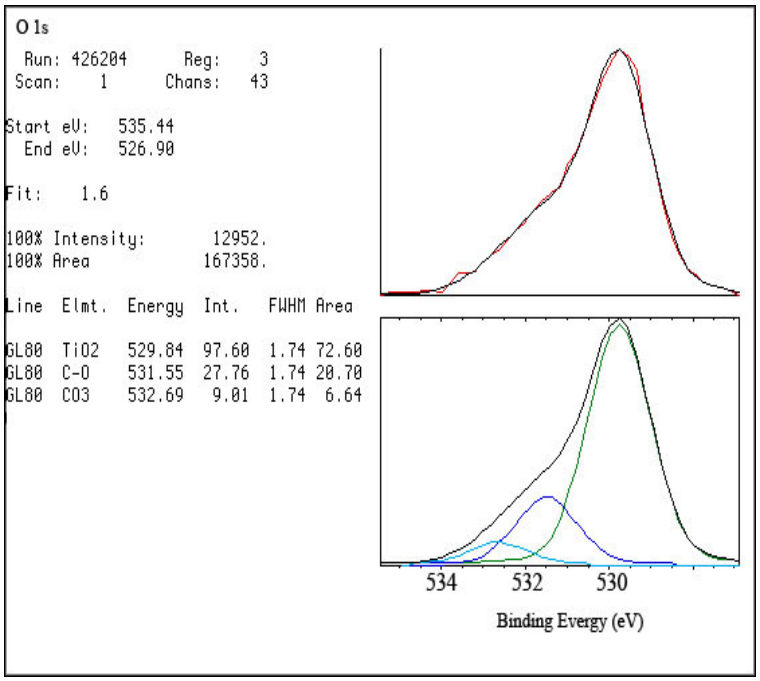

Figure 7.5 Oxygen curve fitting for the green phase

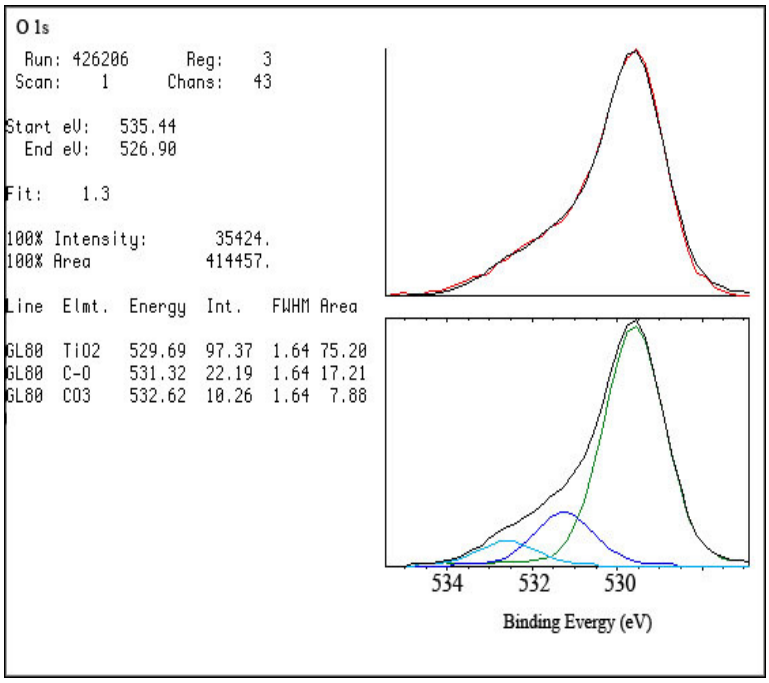

Figure 7.6 Oxygen curve fitting for the blue phase

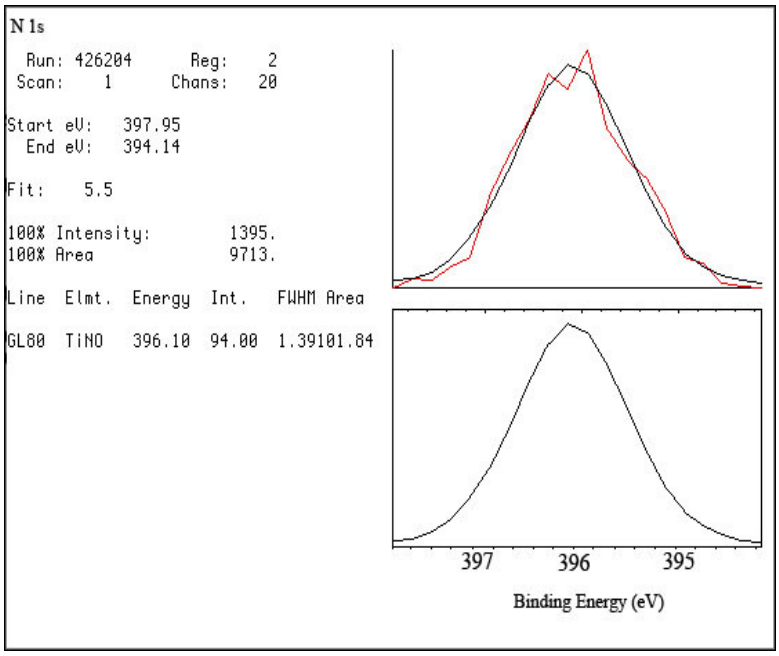

Figure 7.7 Nitrogen curve fitting for the green sample

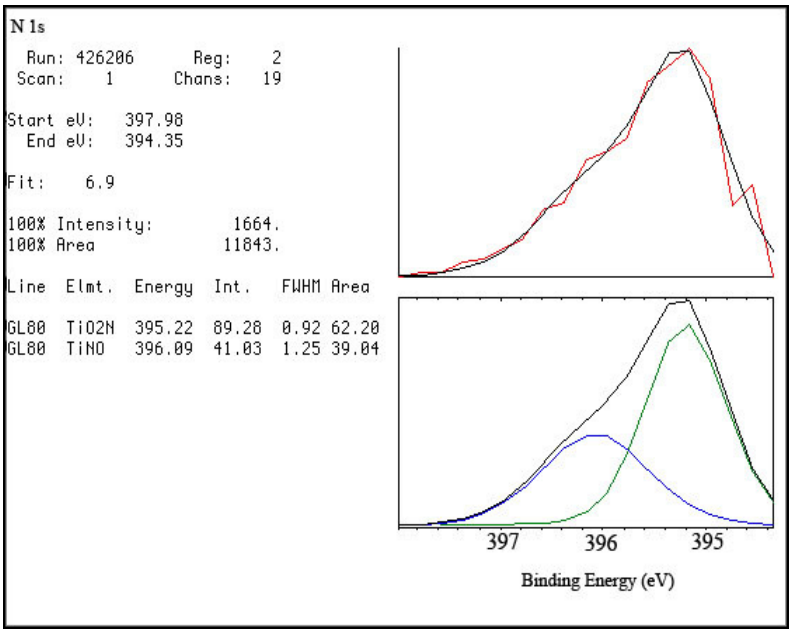

Figure 7.8 Nitrogen curve fitting for the blue sample

Table 7.2 Percentage Atomic Concentration of the TiN_xO_y Samples

SAMPLE	C	N	O	Ca	Ti
'TiON-blue"	30.47	8.62	44.46	0.38	16.07
"TiON-Green"	35.77	4.19	43.66	0.88	15.49

The observation of a blue color in the blue sample was initially thought to be originating from the TiN phase, but the absence of a Ti^{3+} peak, expected between 400 eV and 395 eV, prompted us to consider that the blue color may have resulted from the narrow band gap brought about by an increase in the amount of nitrogen doped into the TiO_2 lattice. Thus, TiO_2 doped with 4.19% nitrogen atomic concentration corresponds to the green-yellow phase, while a nitrogen atomic concentration of 8.62% corresponds to the blue phase.

Chapter 8

Chemical Education Outreach

8.1 CyberLabNet Project

Running chemical instrumentation facilities such as X-Ray Diffraction, Electron Microscopy, NMR and many others is prohibitively expensive for most non-research universities and predominantly undergraduate institutions. However, there is a need to teach students at these institutions how to operate and manage modern chemical instrumentation. This is the case perhaps all over the world. Currently, Dr. Allen D. Hunter at Youngstown State University and his team are developing a solution to this problem. The CyberLabNet package developed by the YSU team and Zethus Software LLC of Youngstown, Ohio, will ultimately allow scientific communities located at different geographical regions (both national and international) to share their resources (research facilities, knowledge, etc.) in a well-organized fashion. Using a cloud computing approach, instruments and sensors ("Nodes") will be connected with each other and the "Cloud" to form a network of resources that can be accessed from anywhere and at anytime. Essentially, each node in the CyberLabNet will be equipped with a hardware tool known as a “symbiote box” which will allow the instrument to communicate with the "cloud" via a software program, CyberLabNet.

The CyberLabNet project has gone through several phases namely, design, development and testing. The latter phase of the CyberLabNet project did involve participation of various collaborators at different regions of the nation and the world.

One of the collaborators is the chemistry department at the University of Eastern Africa Baraton.

8.2 Baraton Chemistry Professors Visit at YSU

Earlier in January 2009, the chemistry department at the University of Eastern Africa, Baraton (UEAB) expressed their desire to visit Youngstown State University to be trained on the modern chemical instrumentation. My role in the CyberLabNet team was to organize and coordinate the visit by Mr.Shadrack S. Mule and Prof. Asafu Maradafu at Youngstown State University. The visit was planned and executed in the summer of 2009. The two professors of chemistry from Baraton spent approximately two months at YSU, being trained on NMR and XRD methods and at the same time they carried out their own research, using facilities available at YSU. While here, the two professors had time to visit various faculty laboratories in the chemistry and physics departments. This enabled them to have an overview of the various resources available for future collaboration. In addition they visited other collaborators with YSU, including Materials Research Laboratory in Struthers, Ohio, and the Youngstown Business Incubator.

The Baraton faculty visit served as an introduction to a sustainable collaboration with the CyberLabNet team and the YSU community at large. Currently, there are plans to co-author research proposals that require international collaboration. Such proposals are hoped to bring in funds that will give students/professors at YSU and UEAB a chance to establish long term collaboration, facilitated in part through the possibilities that CyberLabNet has to offer. In addition, Baraton University is an ideal location for remote testing of the CyberLabNet package. By carrying out testing at Baraton, we can learn

more about factors that may affect the functioning of CyberLabNet. More specifically, we want to know how the internet band width at such a remote location as Baraton affects the transfer of research data from other locations and more particularly, YSU research facilities. Therefore, collaboration with Baraton University is expected to bring in valuable data for both the CyberLabnet team at YSU and for Baraton University.

8.3 Introducing Vernier Probes and Sensors at Baraton University

Vernier probes and sensors are a comprehensive collection of more than 50 compact chemical and physical sensors, manufactured by *Vernier Software & Technology* of Beaverton, OR. They can be used with a variety of computer and calculator platforms, are easy to use (especially for the not yet deeply trained user), and as such are heavily employed in settings such as general chemistry laboratories and experiments. Using Vernier probes students can perform experiments to reinforce various concepts such as in colorimetry, acid-base chemistry, electrochemistry and thermodynamics. While visiting YSU, the Baraton professors acquired a number of Vernier probes and sensors for use in teaching and - to a lesser degree - also in research.

Chapter 9

Summary and Conclusion

One of the major motivating factors in this research was to investigate whether a true TiNF compound, in which nitrogen and fluorine completely occupy the oxygen atomic positions in a TiO_2 lattice, exists. In an attempt to synthesize this compound, we have investigated a novel route involving a thermal decomposition reaction of an appropriate titanium (IV) complex. More specifically, we have outlined and tested a hypothesis that a compound such as bis(diethylamidofluoro) titanium(IV) would undergo a thermal decomposition reaction that leads to the formation of a true TiNF compound. We successfully synthesized and characterized bis(diethylamidofluoro) titanium(IV) via single crystal X-ray diffraction. We further investigated its thermal decomposition and characterized the resulting solid product (expected to be TiNF) by a variety of methods, including PXRD, SEM, and XPS. The TGA data are close to the expected theoretical values. The validity of our hypothesis to prepare TiNF using this approach will need further evidence from mass spectrometry data or/and NMR data, and the obtained material will need to be further investigated under the assumption that it might be unstable under ambient conditions when handled in air. However, the confirmed synthesis of an N, F-doped, extended inorganic bulk TiO_2 phase from a molecular titanium(IV) complex verifies the potential of the overall approach.

We have also investigated the use of urea in the synthesis of TiN_xO_{2-X}. It is evident from the literature that changing the composition of TiO_2 by doping it with

nitrogen, fluorine or other materials can extend the band gap of TiO_2 into the visible region, which enhances the optical properties of this important material. The Wagner group is also interested in using this material as a precursor in the production of ceramic-metallic composites in future work. Thus the motivation here was to find a simple route for preparation of nitrogen-doped TiO_2, as opposed to typical methods such as ammonolysis. The PXRD data shows that reacting TiO_2 anatase with urea at a high temperature such as 1200°C leads to reduction of TiO_2 to form a TiN phase and a TiO_2 rutile phase. Further analysis of the products obtained in this reaction by XPS, on the contrary, shows that there is no Ti^{3+} in the sample! The contradictory data means that a new compound due to the reaction of unstable TiOx and TiN could have been formed. Further analysis would be needed to harmonize the XPS observation and the PXRD data. Most significantly, the presence of a yellow phase and predominant TiO_2-like peaks in the PXRD pattern indicate that this could indeed be a promising alternate route for a simple and inexpensive means for the preparation of nitrogen-doped TiO_2.

The last chapter (Chapter 8) gives an overview of an outreach activity in chemical education involving the CyberLabNet team members at Youngstown State University. This outreach activity is part of the Cyber Instrumentation project, whose major goal is to break the physical barrier between researchers and educators who want to share resources such as chemical instrumentation and databases. A large part of the Cyberinstrumentation project is dedicated to the development of the CyberLabNet software that will ultimately allow a large group of collaborators to share resources in scientific research and education in an organized fashion. The final stages of this project

will involve testing the CyberLabNet software at different sites, to see how various factors such bandwidth, and propagation of data from one collaborator to another, affect the functioning of the software.

The University of Eastern Africa Baraton (UEAB)-Kenya is one of those sites where the testing of the CyberLabNet shall be done. The chemistry department at UEAB expressed their need to be trained on modern chemical instrumentation to allow them to participate in the testing and further development of CyberLabNet. The visit and the training of two chemistry professors, (Mr. Shadrack Mule and Dr. Asafu Maradufu) were planned and executed in the summer of 2009.

REFERENCES

Akiyo Yamamoto, Organotransition Metal Chemistry, John Wiley and Sons New York 1986

Aldrich Catalogue for Inorganics & Organometallics. 1998 – 99

Brown, I. D**.**, *J. Res. Natl. Inst. Stand. Technol.,* 1996, **101**, 341 – 346

Castellani, P.M., Marshall University. Glovebox Instructions. http://science.marshall.edu/castella/research/ (accessed August 2008)

Chaitanya, K. & John E. (1996) Chem.Mater., **8**, 984

Chang, H.H., Huang H.S. & Chen, J.H. (2006) Applied and Environmental Microbiology, **72**, 6111-6116

Cochet-Muchy, D. (1994) Journal of Physics IV, **4**, C2 – 33

Cunman, Z., Zheng, X. & Qian, L. (2005), Journal of Wuhan University of Technology-Mater. Sci. Ed, **20**, No.4

Erlich, P., Linz., W., & Seifert, H.J. (1970) *naturwissenchaftern*, **58**, 219 – 220

Fox, M.A., & Dulay, M.T. (1993) *Chem. Rev*., **93**, 341 - 355

Gole, J.L., & Stout, J.D., (2004) *J. Phys.Chem*., 108, 1230 – 1240

Gomathi, A. & Reshma, S., (2009) *Journal of Solid State Chemistry*, **182**, 72 – 76

Hamid, M., Mazhar M., Zeller M., Molloy K.C., Hunter A.D. (2006) *Inorg.Chem*., **45**, 10457

Heinekey, D.M. University of Washington. Schlenk Techniques. http://depts.washington.edu/chemcrs/bulkdisk/chem317A_win04/syllabus.pdf (accessed August, 2008)

Hongjian, Y. & Dingquan, X. (2005) *Journal of Wuhan University of Technology Mater.Sc.Ed*., **20**, 4

Ismat, S.S., Huang, C.P., et al., NSF Nanoscale Science and Engineering Grantees Conference, Dec 16-18, 2003

Jiping, C.D. & Agrawal, Y.Z. (2001) *Journal of materials science letters,* **20**, 77-79

Kamiya K., Nishijima T., & Tanaka K., (1990) *J. Am. Ceram. Soc*., **73**, 2750

Ko, T.S., Chu, C.P., Chen, H.G., Lu, T.C., Kuo, H.C., & Wang, S.C. (2006) *J.Vac. Sci. Technol*., A **24**(4)

Koscielska, B., Murawaski, L. & Wicikowski, L.(2005) *Materials Science-Poland*, **23**, 1

Li, D., Huang, H., Chen, X., Chen, Z., Li, W., Ye, D. & Fu, X. (2007) *Journal of Solid State Chemistry*, **180**, 2630 – 2634.

Liliane, G. & Hubert P. (2003) Inorg. Chem. Commun., 6, 102

Limin, D., Zhidong, H., Ze, Wu., & Xianyou, Z. (2006) Journal of Rare Earths, **24**, 75-76

Lupeiko, T.G. & Lopatin, S.S. (2004) *Inorganic Materials*, 40, S19 – S32

Maeda, K., Teramura, K., Saito, N., Inoue, Y., Kobayashi, H. & Domen, K.(2006), *Pure Appl. Chem*., 78, 2267 - 2276

Michalow, K.A. Logvinovich D., A. Weidenkaff A., Amberg M., Fortunato G., Heel A., Graule T. & Rekus, M. (2009) *Catalysis today*, **144**, 7 - 12

Miyoshi, J., Diniz, J.A., Barros, A.D., Doi, I.,& Zuben, A.A.G. (2009) *Microelectronics Engineering*, **3**, 267

Nakhutsrishvili, I.G., Dzhishiashvili, D.A., & Mkervalishvili, Z.I. (2003) *Inorganic materials*, **39**, 833-835

Nathan H., Graem A. (2006) *Appl. Organometal. Chem*., **20**: 687

Nicklow, R.A., (2002) MSc. Thesis, Synthesis And Single Crystal X-ray Diffraction Studies of Ca_2NF And Other Compounds, Youngstown State University OH 44555.

Pia W Aldrich Catalogue for Inorganics & Organometallics. 1998 - 99.

Punjab Industry & Export Cooperation. Rubber Stoppers. http://punjabindustryexport.com/prods/rubber/ (accessed August 2008)

Robertson. J. (2004) *Eur.Phys. J.Appl. Phys*., **28**, 265-291

Santamaria, C., Beckhaus, R., Haase, D., Seak, W. & Koch, R. (2001) *Chem-Eur.J*.,**7**, 622

Sheldrick, W.S. (1975) *J.Fluorine Chem*., **4**, 415

Shouxin, L., Xiaoyun, C., & Xi, C. (2006) *C Chin J Catal*., **27(8),** 697-702

Shrout, T. R., (2008) International symposium on the application of ferroelectrics, **3**, 1 – 4

Siebel, H.A., Karen, P., Wagner, T.R. & Woodward, P.M. (2009) J. Mater. Chem., **19**, 471 – 477

Stephen M., Sandra L., & Sean A. (1997) *Chem.Mater*., **9**, 2300

Straus, D.A., M.Kamigaito, Cole, A.P. & Waymouth, R.M. (2003) *Inorg. Chim. Acta*, **349**, 65

Sunandana, C.S., Kumar P.S. (2004) *Bull. Mater. Sci.*, **27**, 1-17

Suresh, G., Vadin, K.G., Mikael, K., Oksana K.N., Elena, K.E., Irina F.M., & Boris R.V. (2001) Polyhedron, 20, 2163 – 2169

Teichner, S.J. (2008) *J. Porous Mater.*, ***15***, 311 – 314

Tessier, F., Maillard, P., Lee, Y., Bleugat, C., & Domen K. (2009) *J. Phys. Chem.*, **113**, 8526

Thirumal, M., Ganguli, K. (2002) *Progress in crystal growth and characterization of Materials*. 147- 154

Thurston, J. H., Whitmire, K. H., (2002) *Inorg. Chem*., **47**, 4194

University of Oregon. Scanning Electron Microscope figure (Courtesy of Museum of Natural Sciences). http://materialscience.uoregon.edu/ttsem/sem_mos.gif (Accessed April 2010)

Wiley-VCH. Powder X-Ray Diffraction. http://www.wiley-vch.de/books/sample/3527310525_c01.pdf (Accessed August, 2008)

Wustefeld, C.,Vogt, T., Lochner, U., Strahle, J., & Fuess, H.(1998) *Angewandte Chemie*, **27**, 929 – 930

Yan, D.S. (1994) *Pure & appl. Chem*., **66(8),** 1629

Appendix A

Selected bond distances (Å) in bis(diethylamidefluoro) titanium

08mz448_0m			
C1—N1	1.475 (8)	C20—H20C	0.9800
C1—C2	1.530 (9)	C21—N6	1.484 (7)
C1—H1A	0.9900	C21—C22	1.531 (9)
C1—H1B	0.9900	C21—H21A	0.9900
C2—H2A	0.9800	C21—H21B	0.9900
C2—H2B	0.9800	C22—H22A	0.9800
C2—H2C	0.9800	C22—H22B	0.9800
C3—N1	1.478 (8)	C22—H22C	0.9800
C3—C4	1.529 (9)	C23—N6	1.482 (8)
C3—H3A	0.9900	C23—C24	1.514 (10)
C3—H3B	0.9900	C23—H23A	0.9900
C4—H4A	0.9800	C23—H23B	0.9900
C4—H4B	0.9800	C24—H24A	0.9800
C4—H4C	0.9800	C24—H24B	0.9800
C5—N2	1.474 (8)	C24—H24C	0.9800
C5—C6	1.532 (10)	C25—N7	1.476 (8)
C5—H5A	0.9900	C25—C26	1.530 (10)
C5—H5B	0.9900	C25—H25A	0.9900
C6—H6A	0.9800	C25—H25B	0.9900
C6—H6B	0.9800	C26—H26A	0.9800
C6—H6C	0.9800	C26—H26B	0.9800
C7—N2	1.479 (8)	C26—H26C	0.9800
C7—C8	1.535 (10)	C27—N7	1.474 (8)
C7—H7A	0.9900	C27—C28	1.532 (10)
C7—H7B	0.9900	C27—H27A	0.9900
C8—H8A	0.9800	C27—H27B	0.9900
C8—H8B	0.9800	C28—H28A	0.9800
C8—H8C	0.9800	C28—H28B	0.9800
C9—N3	1.482 (9)	C28—H28C	0.9800
C9—C10	1.523 (9)	C29—N8	1.474 (8)
C9—H9A	0.9900	C29—C30	1.540 (10)
C9—H9B	0.9900	C29—H29A	0.9900
C10—H10A	0.9800	C29—H29B	0.9900

Appendix B

Table B-1

Principal mean square atomic displacements U in $[TiF_2(NEt_2)_2]$

0.0306	0.0203	0.0142	C1
0.0535	0.0343	0.0146	C2
0.0251	0.0168	0.0156	C3
0.0316	0.0237	0.0182	C4
0.0280	0.0232	0.0119	C5
0.0387	0.0282	0.0207	C6
0.0360	0.0278	0.0028	C7
0.0334	0.0215	0.0181	C8
0.0458	0.0260	0.0137	C9
0.0465	0.0416	0.0154	C10
0.0303	0.0254	0.0117	C11
0.0538	0.0333	0.0251	C12
0.0261	0.0237	0.0091	C13
0.0369	0.0257	0.0149	C14
0.0503	0.0189	0.0161	C15
0.0832	0.0294	0.0139	C16
0.0266	0.0191	0.0158	C17
0.0538	0.0197	0.0143	C18

0.0222	0.0214	0.0142	C19
0.0278	0.0224	0.0184	C20
0.0301	0.0179	0.0109	C21
0.0406	0.0303	0.0143	C22
0.0354	0.0197	0.0169	C23
0.0390	0.0289	0.0205	C24
0.0465	0.0181	0.0099	C25
0.0454	0.0313	0.0183	C26
0.0369	0.0247	0.0122	C27
0.0536	0.0255	0.0213	C28
0.0261	0.0235	0.0182	C29
0.0598	0.0283	0.0190	C30
0.0296	0.0226	0.0069	C31
0.0406	0.0275	0.0137	C32
0.0207	0.0165	0.0112	F1
0.0251	0.0202	0.0126	F2
0.0224	0.0154	0.0099	F3
0.0185	0.0128	0.0104	F4
0.0236	0.0136	0.0094	F5
0.0171	0.0144	0.0119	F6
0.0237	0.0162	0.0093	F7
0.0270	0.0207	0.0165	F8

0.0204	0.0174	0.0149	N1
0.0276	0.0113	0.0106	N2
0.0212	0.0178	0.0160	N3
0.0297	0.0163	0.0074	N4
0.0207	0.0162	0.0111	N5
0.0219	0.0144	0.0077	N6
0.0303	0.0226	0.0086	N7
0.0213	0.0165	0.0123	N8
0.0155	0.0137	0.0109	Ti1
0.0185	0.0132	0.0096	Ti2
0.0160	0.0121	0.0107	Ti3
0.0171	0.0157	0.0120	Ti4

Appendix C

Figure C-1

Rietveld Refinement of TiNxOy compound from urea-TiO_2 reaction